Chinese Journal of
POLYMER SCIENCE

REVIEW

https://doi.org/10.1007/s10118-026-3652-3
Chinese J. Polym. Sci.

Stretchable Organic Photoelectric Conversion Systems: From Molecular Design to Device Applications

Yue-Yue Zhang[a,b], Yi-Li Wang[a,b], Yun-Qi Liu[a,b], and Yun-Long Guo[a,b*]

[a] *Beijing National Laboratory for Molecular Sciences, Key Laboratory of Organic Solids, Institute of Chemistry Chinese Academy of Sciences, Beijing 100190, China*
[b] *School of Chemical Sciences, University of Chinese Academy of Sciences, Beijing 100049, China*

Abstract The rapid development of the Internet of Things and wearable technologies has created substantial demand for stretchable optoelectronic devices. Among these, intrinsically stretchable organic optoelectronic devices are emerging as key technologies for applications in wearable electronics, electronic skin, and health monitoring. This review systematically summarizes the recent progress in this field. We first outline two primary strategies for achieving stretchability: structural engineering (buckling and island-bridge configurations) and intrinsic material design. The review focuses on the latter, providing a comprehensive overview of the design of key components, including insulators, electrodes, and optoelectronic functional layers. Specifically, the design principles for intrinsically stretchable semiconductor active layers are elaborated with a focus on molecular engineering and composite material strategies. Furthermore, we summarize the performance optimization and applications of representative devices, such as organic photodiodes (OPDs), organic phototransistors (OPTs), organic photovoltaics (OPVs), organic light-emitting diodes (OLEDs), and organic light-emitting electrochemical cells (OLECs). The potential of these devices for integrated systems, including human-machine interaction, neuromorphic electronics, and wearable health monitors, is also explored. Finally, the current challenges and future research directions are discussed.

Keywords Organic optoelectronics; Molecular engineering; Intrinsically stretchable devices; Wearable electronic devices

Citation: Zhang, Y. Y.; Wang, Y. L.; Liu, Y. Q.; Guo, Y. L. Stretchable organic photoelectric conversion systems: from molecular design to device applications. *Chinese J. Polym. Sci.* https://doi.org/10.1007/s10118-026-3652-3

* Corresponding author, E-mail: guoyunlong@iccas.ac.cn
Special Topic: Distinguished Young Scholars in Polymer Science
Received January 7, 2026; Accepted March 10, 2026; Published online June 24, 2026

1 INTRODUCTION

The rapid advancement of wearable electronics, flexible human-machine interfaces, soft robotics, and implantable medical devices necessitates the development of functional devices that maintain stable performance under significant mechanical deformation.[1,2] Although conventional silicon-based electronics are well established in terms of performance and integration, their high modulus creates a fundamental mechanical mismatch with soft biological tissues. This incompatibility can lead to device failure under dynamic strains, such as bending and stretching, thereby limiting their utility in applications requiring long-term, comfortable, and high-fidelity biointegration.

Organic and polymeric materials have emerged as ideal platforms for high-performance stretchable optoelectronics owing to their intrinsic low modulus, solution processability, light weight, and tunable functionality.[3,4] These merits make them a focal point of research, paving the way for a new generation of deformable information terminals and biointegrated electronic systems. In terms of functionality, organic optoelectronic devices primarily perform two types of signal conversion: devices such as organic photodiodes (OPDs), organic phototransistors (OPTs), and organic photovoltaics (OPVs) convert optical signals into electrical signals or electrical energy, serving as core units for optical sensing, imaging, commu-

nication, and energy harvesting. Electroluminescent devices, such as organic light-emitting diodes (OLEDs) and organic light-emitting electrochemical cells (OLECs), convert electrical energy into optical signals and play key roles in information display and photobiological modulation (*e.g.*, optical stimulation and therapy).[5,6] Therefore, the development of organic optoelectronic devices that combine excellent stretchability with high optoelectronic efficiency is crucial for realizing the practical application of next-generation flexible integrated optoelectronic systems.

Achieving synergistic optimization of mechanical–optical–electrical properties at the device level presents intrinsic challenges in materials science. The high optoelectronic performance of organic semiconductor materials typically relies on highly ordered molecular packing (such as close π-π stacking) to enable efficient exciton diffusion and charge transport. Molecular backbones are often required to possess a certain degree of rigidity and planarity. Conversely, achieving intrinsic stretchability necessitates introducing chain segment mobility, constructing energy-dissipation networks, or appropriately reducing crystallinity, which usually implies a compromise in the orderliness of molecular packing.[4,7] Therefore, the central design challenge is to impart stretchability without substantially compromising the optoelectronic characteristics of the material.

Initial approaches circumvented this material-level trade-off by employing structural engineering (*e.g.*, buckling and island-bridge designs) to confer device-level stretchability.[8,9] However, these strategies have limitations in terms of mechanical robustness, strain distribution uniformity, and integration density. More recently, a deeper understanding of multiscale structure-property relationships has enabled a paradigm shift toward the rational design of functional materials. Through molecular engineering and composite strategies, optoelectronic materials that exhibit high charge-carrier mobility and excellent extensibility have been developed.[10,11] This progress has spurred rapid advancements in intrinsically stretchable organic optoelectronic devices.

In this review, we have systematically described the field of stretchable organic optoelectronic devices. First, we introduce the basic structures and work mechanisms of OLEDs, OPDs, OPTs, and OPVs. Subsequently, we delve into the two primary paradigms for achieving stretchability—structural engineering and intrinsic design–with a special focus on strategies for synergistically optimizing the properties of the constituent semiconductor, electrode, and dielectric layers. Then, we categorize and summarize the performance optimization and application expansion of several representative types of intrinsically stretchable organic optoelectronic devices and explore innovative application examples of these devices in integrated systems such as human-machine interaction/intelligent interfaces and wearable health monitoring, highlighting their unique advantages in constructing "soft optoelectronics-biology interfaces." Finally, we summarize the key challenges in this field and discuss future research directions and development opportunities.

2 DESIGN OF STRETCHABLE MATERIALS AND DEVICES

2.1 Organic Optoelectronic Devices

OLEDs are composed of organic light-emitting materials (emissive layer, EML) sandwiched between two electrodes, the anode and cathode (Fig. 1a). When a voltage is applied across OLEDs, electrons are injected into the electron injection layer (EIL) and then transported through the electron transport layer (ETL) to the EML. Concurrently, holes are injected into the hole

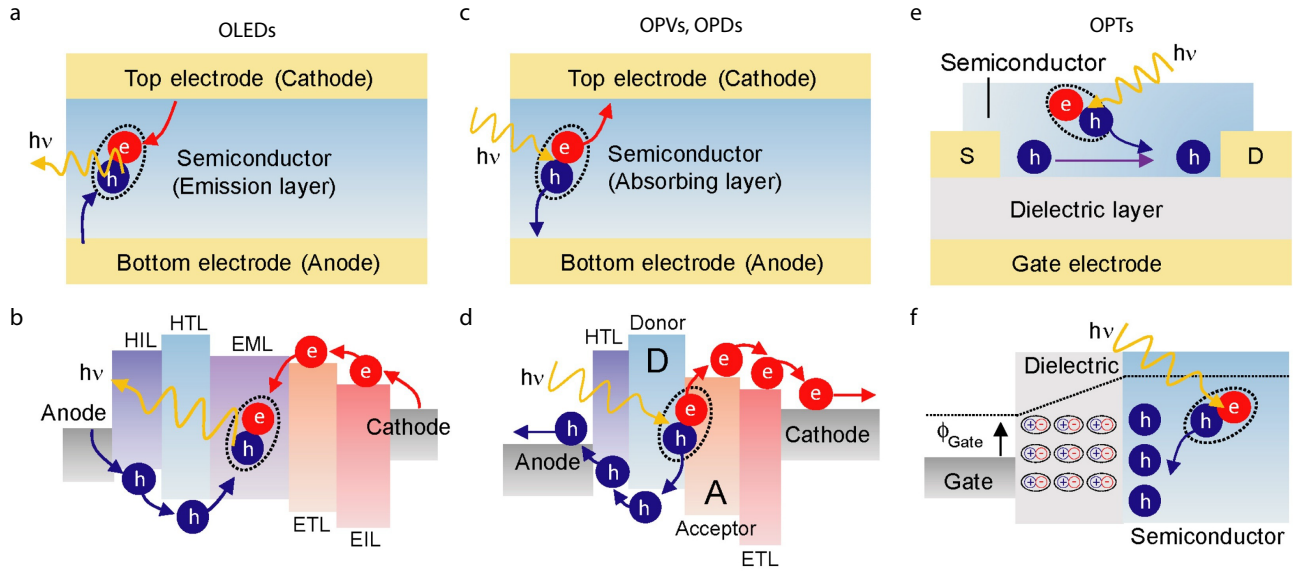

Fig. 1 Structure schematics of typical stretchable organic photoelectronic devices. (a) OLEDs; (b) Band diagram of the OLEDs: OLEDs emit light by recombination of electron-hole pairs in the middle of the organic layer; (c) OPVs and OPDs; (d) Band diagrams of the OPDs and OPVs, which separate charges from light irradiation and collect both carrier types by an applied electric field between the top and bottom electrodes; (e) OPTs; (f) Band diagram of the OPTs: OPTs form a conductive channel by accumulating either electrons or holes at the dielectric-semiconductor interface under an applied gate voltage (Reproduced with permission from Ref. [6]; Copyright (2021), Elsevier B.V. All rights reserved).

https://doi.org/10.1007/s10118-026-3652-3

injection layer (HIL) and migrate through the hole transport layer (HTL) toward the EML. Electrons and holes recombine to form excitons, which then radiatively decay to emit light (Fig. 1b).

OPDs and OPVs employ a structure similar to OLEDs, but operate *via* a reverse mechanism. Both OPDs and OPVs consist of a photosensitive layer sandwiched between an anode and a cathode, which is capable of converting light into electrical signals (Fig. 1c). In most OPDs and OPVs, the active layer is composed of blended donor and acceptor materials, forming a bulk heterojunction (BHJ) structure. When the energy of the incident light is equal to or greater than the bandgap of the donor (p-type), electron-hole pairs (excitons) are generated within the active layer. Driven by the gradient energy distribution, these excitons diffuse into the donor/acceptor interface and dissociate into free holes and electrons. The holes and electrons are then transported through the HTL and ETL, respectively, toward the anode and cathode. Finally, the collected charge carriers generate a photocurrent in the device (Fig. 1d).

OPTs are a class of photosensitive organic field-effect transistors (OFETs) that integrate the light detection capability of photodiodes with the signal amplification function of transistors. The OPTs consist of three terminal electrodes (gate, source, and drain), a dielectric layer, and a photoresponsive semiconductor layer (Fig. 1e). In the absence of light, the OPTs operate identically to the conventional OFETs. Under illumination, the photoresponsive semiconductor absorbs photons with sufficient energy to generate bound electron-hole pairs (excitons). These excitons are efficiently separated by an externally applied gate bias, resulting in photogenerated current (Fig. 1f).

2.2 Stretchable Devices Design

The limited strain capability of soft and rigid functional materials prompted early investigations into geometrical engineering strategies for achieving structural stretchability in devices. Conventional approaches to structural stretchability include the integration of rigid film devices with pre-strained elastomeric substrates to form buckling configurations or the fabrication of device matrices interconnected by stretchable bridges, the so-called island-bridge architecture. Meanwhile, the development of stretchable functional materials is paving the way for intrinsically stretchable devices as promising alternatives.

2.2.1 Buckling strategy

The most straightforward method for realizing stretchable devices is to adopt a buckling structure. The functional layers are either deposited directly on a pre-strained elastomer using solution spin-coating or evaporation, or they are first fabricated on an ultrathin flexible substrate, followed by their transfer and bonding onto a pre-strained elastomeric substrate.[12] After the device fabrication, a release or relaxation process is required. Upon complete strain release, the device forms wavy or buckling configurations, which enable it to withstand significant strain or stretching.[9,13,14] Bao *et al.*[9] demonstrated the first stretchable organic solar cell using a buckling strategy. The device could reversibly withstand 27% strain and exhibited comparable performance when fabricated on pre-strained polydimethylsiloxane (PDMS) to that on a glass substrate. Employing a similar strategy in a later study,[15] a poly(3-hexylthiophene-2,5-diyl) (P3HT):(6,6)-phenyl-C61-butyric acid methyl ester (PCBM) bulk-heterojunction solar cell was fabricated from an ultra-thin (<2 μm) polyethylene terephthalate (PET) substrate onto a pre-strained elastomer. This induced aperiodic wrinkling, allowing the device to sustain strains exceeding 300%.

In principle, this strategy can transform virtually any high-performance flexible electronic device into a stretchable device that is suitable for large-scale device architectures. However, uncontrolled substrate release can lead to small bending radii at the sharp corners and extreme bending regions, inducing large flexural strains that may damage the device. Furthermore, random buckling can evolve during cyclic stretching owing to variations in the random bonding regions between the ultrathin device and elastomeric substrate. Poor mechanical stability remains a critical drawback of stretchable devices based on random buckling.[13,16]

To achieve controllable stretch-release cycles, Sun et al. developed a programmable buckling process by laser-ablating long-period gratings on an elastomer substrate.[17] However, developing a simple and low-cost technique remains a challenge. Subsequently, they proposed a simple and versatile stencil-pattern transfer technique for fabricating ordered buckles in stretchable organic optoelectronic devices.[18] A periodic metal film was deposited onto the surface of the adhesive and elastomeric substrate *via* a stencil and used as a barrier layer to modify the surface viscidity distribution of the substrate without affecting its elasticity. When an ultrathin optoelectronic device was attached to a pre-stretched substrate, the bonding and nonbonding regions between the device and substrate were defined by the periodic barrier layer. Controllable and ordered buckles were achieved after releasing the pre-strained substrate (Fig. 2a). The first stretchable polymer solar cell (SPSC) with a periodic buckling structure was fabricated. Both stretchable organic light-emitting diodes (SOLEDs) and SPSCs with periodic buckles exhibited excellent mechanical robustness after 20000 and 12000 stretch-release cycles between 0% and 20% tensile strain, respectively (Fig. 2b).

2.2.2 Island-bridge structure

Stretchability in devices can also be achieved by fabricating a matrix of devices with stretchable interconnect structures, a configuration known as an island-bridge structure.[19] These interconnects typically take the form of in-plane buckled (*e.g.*, serpentine) structures[20] or soft elastic composites.[21] An important advantage of island-bridge structure is that the electrical functionality of the devices remains almost entirely decoupled from the applied stretching until mechanical failure (for example, delamination or fracture) occurs.[22]

A typical island-bridge design was first demonstrated by Rogers *et al.*[8] They employed a hemispherical elastomeric transfer element to achieve this configuration, utilizing an electrically interconnected array of single-crystalline silicon photodiodes and current-blocking p-n junction diodes assembled in a passive matrix layout (Fig. 2c). The resulting hemispherical focal plane arrays, when combined with imaging optics and hemispherical housings, yield electronic cameras with sizes and shapes comparable to those of the human eye.

There is a steep strain variation at the deformable-rigid interfaces, as the rigid units constrain the elastomer under

https://doi.org/10.1007/s10118-026-3652-3

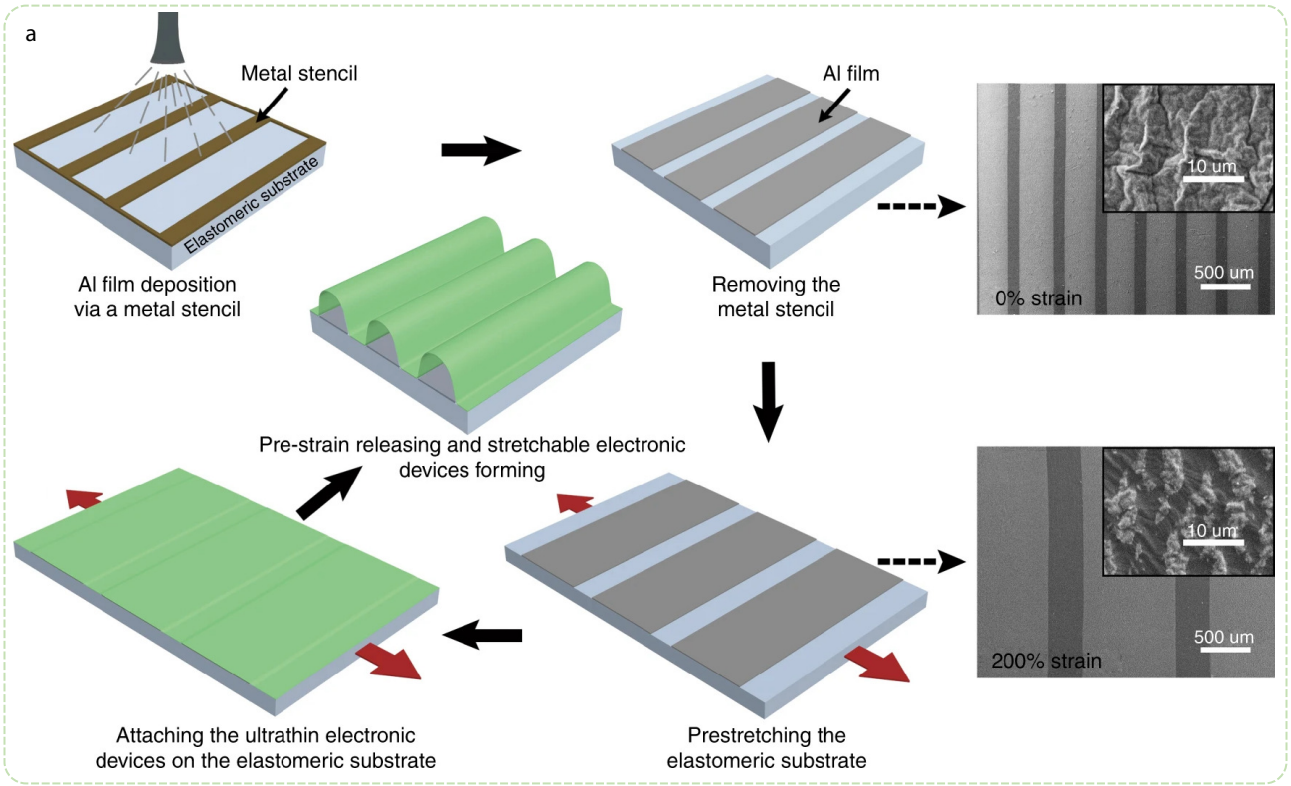

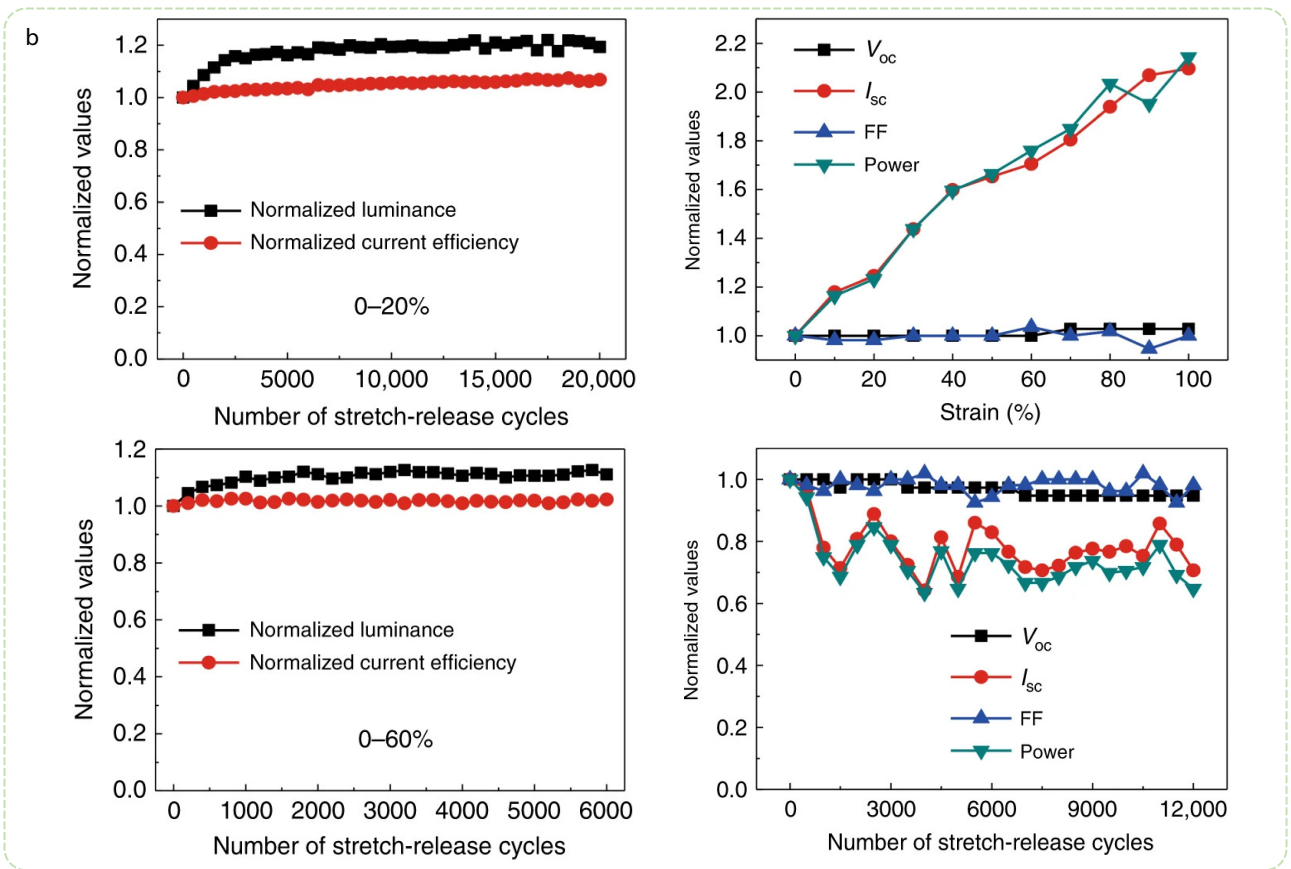

https://doi.org/10.1007/s10118-026-3652-3

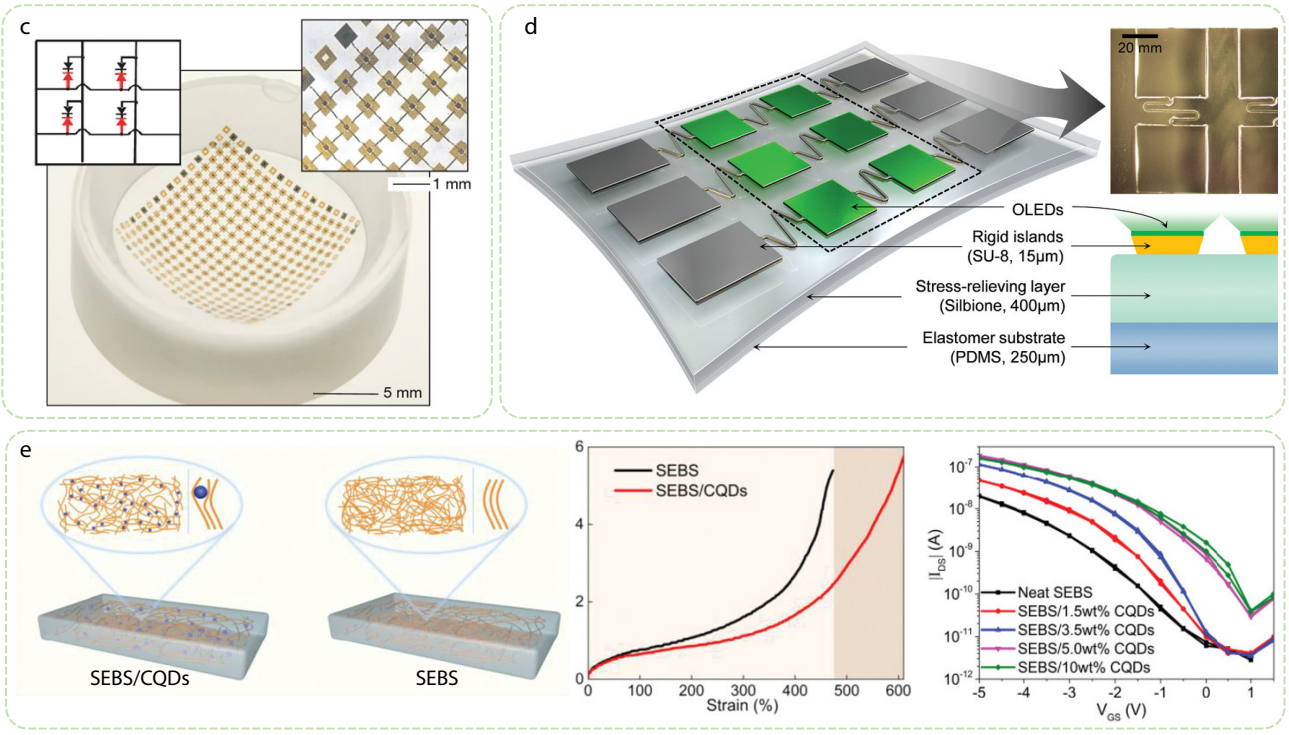

Fig. 2 (a) Schematic diagram showing the fabrication process for the stretchable electronic devices; (b) Characterization of SOLEDs and SPSCs (Reproduced with permission from Ref. [18]; Copyright (2018), The Authors, published by Springer Nature). (c) Photograph of the array integrated on a hemispherical glass substrate (main frame), optical micrograph of a part of the array (upper right inset) and circuit diagram showing the BDs (black), PDs (red) and electrode crossovers (arcs) in a 2-by-2 section of the system (upper left inset) (Reproduced with permission from Ref. [8]; Copyright (2008), Springer Nature). (d) Schematic diagrams of the hybrid stretchable platform, on which OLEDs are deposited. Both tilted top-view and cross-sectional view diagrams are provided; the inset photograph on the top, right side shows the microscope image of SU-8-based rigid islands and serpentine interconnectors fabricated on top of a Silbion layer (Reproduced with permission from Ref. [20]; Copyright (2020), Wiley-VCH GmbH). (e) Schematic diagrams illustrating the interaction between SEBS molecular chains and CQDs. The mechanical properties of thin films and the electrical properties of transistors (Reproduced with permission from Ref. [30]; Copyright (2022), Wiley-VCH GmbH).

them from expanding during stretching. The large strain variation could cause the delamination of the device units from the elastomer substrate. The interface between the device units and interconnects may also detach because of localized strain under stretching. To suppress localized strain at these rigid-soft interfaces, thin layers of a stiff material, such as SU-8 photoresist[23,24] or polyimide,[25] can be incorporated within the elastomer to form "strain-insulated islands." Yoo *et al.*[20] proposed a hybrid stretchable platform by introducing a thick, ultra-soft silicone elastomer layer (Silbione; Young's modulus≈0.9 kPa) between the PDMS substrate and SU-8 layer (Fig. 2d). This elastomer layer effectively functions as an adhesive, preventing SU-8 patterns from delaminating and maintaining their structural integrity during stretching. Using this method, they demonstrated stretchable OLEDs that could withstand repeated stretching cycles up to 140%. The planar rigidity of the device islands ensures that the fabricated OLEDs are free from optical artifacts such as diffraction and blurring. Furthermore, the all-elastomer fabrication process shows considerable application potential, as it significantly reduces the manufacturing complexity.[26] Bao *et al.*[27] reported an all-elastomer fabrication process, choosing both elastiff and substrate materials from the same family of elastomers with various cross-linking densities to achieve vastly different mechanical properties, while sharing similar chemical compositions for strong interfacial interactions. The resulting device density was at least two orders of magnitude higher than that reported for "rigid-island" stretchable electronics because of the broad tunability in the thickness and modulus of the elastomeric layers.

2.2.3 Intrinsic stretchability

As discussed, devices with geometrically stretchable structures are typically fabricated using complex processes. Although they can maintain stable performance under mechanical deformation, significant limitations persist. For instance, buckling configurations can only withstand uniaxial tensile deformation. When applied in sensors, these structures may alter their sensing characteristics upon bending and prevent intimate contact between the device and the target object. While island-bridge designs have expanded the applications of high-performance rigid devices, their stretchability is governed by the surface area ratio between the stretchable interconnects and rigid islands, and a trade-off between stretchability and device density is inevitable.[16] These strategies, particularly in the context of stretchable displays, inevitably compromise device performance, stretchability, and resolution.[20]

Unlike structurally stretchable devices, intrinsically stretchable devices are fabricated by vertically stacking multiple stretchable functional layers within a single unit. These devices can conform seamlessly to three-dimensional surfaces

without wrinkling and can withstand deformation in multiple directions. This design necessitates that each internal functional layer possesses stretchability compatible with the elastic substrate and that excellent mechanical compatibility exists between the layers. Such requirements are crucial for maintaining stable and efficient device performance during stretching. The fabrication of intrinsically stretchable devices typically involves two main approaches.[28] The first involves the sequential deposition of layers using solution-based methods, which require the use of orthogonal solvents between layers to prevent interlayer dissolution. The second approach employs lamination techniques in which individual layers are fabricated independently and then assembled. This method offers broader material compatibility and can be integrated with photolithography to achieve high-precision and highly integrated device arrays.[29]

2.3 Stretchable Materials Design

The primary goal in designing stretchable materials is to retain reliable high-performance operations despite repeated mechanical deformation. This section focuses on design strategies for stretchable functional layers, covering three fundamental components: insulators, electrodes, and semiconductors.

2.3.1 Stretchable insulators

Stretchable insulators are pivotal materials for the development of stretchable electronics, and have been employed as elastomeric substrates and encapsulation layers. The design of stretchable substrates must consider physical properties, such as toughness, stretchability, and thickness, to ensure operational stability under stress. Optical characteristics such as transparency should also be considered to enable effective light absorption and emission depending on the specific device type. Furthermore, because the construction of functional devices necessitates the vertical stacking of other layers, compatibility with these adjacent stretchable layers is crucial to maintain intimate interfaces during repeated mechanical deformation. Owing to these requirements, a wide range of stretchable insulators including polyurethane (PU), poly(styrene-butadiene-styrene) (SBS), poly(styrene-ethylene-butylene-styrene) (SEBS),[27] Ecoflex,[31] and PDMS have been widely applied. Jeong *et al*.[32] employed a bilayer polymer for encapsulating implantable optoelectronic devices. The inner layer, composed of PDMS and Parylene C, served as a waterproof barrier against biofluid penetration, whereas the outer layer, an ultrasoft silicone gel (Ecoflex GEL), functioned as a mechanical buffer. This approach achieves lightweight construction and thermomechanical compatibility, which cannot be achieved with traditional encapsulation materials such as metals and glass.

Stretchable insulators, such as PU and SEBS, are also widely employed as dielectric layers in stretchable OFETs and OPTs. However, the typically low dielectric constant (k) of these elastomeric insulators often compromises the electrical performance of the devices. Hence, the development of new dielectric elastomers with high dielectric constants (high-k) for use as gate dielectrics is imperative for fabricating high-performance stretchable OFETs and OPTs. Pei *et al*.[33,34] developed a polyurethane-*co*-poly(ethylene glycol) (PU-*co*-PEG) dielectric material that exhibited high stretchability (up to 50% strain) and high dielectric constant (up to 13 at 12 Hz). Field-effect transistors (FETs) employing PU-*co*-PEG as the gate dielectric demonstrated a high charge carrier mobility and low operating voltage. Our group[30,35] fabricated a hybrid polymer dielectric, SEBS/Carbon Quantum Dots (CQDs), modulated through van der Waals interactions. This material exhibited a remarkable tensile strain of 620% and large-area film uniformity (exceeding the size of an A4 sheet). Intrinsically stretchable organic field-effect transistors (ISOFETs) based on this hybrid film demonstrated a low operating voltage below 5 V. While balancing stretchability with a high dielectric constant, Bao *et al*.[36,37] developed a high-dielectric-constant self-healing elastomer (SHE), PDMS-$MPU_{0.6}$-$IU_{0.4}$, for use in stretchable polymer transistors, thereby endowing the devices with self-healing capability. When a transistor array was severed, it immediately showed complete disconnection of the circuit pathway. Over time, all transistors were capable of autonomous self-healing, with recovery efficiencies exceeding 77% in all cases. This demonstrates the potential of integrating stretchable and self-healing functionalities into more complex systems in the future.

2.3.2 Stretchable electrodes

Stretchable electrodes are vital components of stretchable devices. Materials such as metal nanoparticles, metal nanowires, liquid metals, carbon nanotubes (CNTs),[38] graphene, and conductive polymers are viable for stretchable electronics. Two primary strategies have been pursued to develop stretchable electrodes: one involves designing conductive materials into specific geometries, such as in-plane buckling[12,39–41] and nanomeshes;[42–44] the other focuses on embedding or attaching various conductive materials within or onto an elastic polymer substrate, effectively leveraging the high conductivity of metals and the intrinsic stretchability of elastomers.

Spherical nanoparticles have a percolation threshold (V_c) that is 10–100 times higher than that of high-aspect-ratio nanoscale components. Charge transport between spherical nanoparticles involves numerous nanoparticle-nanoparticle junctions, leading to high contact resistance and charge carrier scattering. Kotov *et al*.[45] fabricated highly conductive and stretchable polyurethane/gold nanoparticle (PU/NP) composites *via* both layer-by-layer (LBL) and vacuum-assisted flocculation (VAF) methods. Both composites achieved high conductivity with low-aspect-ratio nanoparticles. However, the strong strain sensitivity of percolation-governed conductivity remains a challenge for device miniaturization and cycling stability.[46]

High-aspect-ratio silver nanowires (AgNWs) have been widely adopted as stretchable electrodes.[47–50] They can be dispersed in solvents and deposited over large areas on flexible/stretchable substrates using simple techniques, such as spray coating. The direct deposition of AgNWs is challenging because of their high surface roughness and weak adhesion to substrates, which makes them susceptible to damage, cracking, or delamination when exposed to complex environmental conditions involving oxygen, moisture, or various mechanical stresses.[51] To enhance the potential of AgNWs-based stretchable transparent electrodes for flexible and stretchable electronics, research efforts have been dedicated to optimizing the relevant fabrication processes.[52–54] Yu *et al*.[55] proposed the concept of an interfacial percolation network (PN). The interfacial PN was composed of a 2D AgNWs PN and a protruding 3D AgNWs PN embedded on the sur-

https://doi.org/10.1007/s10118-026-3652-3

face and in the near-surface region of an elastic polymer matrix. The protruding PN comprised a poly(styrene-isobutylene-styrene) (SIBS) elastomer host with AgNWs and polypropylene-graft-maleic anhydride (PP-*g*-MAH) domains concentrated as fillers in the near-surface region of the matrix. The protrusion of the AgNWs enabled physical connection between the electrical conduction channels in the surface and bulk layers. The resulting electrode exhibited a high electrical conductivity of 13500 S·cm^{-1} and a stretchability of 660%, while the resistance change under strain was several orders of magnitude lower than that of 2D PN and conventional 2D+3D PN structures. Ye *et al*.[56] developed a highly stretchable and stable composite electrode, termed Strem-AT, by embedding AgNWs into a thermoplastic polyurethane (TPU) subsurface *via* a simple and rapid spray-transfer technique, forming an interpenetrating AgNWs/TPU conductive network. In this structure, the TPU matrix dissipates stress, mitigating the strain on the AgNWs during deformation. The resulting intrinsically stretchable organic photovoltaics (ISOPVs) achieved a power conversion efficiency (PCE) of over 12.5% and maintained 76% of its initial efficiency after 1000 cycles at 50% strain.

Two-dimensional materials such as graphene offer great promise for both conventional semiconductor applications and emerging fields such as flexible electronics. Lee *et al*.[57] demonstrated a highly efficient intrinsically stretchable OLED (ISOLED) that uses graphene-based 2D-contact stretchable electrodes (TCSEs). The TCSEs included a layer of graphene and graphene scrolls on top of the AgNWs networks embedded in the SEBS elastomer matrix. The graphene layer modified the work function, promoted charge spreading, and impeded the inward diffusion of oxygen and moisture, thereby achieving significant improvement in charge injection and environmental stability. Bao *et al*.[58] developed a transparent conductive graphene-based architecture for use as a stretchable electrode by creating graphene nanoscrolls, termed multilayer graphene/graphene scrolls (MGG), within stacked graphene layers. Under strain, these scrolls bridged the fragmented graphene domains to maintain the percolation network, thereby ensuring an excellent electrical conductivity. A three-layer MGG supported on an elastomer retained 65% of its original conductivity at 100% strain, whereas a typical single-layer graphene electrode completely lost its conductivity at 5% strain. A stretchable all-carbon transistor fabricated using MGG as the electrode exhibited over 90% transmittance and retained 60% of its initial current output when subjected to 120% strain applied parallel to the charge-transport direction.

Conductive polymers, particularly poly(3,4-ethylenedioxythiophene):poly(styrenesulfonate) (PEDOT:PSS), demonstrate considerable promise for practical applications. Numerous strategies have been proposed to enhance the electrical conductivity and stretchability of PEDOT:PSS thin films.[59] Bao *et al*.[60] employed ionic liquids (ILs) to improve the stretchability and conductivity of PEDOT:PSS. The ionic liquid additives disrupted the hydrogen bonding between PSS and PEDOT chains and facilitated the formation of PEDOT nanofibrils, leading to enhanced electrical conductivity. Someya *et al*.[61] achieved improved stretchability of PEDOT:PSS electrodes by incorporating the zwitterion 4-(3-ethyl-1-imidazolio)-1-butanesulfonate (ION E) additive. ION E modulated the crystalline structure of PEDOT:PSS and strengthened the interfacial adhesion between the PEDOT:PSS layer and PU substrate through enhanced hydrogen bonding, leading to a significant increase in the overall stretchability of the composite. Unlike small molecules, polymeric dopants can form physically cross-linked interpenetrating networks with PEDOT:PSS, resulting in a more stable plasticizing effect. Bao *et al*.[62] designed a cross-linkable supramolecular additive, TopoE, based on a polyrotaxane (PR) structure. The PR consists of a poly(ethylene glycol) (PEG) backbone and sliding cyclodextrins functionalized with PEG methacrylate (PEGMA) side chains. They systematically introduced PR into soft conductive membranes made of the conductive polymer PEDOT:PSS. The cyclodextrins could slide back and forth along the chains, thus preventing crystallization of PEG and providing better stretchability. The blended polymers could be photopatterned down to two-micrometer feature sizes and exhibited enhanced conductivity. Hu *et al*.[63] proposed a new plasticization strategy based on the non-covalent interaction between interpenetrated highly polar networks, termed as "mutual plasticization". Highly conductive and stretchable thin-film conductors were obtained through the side-chain engineering of a PR additive and the introduction of ILs as secondary dopants. The PR-IL-PEDOT:PSS thin film showed an electrical conductivity of up to 1603 S·cm^{-1} with negligible variation under 100% strain.

2.3.3 Stretchable optoelectronic functional layer

Conjugated polymer semiconductors are the key components of the active layers of organic optoelectronic devices. Their structures typically consist of rigid π-conjugated backbones and flexible alkyl side chains. Charge transport can occur along the backbone *via* intrachain pathways and between chains *via* π-π stacking.[4,64] However, because of the rigidity of the backbone, the elongation at break of conjugated polymers is typically less than 10%, posing significant challenges for stretchable applications. The realization of stretchability in polymer semiconductors generally follows two strategic approaches: one involves rational molecular-level design to modify the molecular weight[65,66] and chemical structure of the polymer, and the other involves the incorporation of additional components (such as insulating elastomers, plasticizer molecules, or cross-linkers) to form polymer composite films.

Molecular structure design. The properties of a material are determined by its molecular structure. The central challenge in designing molecules for intrinsically stretchable polymer semiconductors is to strike a balance between electrical performance and mechanical robustness. Long-range ordered crystalline domains are generally accepted to be essential for high charge carrier mobility, whereas partially disordered amorphous regions are required to confer mechanical deformability. Currently, the primary strategies for molecular design are backbone and side-chain engineering.

The most straightforward approach to reduce the crystallinity of conjugated polymers is to decrease the effective conjugation length of the polymer chains. This can be rationally achieved by incorporating flexible conjugation break spacers (CBSs) into the polymer backbone to disrupt the conjugation. While CBSs can disrupt interchain charge transport and reduce charge carrier mobility along the backbone, they simultaneously enhance the intrinsic stretchability and me-

https://doi.org/10.1007/s10118-026-3652-3

chanical durability of conjugated polymers. In recent years, various spacer units, including alkyl chains,[67,68] siloxanes, and other flexible linkers, have been employed to construct stretchable polymer semiconductors.

Bao *et al.*[69] systematically investigated CBSs (10 mol%) with different chain lengths and rigidities, including ethylene, dibutylbenzene (DBB), hexane (C6), and dodecane (C12), which were incorporated into the backbone of diketopyrrolopyrrole (DPP)-based polymer semiconductors (Fig. 3a). Compared to the fully conjugated DPP polymer, longer flexible CBSs led to a higher crack-onset strain (25%–100%) and a lower elastic modulus (1.3–0.13 GPa) (Fig. 3b), while the charge carrier mobility decreased by only 40%. Mobility values >1 $cm^2 \cdot V^{-1} \cdot s^{-1}$ were maintained for partially conjugated

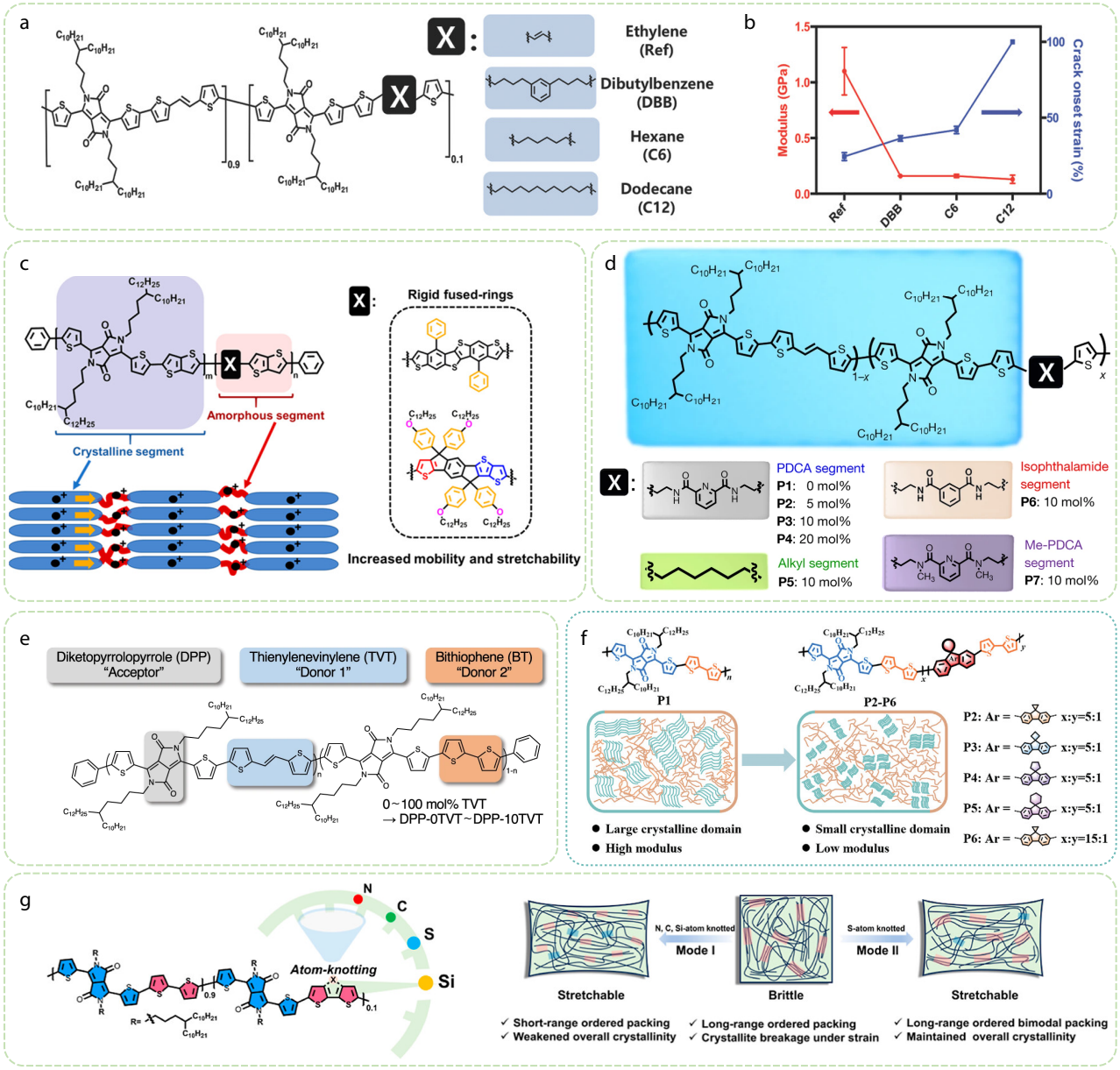

Fig. 3 (a) Chemical structures of DPP-based semiconducting polymers containing 10 mol% of conjugation breakers; (b) Elastic modulus (red, left) and crack onset strain (blue, right) of the polymer semiconductors. Elastic modulus and crack onset strain were measured by the film-on elastomer method (Reproduced with permission from Ref. [69]; Copyright (2018), WILEY-VCH Verlag GmbH & Co. KGaA, Weinheim). (c) Design of intrinsically stretchable semiconducting polymers (Reproduced with permission from Ref. [77]; Copyright (2021), American Chemical Society). (d) Chemical structures of polymers **P1** to **P7** (Reproduced with permission from Ref. [80]; Copyright (2016), Macmillan Publishers Limited, part of Springer Nature. All rights reserved). (e) Chemical structure of terpolymers used in this study. Based on the TVT unit fraction, terpolymers were named as DPP-0TVT (0 mol% TVT)–DPP-10TVT (100 mol% TVT) (Reproduced with permission from Ref. [11]; Copyright (2021), The Authors, published by Springer Nature). (f) Chemical structures of the terpolymers P2-P6 after incorporating the non-centrosymmetric spiro[cycloalkane-1,9′-fluorene] units into the backbone of the DPP-based conjugated polymer P1, and illustration of the microstructures of the terpolymers and P1 (Reproduced with permission from Ref. [82]; Copyright (2023), Wiley-VCH GmbH). (g) Schematic illustration of the proposed dual-mode stretchability enhancement mechanism (Reproduced with permission from Ref. [83]; Copyright (2024), American Chemical Society).

https://doi.org/10.1007/s10118-026-3652-3

polymer semiconductors at 0% strain. When a DPP polymer containing C12 alkyl non-conjugated units was used as the semiconductor layer in stretchable OFETs, the devices retained mobilities >0.36 $cm^2 \cdot V^{-1} \cdot s^{-1}$ even under 100% strain, and exhibited stable electrical performance after 100 stretching cycles at 50% strain. This demonstrates that a small fraction of conjugation breakers can effectively tune the mechanical properties of polymer semiconductors without significantly compromising their charge transport performance.

This strategy has predominantly been applied to stretchable p-type semiconducting polymers, with very few reports on n-type polymer semiconductors. In 2020, Gu *et al*.[70] first reported a series of naphthalene diimide (NDI)-based polymers incorporating alkyl CBSs of different lengths, denoted as PNDI-C_x (x=0, 3, 4, 5, 6, 7). For the first time, the Kuhn length (L_k) has been employed to quantitatively characterize the flexibility of polymer semiconductors. Small-angle neutron scattering (SANS) and oscillatory shear rheometry revealed a dramatic reduction in the Kuhn length from 52.1 nm for PNDI-C_0 to 3.6 nm for PNDI-C_6. The increased length of the alkyl CBSs led to a decreased elastic modulus and glass transition temperature (T_g), along with an increased crack-onset strain, notably reaching 400% for PNDI-C_4. This study underscores the critical role of backbone rigidity in designing stretchable conjugated polymers, although it did not explore the electrical properties of the polymers. Higashihara *et al*. conducted a systematic study. They successfully incorporated CBSs containing ester groups, amide groups, and ester-functionalized bulky branched chains into the backbone of NDI-based polymers to develop stretchable n-type semiconducting materials.[71,72] In 2023, they reported the design, synthesis, and application of OFETs of stretchable n-type semiconducting polymers featuring heteroatom-based CBSs.[73] The results indicated that polymers with thioether CBSs exhibited higher charge carrier mobility after both a single strain event and repeated stretch-release cycles than those containing polar ethylene oxide CBSs. This was primarily attributed to the fact that the highly polar ethylene oxide moieties can lead to severe aggregation and pronounced phase separation. Notably, density functional theory (DFT) calculations revealed a smaller bond angle for C—S—C (98.9°) than for C—O—C (113.3°), resulting in a more bent conformation along the polymer backbone, which provided a stronger capacity for strain energy dissipation between chain segments.

Although flexible CBSs can reduce the backbone rigidity of polymer semiconductors and enhance stretchability, maintaining a satisfactory electrical performance remains challenging. In recent years, researchers have introduced conjugated rigid fused-rings as replacements for flexible CBSs by incorporating them into the polymer backbone. These conjugated linkers maintain conjugation along the polymer backbone, facilitating efficient charge transport along the chain.[74–76] Bao *et al*.[77] incorporated conjugated rigid fused-ring structures with various bulky side chains, such as benzene-substituted dibenzothiopheno[6,5-*b*:6′,5′-*f*]thieno[3,2-*b*]thiophene (Ph-DBTTT) and indacenodithiophene (IDT), into the backbones of DPP-based polymer semiconductors (Fig. 3c). In the Ph-DBTTT system, the rigid fused-rings did not yield high charge transport properties because of the disruption of the molecular packing in the crystalline domains. In the PIDT system, the PIDT-3T-OC12-10% polymer, featuring an asymmetric IDT backbone and bulky alkoxy-functionalized side chains, exhibited enhanced stretchability while maintaining or even improving charge carrier mobility. Compared to the reference polymer PDPPTT, it demonstrated the highest hole mobility of (1.08±0.09) $cm^2 \cdot V^{-1} \cdot s^{-1}$. Moreover, ISOFETs based on PIDT-3T-OC12-10% retained a mobility of 0.27 $cm^2 \cdot V^{-1} \cdot s^{-1}$ even under 75% strain (parallel direction). Notably, after 500 stretching cycles, the devices maintained mobilities as high as 0.22 $cm^2 \cdot V^{-1} \cdot s^{-1}$ (parallel) and 0.38 $cm^2 \cdot V^{-1} \cdot s^{-1}$ (perpendicular), significantly outperforming the PDPPTT-based devices.

An alternative strategy involves incorporating dynamic non-covalent bonds (*e.g*., hydrogen bonds[78] and metal–ligand coordination units[79]) as non-covalent crosslinking sites in polymer semiconductors. This approach not only promotes the interchain packing order and enhances the charge carrier mobility but also provides an additional strain energy dissipation mechanism through the reversible breakage of these bonds, thereby improving stretchability. Bao *et al*.[80] incorporated a small fraction of 2,6-pyridinedicarboxamide (PDCA) groups as hydrogen-bonding units into the backbone of DPP-based conjugated polymers (Fig. 3d). They also introduced alkyl spacers to link the hydrogen-bonding units with conjugated segments in the polymer backbone, thereby enhancing the flexibility of the dynamic motifs. The hydrogen bonds could be readily broken under tensile strain and spontaneously reformed during recovery, leading to a reduction in the tensile modulus of the thin film from about 1 GPa to about 0.25 GPa and a significant increase in the crack-onset strain (COS) from 5%–10% to over 100%. Transistor devices based on P3 (10 mol%) exhibited charge carrier mobility of 1.3 $cm^2 \cdot V^{-1} \cdot s^{-1}$. This work represents the first demonstration of a high-mobility conjugated polymer capable of complete healing after mechanical damage achieved through a combination of solvent and thermal annealing. Furthermore, they systematically investigated the influence of flexibility and strength of hydrogen-bonding interactions on the mechanical and electronic properties of conjugated polymers. [81] The H-bonding strength with a self-association constant >0.7 and flexible linkers were desired for efficient strain energy dissipation and favorable charge transport, thereby preserving the electrical performance during stretching.

As discussed above, most strategies for enhancing the stretchability of polymer semiconductors inevitably compromise electrical performance. Random copolymerization is a simple yet effective approach to improve stretchability without sacrificing charge carrier mobility. Bao *et al*.[11] incorporated thienylenevinylene (TVT) and bithiophene (BT) units into a DPP-based conjugated polymer system (Fig. 3e) with molar percentages varying from 0% TVT (100% BT, DPP-0TVT) to 100% TVT (0% BT, DPP-10TVT). All resulting terpolymers exhibited mobilities greater than 1 $cm^2 \cdot V^{-1} \cdot s^{-1}$, while those containing 20%–80% TVT demonstrated significantly higher crack-onset strains (>100%) than their corresponding homopolymers. DPP-8TVT (80% TVT) maintained a stable mobility over 1000 stretching cycles at 25% strain. Notably, this strategy has also been successfully extended to the develop-

ment of intrinsically stretchable n-type polymer semiconductors using NDI-TVT-BT terpolymers.

Zhang *et al*.[82] reported terpolymers as intrinsically stretchable semiconducting polymers by incorporating non-centrosymmetric spiro[cycloalkane-1,9'-fluorene] (spiro-fluorene) units into the conjugated backbones (Fig. 3f). These terpolymers entailing DPP, bithiophene, and spiro-fluorene units in their backbones simultaneously exhibited good ductility and high charge mobility. The polymer series simultaneously maintained high charge mobilities (>1.0 $cm^2 \cdot V^{-1} \cdot s^{-1}$) even at 100% strain and after 500 repeated stretch-release cycles under 50% strain. The terpolymer P2, in which cyclopropane is linked to the spiro-fluorene unit, is among the best reported intrinsically stretchable polymer semiconductors with record mobility up to 3.1 $cm^2 \cdot V^{-1} \cdot s^{-1}$ at even 150% strain and 1.4 $cm^2 \cdot V^{-1} \cdot s^{-1}$ after repeated stretching and releasing cycles for 1000 times.

Structurally innovative molecular designs offer new avenues for developing intrinsically stretchable polymer semiconductors. Our group[84] proposed a molecular-scale geometric design strategy, *ortho*-isomerized (*o*,*o*-F, *o*-OMe, and *o*-OC8) and *meta*-isomerized (*m*,*m*-OC10C12) bithiophene-benzene units were incorporated into the regioregular backbone of poly[(2,5-bis(4-decyltetradecyl)-3,6-di(thiophen-2-yl)-2,5-dihydropyrrolo[3,4-*c*]pyrrole-1,4-dione)-*co*-(2,2′-dithiophen)] [P(DPP-BT)], with a series of synthesized zigzag-structured polymer semiconductors. Based on an appropriate modification ratio, molecular-scale structural design can endow polymer semiconductors with better mechanical and electrical properties with the assistance of heteroatom embedment and alkyl-chain attachment. Compared to the reference polymer P(DPP-BT), zigzag-structured *o*-OC8-5% yielded a high COS value of 110%, with the highest field-effect carrier mobility of up to 1.92 $cm^2 \cdot V^{-1} \cdot s^{-1}$. It could afford 1.43 and 1.37 $cm^2 \cdot V^{-1} \cdot s^{-1}$ under 100% strain with charge transport parallel and perpendicular to the stretching direction, respectively. In addition, even after undergoing cyclic stretching for over 1000 cycles under 25% strain, *o*-OC8-5% maintained above 1.10 $cm^2 \cdot V^{-1} \cdot s^{-1}$ along both stretching directions. Our group[83] has also proposed an atomic junction strategy. Based on the model-conjugated polymer P(DPP-BT), we appended bridging atoms of different sizes, including nitrogen (N), carbon (C), sulfur (S), and silicon (Si), onto adjacent β-C atoms in BT units, affording various bending angles (BAs) in the modified polymer chains to bend polymer conformations (Fig. 3g). In addition to undermining film crystallinity, bent chain conformations induced by atom knotting could also promote bimodal stacking for preserved crystallinity and direct stretchability enhancement. This strategy provides important molecular design guidelines for the design of high-mobility, intrinsically stretchable polymer semiconductors.

Side-chain engineering has also been used to develop intrinsically stretchable polymer semiconductors. Molecular design *via* side-chain engineering can effectively enhance the chain entanglement between polymers and construct cross-linked network structures.[7] Several novel side chains have been designed and developed to improve the stretchability of conjugated polymers, including but not limited to non-conjugated flexible side chains (alkyl chains,[85,86] carbosilane,[87,88] polyethylene glycol-type ether chains,[89,90] and poly(butyl acrylate)[91]), side chains containing dynamic hydrogen-bonding sites (urea,[92,93] amide,[94–97] urethane[98]), functional flexible side chains with cross-linking sites (siloxane[99]), and asymmetric/symmetric conjugated side chains.[100,101]

Gu *et al*.[86] designed four DPP-based donor-acceptor (D-A) polymers with increasing side chain lengths from 2-hexyl decyl (C2C6C8) to 2-octyl dodecyl (C2C8C10), 2-decyl tetradecyl (C2C10C12), and 2-dodecyl hexadecyl (C2C12C14) and systematically investigated the chain packing mechanism and structure-morphology-electrical property relationships (Fig. 4a).

Bao *et al*.[96] conducted a detailed study on the influence of the location (side chain and main chain) of the PDCA unit in DPP-based polymers on the number of hydrogen bonds and the consequent effect on crystallinity (Fig. 4b). They found that polymers with PDCA units along the main chain had a limited number of hydrogen bonding sites. In contrast, PDCA incorporated into the side chains readily facilitated nearly quantitative formation of intermolecular hydrogen bonds, even at a low unit content (<10 mol%). Increasing the amount of PDCA on the side chains did not compromise the polymer solubility or charge carrier mobility, even though the films were cross-linked via hydrogen bonding. Similarly, Wu *et al*.[98] synthesized four DPP-based copolymers incorporating urethane-containing side chains ($PDPP_{urethane}$-TT, $PDPP_{urethane}$-BT, and $PDPP_{urethane}$-TVT) (Fig. 4c). The urethane-containing side chains serve as dynamic bonding motifs, facilitating stress dissipation within the polymer film during mechanical deformation. This approach not only preserved the initial electrical characteristics of the film but also maintained the molecular orientation under strain. Specifically, the $PDPP_{urethane}$-TVT film retained its electrical and molecular packing properties, even when subjected to strains of up to 100%. The hydrogen bonds between the urethane groups can re-form after mechanical deformation, endowing the copolymers with self-healing properties.

Bao *et al*.[100] incorporated four types of bulky side groups—naphthalene (NaPh), biphenyl (PhPh), thienylphenyl (ThPh), and alkylphenyl (C4Ph)—into DPP-based polymers in an asymmetric fashion (Fig. 4d). The bulky side groups in this design strategy play particularly important roles: reducing the strong aggregation tendency of fused-ring building blocks, decreasing the crystallinity of the polymer semiconductor films, and providing additional strain energy dissipation pathways, such as conformational change and chain re-orientation in the amorphous regions during stretching. The polymer PDPP-C4Ph with alkylbenzene showed increased mobilities (about 1 $cm^2 \cdot V^{-1} \cdot s^{-1}$), and was attributed to its larger crystal coherence length, the devices were observed to retain their mobilities as high as about 0.1 $cm^2 \cdot V^{-1} \cdot s^{-1}$ (parallel direction) and about 0.3 $cm^2 \cdot V^{-1} \cdot s^{-1}$ (perpendicular direction) even after 500 cycles (25% strain).

Reported intrinsically stretchable n-type polymer semiconductors are scarce, and most suffer from poor electron mobility at high stretching strains. Qiu *et al*.[102] designed and synthesized a series of PBIBDF polymers with different side chains, including alkyl and hybrid siloxane-based chains (de-

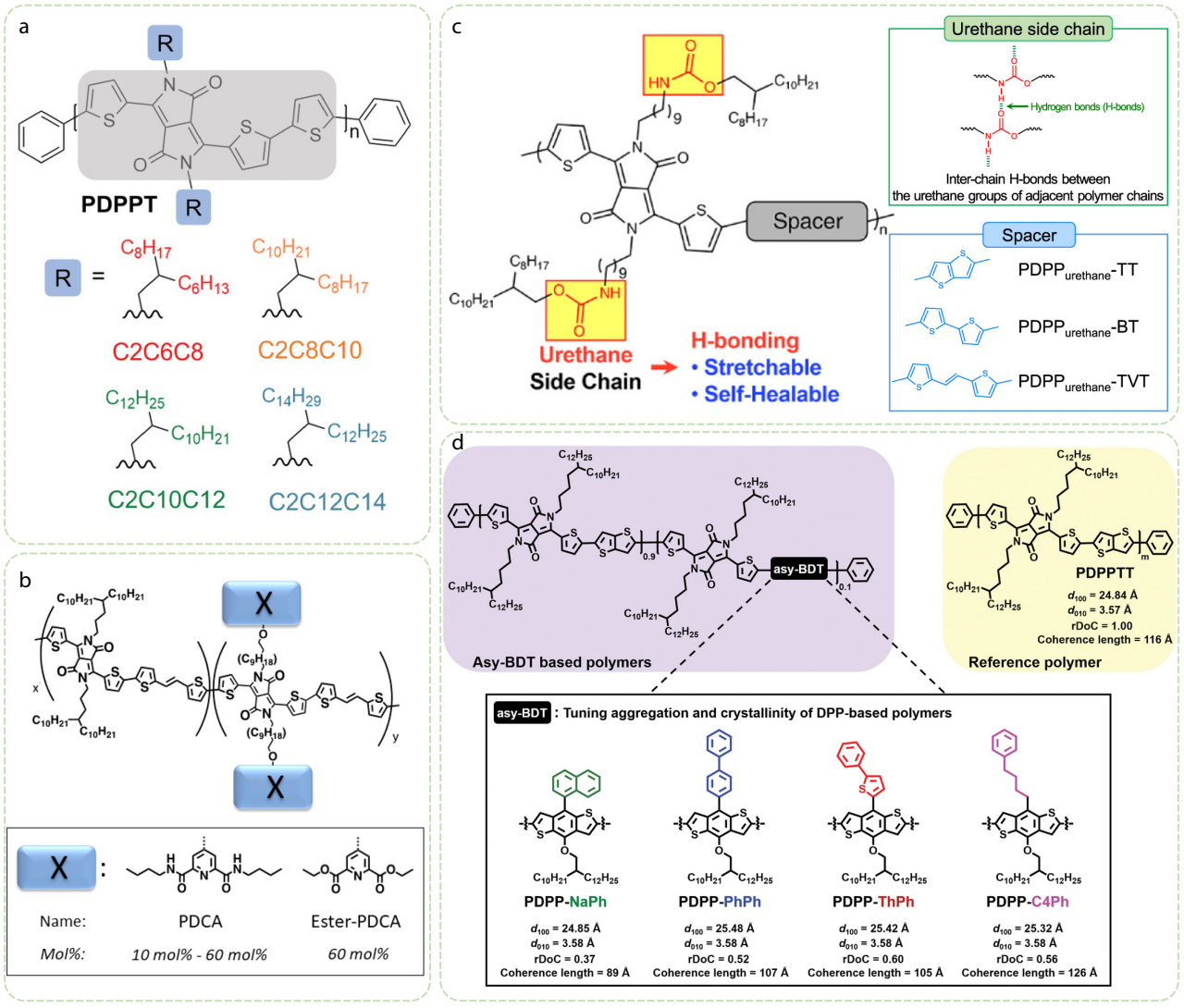

Fig. 4 (a) Schematics of PDPPT polymers with different side-chain structures (Reproduced with permission from Ref. [86]; Copyright (2021), Wiley-VCH GmbH). (b) The chemical structure of the DPP-based polymers and their respective H-bonding groups PDCA units (Reproduced with permission from Ref. [96]; Copyright (2019), American Chemical Society). (c) Molecular structures of $PDPP_{urethane}$ copolymers (Reproduced with permission from Ref. [98], Copyright (2020), American Chemical Society). (d) The chemical structure of the asymmetric benzodithiophene (asy-BDT) based polymers used in this study and the reference polymer PDPPTT (Reproduced with permission from Ref. [100]; Copyright (2022), Wiley-VCH GmbH).

noted as C-PBIBDF, CC-PBIBDF, Si-PBIBDF, and CSi-PBIBDF), to investigate the influence of the side-chain density and type on the macroscopic film morphology and microscopic molecular stacking of the polymers. Replacing the branched alkyl side chains with linear hybrid siloxane-based chains increased the side-chain density, which substantially reduced the film crystallinity and enhanced the flexibility of the polymer chains. The CSi-PBIBDF polymer exhibited significantly improved mechanical properties while retaining high electron transport performance. Due to the stretch-induced alignment of the polymer chains, the CSi-PBIBDF film under 100% strain parallel to the stretching direction demonstrated a higher electron mobility of 0.21 $cm^2 \cdot V^{-1} \cdot s^{-1}$ compared to its unstretched state.

In summary, molecular structure design is an effective strategy for achieving both a high charge carrier mobility and intrinsic stretchability in polymer semiconductors. Although this approach has been extensively and successfully applied to the development of p-type polymer semiconductors, the advancement of intrinsically stretchable, high-performance n-type counterparts faces considerable challenges, primarily because of the paucity of strongly electron-deficient building blocks. [103] Nevertheless, progress in this domain is expected to accelerate the development of wearable and implantable electronic devices.

Composite strategy. Molecular structural design offers notable advantages in terms of structural homogeneity, tunable performance, and long-term stability. However, their synthetic complexity, challenges in balancing multiple properties, and limitations in general applicability have motivated researchers to explore more flexible and readily adjustable complementary pathways. Composite strategies not only sig-

nificantly lower processing barriers and enhance compatibility with existing techniques but also readily enable the introduction of various fillers to achieve multifunctionality. Blending conjugated polymers with other additives such as elastomers, crosslinkers, or plasticizing molecules constitutes an effective strategy for improving elasticity without altering the chemical structure of the conjugated polymer. The additive molecules form multilayered or highly networked fibrous architectures, which grant the conjugated polymer backbones greater freedom of dynamic motion, effectively reduce the modulus of the resulting thin films, and significantly enhance the stretchability.

The potential of elastomer blending has been demonstrated in the development of stretchable conductive composites.[21,104,105] In 2015, Jeong *et al*.[106] reported the first stretchable semiconducting composite based on P3HT/SEBS (Fig. 5a). The P3HT nanofibrils in the solution were phase-separated from the air surface of the rubber matrix during spin-coating and formed a network of bundles by side-to-side self-assembly. The networks of bundles and indentations were the most important factors for producing high stretchability. The transistors made of the active channel layer showed a high stretchability of up to $\varepsilon \approx 0.5$, during repeated cycles of stretching, as well as excellent air stability and a stable threshold voltage near zero.

In 2017, Bao *et al*.[107] introduced the concept of polymer nanoconfinement, which was shown to enhance the stretchability of polymer semiconductors without compromising the charge carrier mobility. The DPP-DTT/SEBS blend film (CONPHINE-1 film, 70 wt% SEBS), fabricated *via* the phase-separation-induced elasticity method for conjugated polymer/elastomer systems (CONPHINE) (Fig. 5b), exhibited no visible cracks even under 100% tensile strain and demonstrated a high hole mobility of 1.32 $cm^2 \cdot V^{-1} \cdot s^{-1}$. The nanoconfinement effect resulting from phase separation reduces large crystal domains while maintaining a highly aggregated structure, thereby providing both high stretchability and efficient charge transport. ISOFETs based on the CONPHINE-1 film exhibited typical field-effect characteristics, with an average mobility of 0.59 $cm^2 \cdot V^{-1} \cdot s^{-1}$. Building on this, they introduced a solution-shearing method utilizing a patterned microgroove-coated blade.[108] By synergistically combining this technique with the nanoconfinement effect, macroscale alignment of the conjugated polymer nanostructures along the charge-transport direction was achieved. The nanoconfined spatial environment modulated the polymer chain conformation and promoted short-range π-π ordering, which substantially reduced the energetic disorder and, thus, the activation barrier for charge carrier transport. Consequently, the mobility of the stretchable conjugated polymer film was en-

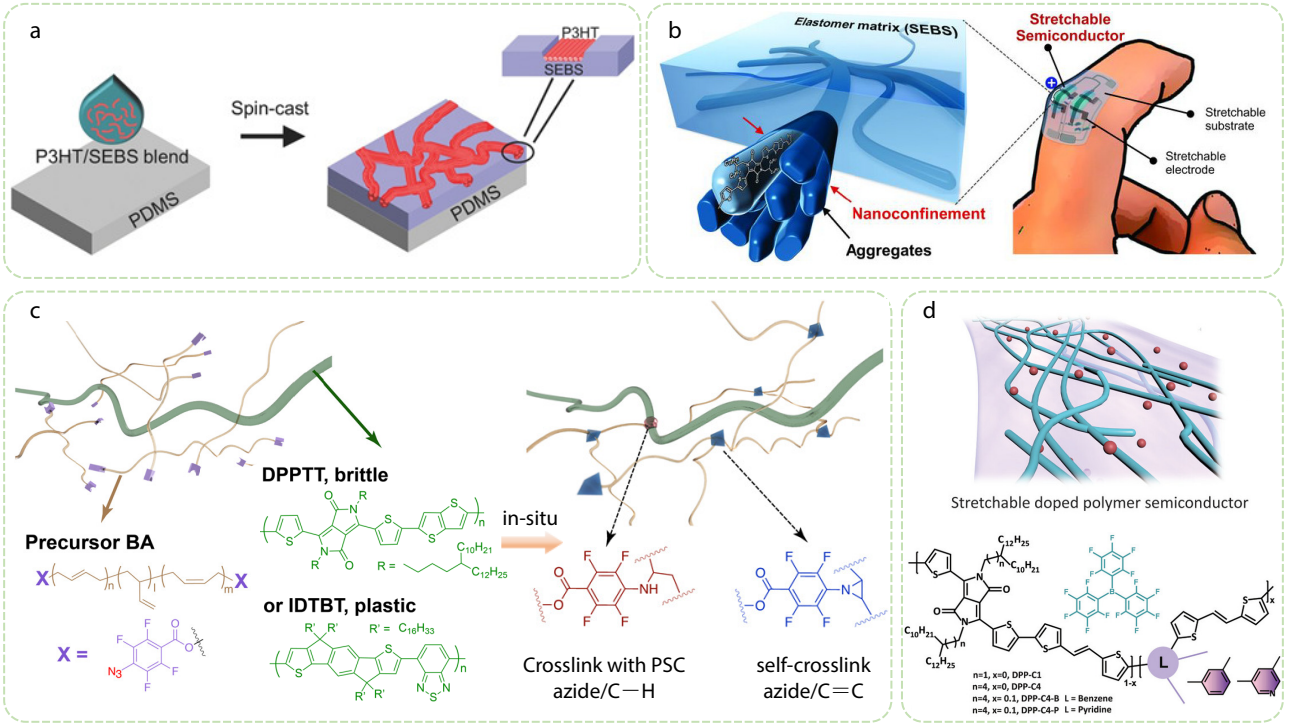

Fig. 5 (a) Schematic illustration of coating polymer blend solutions of P3HT and SEBS. P3HT nanofibrils were phase separated onto the top surface of the SEBS rubber matrix (Reproduced with permission from Ref. [106]; Copyright (2015), WILEY-VCH Verlag GmbH & Co. KGaA, Weinheim). (b) A 3D schematic of the desired morphology composed of embedded nanoscale networks of polymer semiconductor to achieve high stretchability, which can be used to construct a highly stretchable and wearable TFT (Reproduced with permission from Ref. [107]; Copyright (2017), The American Association for the Advancement of Science). (c) For semiconductors, DPPTT network is covalently embedded into the *in situ* formed elastic rubber matrix generated by iRUM precursor BA. In iRUM-s, the number of covalent crosslinking sites created through azide/C=C cycloaddition is much higher than that created through azide/C—H insertion (Reproduced with permission from Ref. [110]; Copyright (2021), The Authors, published by Springer Nature). (d) Schematic illustration of doped stretchable polymer semiconductor and chemical structures of the four conjugated polymers and the BCF (Reproduced with permission from Ref. [111]; Copyright (2024), Wiley-VCH GmbH).

https://doi.org/10.1007/s10118-026-3652-3

hanced threefold and remained stable under strains of up to 100%, providing a foundation for large-area fabrication of high-performance polymer films. Furthermore, the molecular weights of both the conjugated polymer and SEBS elastomer significantly influenced the morphology, mechanical properties, and electrical performance.[109] A higher molecular weight of the polymer semiconductor promotes a greater degree of polymer aggregation, which beneficially impacts charge transport. Conversely, the molecular weight of the elastomer could be precisely tuned to simultaneously optimize the mechanical robustness and electrical characteristics of the hybrid film.

Physical blending strategies lack covalent crosslinking sites and often exhibit uncertain long-term mechanical stabilities. Bao *et al*.[110] developed a covalently-embedded *in situ* rubber matrix (iRUM) by thoroughly mixing iRUM precursors with electronic polymer materials. The composite film morphology was precisely controlled by exploiting the differential reactivity of the azide groups with C—H versus C=C bonds (Fig. 5c). The high covalent crosslinking density provides both exceptional elasticity and strong solvent resistance. When applied to stretchable transistors, the iRUM-semiconductor film retained its mobility after being stretched to 100% strain. Furthermore, it exhibited a record-high mobility retention of 1 $cm^2 \cdot V^{-1} \cdot s^{-1}$ after 1000 stretching-releasing cycles at 50% strain. The cycling life was stably extended to 5000 cycles, which is five times longer than that of previously reported semiconductors.

Small molecular additives have been used to enhance the mechanical properties of conjugated polymers, such as cycloparaphenylenes (CPPs),[112] 2,3,5,6-tetrafluoro-7,7,8,8-tetracyanoquinodimethane (F4-TCNQ),[113] and dioctyl phthalate (DOP).[114] Shih *et al*.[111] proposed an innovative strategy that employed tris(pentafluorophenyl)borane (BCF) as a Lewis acid dopant (Fig. 5d) to enhance the charge-carrier mobility and modulate the crystallization behavior, thereby improving the stretchability of polymer semiconductors. The doping mechanism of BCF relies on the interaction between the boron atom and the nitrogen or sulfur atoms within the conjugated polymer backbone. By tailoring the side-chain length and backbone structure of the polymer, sufficient free volume was provided to effectively accommodate the dopant molecules, leading to enhanced doping efficiency. With the addition of a small amount of BCF, DPP-C4-B (0.1 wt% BCF) maintained a relatively high initial mobility of 0.91 $cm^2 \cdot V^{-1} \cdot s^{-1}$, retained a mobility of about 0.81 $cm^2 \cdot V^{-1} \cdot s^{-1}$ perpendicular to the stretching direction even at 100% strain, and exhibited stable mobility retention over 1000 repeated stretching cycles at 30% strain.

3 INTRINSICALLY STRETCHABLE ORGANIC OPTOELECTRONIC DEVICES

Based on the aforementioned material strategies, a variety of high-performance stretchable functional materials have been developed in recent years and successfully applied in the fabrication of various intrinsically stretchable organic photoelectronic devices. Representative devices include photodiodes, phototransistors, organic photovoltaics, organic light-emitting diodes, and organic light-emitting electrochemical cells. This section summarizes recent progress in these types of devices.

3.1 Organic Photodiodes

Intrinsically stretchable and skin-conformable photodiodes (PDs) are crucial for enabling next-generation wearable electronics in applications such as optical biometric monitoring and biomedical imaging. Despite recent progress in the development of elastomeric semiconductors, intrinsically stretchable organic photodiodes (ISOPDs) featuring elastomeric bulk heterojunction (e-BHJ) photoactive layers that exhibit low electronic noise are still in their early stages. In 2021, Kippelen *et al*.[41] reported a skin-like e-BHJ composed of an elastomer SEBS blended with the donor polymer P3HT and the acceptor indene-C60 bisadduct (ICBA), which demonstrated a tensile modulus of 2.4 MPa and a fracture strain of 189%. The elastomeric OPDs (e-OPDs) based on pre-strained PEDOT:PSS and eutectic gallium-indium (EGaIn) electrodes exhibited noise-equivalent power (NEP) values in the tens of picowatts range and detectivity (D^*) values of approximately 10^{10} Jones at 653 nm, with these performance metrics retained up to at least 60% strain. The significant performance degradation beyond 60% strain was attributed to the failure of the 30% pre-strained PDMS/PEDOT:PSS electrode rather than the e-BHJ layer itself.

To address this challenge, Yun *et al*.[115] developed conductive polymers with tunable work functions and excellent performance, demonstrating an all-polymer-based intrinsically stretchable polymer photodiode (ISPPD). A stretchable cathode (c-PEDOT:PSS) was realized by coating a polyethyleneimine ethoxylated (PEIE) layer onto modified PEDOT:PSS (m-PEDOT:PSS), while a stretchable anode (a-PEDOT:PSS) was developed by blending a fluorinated ionomer (FI) with m-PEDOT:PSS. The mechanical stability and D^* of the ISPPD were enhanced using a mechanically robust elastomeric photoactive layer (PTB7-Th/N2200/SEBS) and conductive polymer-based stretchable transparent electrodes with modulated work functions. Consequently, the ISPPD exhibited high D^*>10^{13} Jones under a large deformation of 100% strain, and could be effectively used for measuring a photoplethysmography (PPG) signal with a high signal-to-noise ratio (SNR) >20 dB at the inner wrist, where a strain of approximately 33% occurs.

Our group[116] reported a spatially modularizable-assembled elastic (SMAE) photoactive film for ISOPDs, exhibiting a photoresponse in the visible to near-infrared (NIR) range based on a scalable solution-processed strategy, demonstrating the feasibility of scalable encrypted imaging and real-time signal detection (Fig. 6a). The stretchable photoactive layer, composed of the polymer donor PM6, small-molecule acceptor Y6, and SEBS elastomer, exhibited a relatively uniform spatial distribution and ideal packing, which facilitated the generation and transport of the photogenerated charge carriers. The resulting NIR-ISOPDs achieved an ultralow detection limit of 1.82 $nW \cdot cm^{-2}$, a broad dynamic range of about 108 dB, and an excellent specific detectivity (D^*_{noise}) over 10^{12} Jones at 850 nm (one of the best performance among the previously reported stretchable NIR OPDs). Furthermore, record-high mechanical deformation (up to 100% strain) and durability (>1000 stretching cycles at 40% strain) were achieved simultaneously in our NIR-ISOPDs.

https://doi.org/10.1007/s10118-026-3652-3

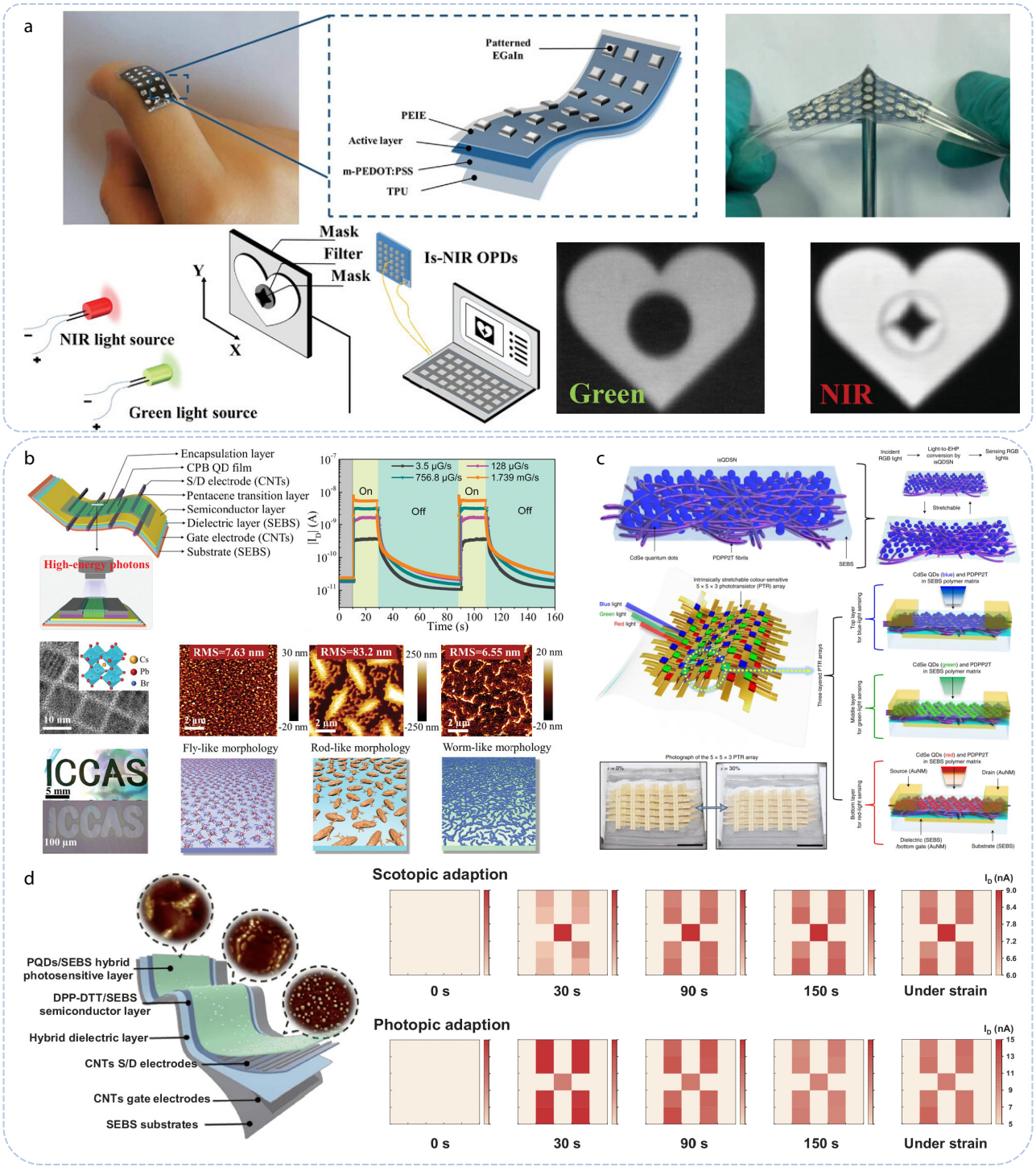

Fig. 6 (a) Device structure of NIR-ISOPDs. ISOPDs under large deformation. Schematic diagram of the single-pixel scanning imaging. Imaging results under green light and NIR light at initial state (Reproduced with permission from Ref. [116]; Copyright (2024), Wiley-VCH GmbH). (b) Schematic illustration of ISTPTs with a worm-like CPB QD film as the photosensitizer. Device response to X-ray pulse upon switching X-ray source on and off under various dose rates (Reproduced with permission from Ref. [119]; Copyright (2021), Wiley-VCH GmbH). (c) Schematic of the isQDSN, which consists of QDs and semiconducting polymer fibrils (PDPP2T) in the SEBS elastomer matrix. Schematic showing the intrinsically stretchable phototransistor array using isQDSN as a photoabsorption layer (Reproduced with permission from Ref. [120]; Copyright (2022), The Authors, under exclusive licence to Springer Nature Ltd.). (d) Schematic of the ISNVaT based on elastic heterojunction. Resulting current mapping of the 5 × 5 ISNVaT array at different time (0, 30, 90, 150 and 150 s under 50% stretching strain) and under different conditions to simulate scotopic and photopic adaptation (Reproduced with permission from Ref. [35]; Copyright (2024), The Authors, published by Springer Nature).

https://doi.org/10.1007/s10118-026-3652-3

The stretchability of the composite photoactive layer is typically enabled by an elastic polymer matrix.[117] Recently, Shih *et al*.[118] employed isomeric linkers (DTL) with tunable dipole moments to tailor the microstructure of PDPP polymers and applied them to ISOPDs. PDPP-(2,4)-DTL exhibited a microstructure characterized by reduced long-range crystallinity and enhanced short-range aggregation, demonstrating a COS of approximately 120% and significantly higher hole mobility of approximately 1.6 $cm^2 \cdot V^{-1} \cdot s^{-1}$. The photoactive layer for the ISOPDs consisted of an intrinsically stretchable polymer donor, PDPP-(2,4)-DTL, and the small-molecule acceptor, Y6. Although small-molecule acceptors generally compromise film stretchability, the PDPP-(2,4)-DTL:Y6 blend still achieved a high COS of 100%. The resulting device exhibited a higher external quantum efficiency (EQE) and detectivity relative to the control, maintained a D^* above 10^{11} Jones under 80% strain, and retained a stable photoresponse after hundreds of stretching cycles.

3.2 Organic Phototransistors

OPTs are a class of light-sensitive organic field-effect transistors that integrate the light-detection capability of a photodiode with the signal amplification function of the transistor. A primary challenge in fabricating stretchable OPTs is the development of stretchable active layers that are light-responsive. The exceptional photoresponsive characteristics of quantum dots (QDs) make them an effective strategy for designing composite materials or heterojunctions. In 2021, our group[119] developed a stretchable photosensitive heterojunction composed of a worm-like inorganic perovskite quantum dot (PQDs) film and a hybrid polymer semiconductor (PDPPTT/SEBS). Specifically, a surface-energy-induced self-assembly method was employed to fabricate easily transferable PQDs films with diverse morphologies, ranging from rod-like to worm-like (Fig. 6b). By laminating this film on top of the hybrid polymer semiconductor, the first intrinsically stretchable X-ray phototransistor was realized. The phototransistors could withstand high tensile strains of up to 100% and severe mechanical deformation with negligible degradation in the photoresponsive performance. For X-ray detection, they exhibited high sensitivity (>2×10^9 $\mu C \cdot Gy^{-1} \cdot cm^{-3}$), a fast response speed (<0.1 s), and a low detection limit (about 79 $nGy \cdot s^{-1}$, significantly below the dose rate for a typical chest X-ray of about 45 $\mu Gy \cdot s^{-1}$). For ultraviolet (UV) light detection, the devices demonstrated high light-current/dark-current (I_{light}/I_{dark}) ratio (5×10^6), photoresponsivity (2600 $A \cdot W^{-1}$), detectivity (5.5×10^{14} Jones), and EQE (10 250%).

Similarly, Son *et al*.[120] reported an intrinsically stretchable multispectral multiplexed phototransistor array. Its color-sensitive and shape-tunable characteristics were realized using an intrinsically stretchable quantum-dot semiconductor nanocomposite (isQDSN) comprising an organic semiconducting polymer (PDPP2T-TT-OD), size-tunable quantum dots (R, G, or B QDs), and an SEBS elastomer matrix. Separately fabricated R, G, and B phototransistor arrays were stacked into a multiplexed phototransistor array (a 5 × 5 × 3 array: a 5 × 5 R-sensitive array at the bottom, a 5 × 5 G-sensitive array in the middle, and a 5 × 5 B-sensitive array on the top) using a transfer technique (Fig. 6c). The photoresponse of the R, G, and B phototransistors to periodic on/off light illumination showed minimal variation before and after applying a 30% strain perpendicular to the channel direction. The device also endured 1000 stretching cycles at a strain of 30%. A photoresponsivity of about 0.013 $mA \cdot W^{-1}$ and photodetectivity of about 3.8×10^6 Jones were obtained from the green phototransistor under 30% strain when illuminated with green light. Oh *et al*.[121] reported an intrinsically stretchable OPT (ISOPT) based on a hybrid multilayer semiconductor film (PSC/QDs/PSC), achieving a broad spectral sensitivity from NIR to visible range. A blend of SEBS and DPPT-TT was used as the top and bottom polymer semiconductor (PSC) layers, with the middle layer consisting of a CdSe/ZnS quantum dot film. Under illumination at different wavelengths, the phototransistor exhibited distinct photoresponse characteristics, benefiting from the efficient separation of photogenerated carriers. The device maintained its performance even under a 50% strain and endured 10,000 stretching cycles. Notably, a phototransistor array patterned with a unique dodecagonal source/drain (S/D) electrode layout remained responsive to both NIR and visible-light stimuli even when subjected to a substantial in-plane strain of up to 38%.

Our group[122] demonstrated an ISOPT based on a stretchable n-type hybrid polymer semiconductor, and implemented X-ray imaging. The similar surface energies of the polymer semiconductor FIID-CF3TVT and elastomer SEBS ensured the formation of uniform microphase separation and a spatially nanoconfined morphology within the hybrid system. The off-center spin-coating (OCSC) method significantly enhances electron transport efficiency. The optimized stretchable hybrid polymer semiconductor exhibited ultrahigh photosensitivity of 1.52×10^4 $\mu C \cdot Gy_{air}^{-1} \cdot cm^{-2}$, an ultralow detection limit of 37.7 $nGy_{air} \cdot s^{-1}$, and excellent mechanical stability, enduring 1000 stretching cycles at 25% strain. Notably, even at a low dose rate of 3.65 $\mu Gy_{air} \cdot s^{-1}$, the polymer film successfully achieved clear X-ray imaging of a hexagonal nut. Furthermore, we developed a universal detachable interface technique that allows the uniform, damage-free, and reproducible integration of micropatterned stretchable electrodes for pixel-dense intrinsically stretchable organic transistor arrays.[123] Benefiting from the ideal heterocontact and short channel length (2 μm) in our transistors, a switching current ratio exceeding 10^6, a device density of 4.1×10^4 transistors$\cdot cm^{-2}$, an operational voltage down to 5 V, and excellent stability were simultaneously achieved. The resulting stretchable transistor-based image sensors exhibited ultrasensitive X-ray detection and high-resolution imaging capabilities.

Introducing controllable defects into charge-carrier transport channels/interfaces enables adaptive and synaptic functionalities in phototransistors. Our group[35] reported an intrinsically stretchable neuromorphic vision-adaptive transistor (ISNVaT) based on defect-tunable viscoelastic perovskite films (Fig. 6d). In this architecture, perovskite quantum dots are microspherically distributed within an elastomer matrix *via* a surface-energy-induced strategy, resulting in a strain-insensitive quasi-continuous microsphere (QCM) morphology. These viscoelastic perovskite films not only ensured intrinsic stretchability and retained broadband photosensitivity from the near-infrared to the visible and ultraviolet regions, but also provided tunable charge-trapping defects that effec-

tively guided photoadaptation and synaptic behaviors. By constructing a layered heterojunction using a QCM perovskite film and an elastic semiconductor layer, the resulting device exhibited trichromatic photoadaptation and high biaxial stretchability (up to 100%). The ISNVaT successfully emulated the visual adaptation functions of the human eye, including the active processes of natural photopic and scotopic adaptation, with an ultralow energy consumption of 15 aJ and a record-high paired-pulse facilitation (PPF) index of 270%. Furthermore, a fast adaptation speed (<150 s) was realized, which was able to realize adaptive imaging beyond the human eyes (3–30 min) (Fig. 6d), which was expected to reproduce the visual perception-adaptation-imaging loop for advanced intelligent neuromorphic electronics. thereby paving the way for the next-generation skin-like artificial intelligence systems.

3.3 Organic Photovoltaics

The active layers in OPVs consist of blended donor and acceptor materials. Enhancing the stretchability of the binary active layer system through material design has proven to be an effective approach, involving modifications to both conjugated polymer donors[124–127] and small-molecule acceptors (SMAs). Conventional SMAs, characterized by rigid structures comprising fused-rings, typically exhibit brittleness (ultimate strain ε_u<5%).[128] This inherent rigidity often results in the poor mechanical stretchability of the active layer, leading to a rapid decline in the initial PCE under strain. Significant research efforts have recently been dedicated to the development of polymerized small-molecule acceptors (PSMAs).[129,130] Recently, a functionalization strategy for SMAs was reported. Shao *et al.*[128] designed a new SMA named BTP-Si4, which exhibits a "plasticizing" effect (Fig. 7a). This material can infiltrate the amorphous regions of the polymer donor, effectively reducing the overall crystallinity of the photoactive film by increasing the free volume of the polymer chains. Under external stress, polymer chains can slide and reorient, thereby substantially enhancing the mechanical stretchability of the film. Stretchable OPVs fabricated from the blend film of this SMA and the polymer donor PNTB6-Cl achieved a PCE of 14.6% along with robust mechanical properties, retaining 82% of their initial PCE even under a substantial tensile strain of 80%.

Incorporating a third component into binary systems, characterized by high efficiency but poor stretchability, has emerged as a highly versatile strategy for enhancing the stretchability of the active layer. This approach includes the addition of a third donor,[124,131] an acceptor,[132] or highly elastic polymers.[133] Hao *et al.*[134] introduced the concept of effective elastomer density (De) as a unified molecular descriptor to quantitatively evaluate the effect of elastomer structures on ISOPVs morphology and functionality. It was demonstrated that increasing De enhances stretchability by inducing domain coarsening and surface roughening in amorphous regions, but simultaneously prolongs exciton lifetimes and suppresses charge extraction and transport. Notably, ISOPVs achieved an optimal balance at a critical De of 1.5 mol·m^{-3}, delivering a high initial PCE of 14.3% and retaining 80% of the initial PCE at a strain of 30.6%. This descriptor-based framework provides predictive and generalizable guidelines for the molecular design of elastomers in stretchable optoelectronic devices. Ye *et al.*[135] proposed a general toughening strategy based on styrene-ethylene-ethylene-propylene-styrene block copolymer (SEEPS). By defining a toughening parameter η derived from dynamic mechanical analysis, the authors established a quantitative correlation between elastomer and acceptor compatibility and mechanical enhancement capability. The resulting ISOPVs based on D18:L8-BO achieved an efficiency of 16.7%, retained 80% of their initial PCE under 52% strain, and maintained approximately 80% of their initial performance after 500 stretch-

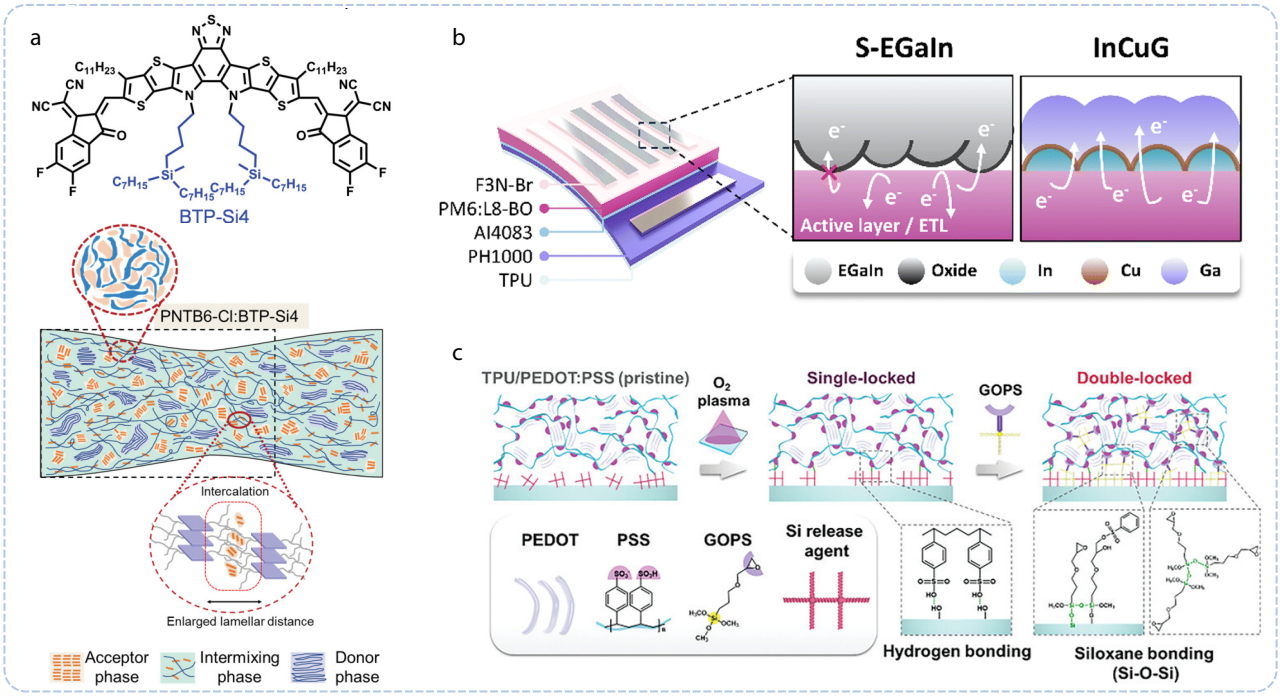

https://doi.org/10.1007/s10118-026-3652-3

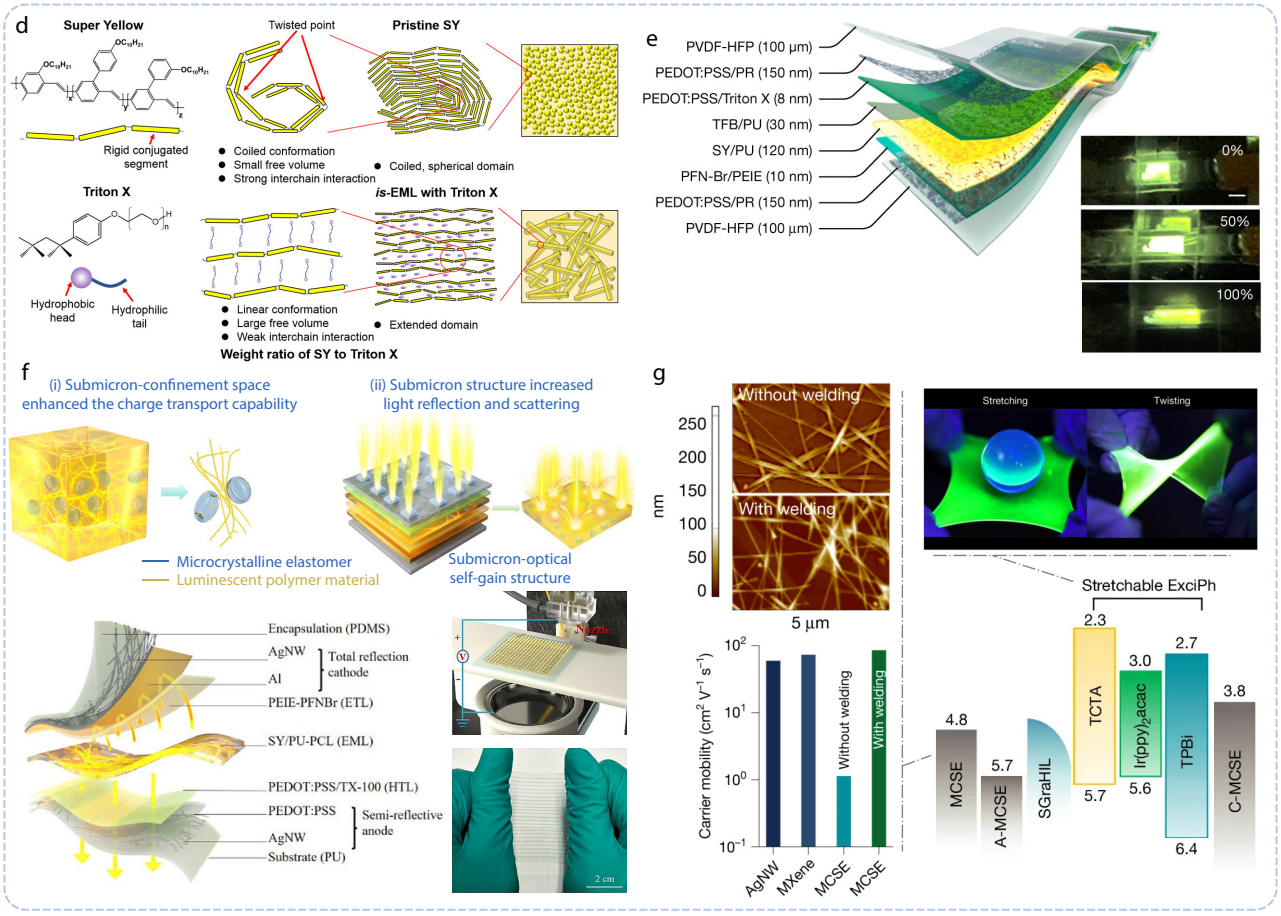

Fig. 7 (a) Molecular structures of acceptor BTP-Si4. Schematic illustration of the morphology of blend films (Reproduced with permission from Ref. [128]; Copyright (2025), The American Association for the Advancement of Science). (b) Schematic illustration of IS-OSCs utilizing two liquid metal deposition techniques (Reproduced with permission from Ref. [136]; Copyright (2024), The Royal Society of Chemistry). (c) Schematic diagram of single-locked and double-locked process (Reproduced with permission from Ref. [138]; Copyright (2023) Wiley-VCH GmbH). (d) Schematics comparing the microstructures of pristine Super Yellow (SY) and is-EMLs (Reproduced with permission from Ref. [139]; Copyright (2021), The American Association for the Advancement of Science). (e) Device structure of the intrinsically stretchable APLED. Photographs of a stretchable yellow-light APLED with increased strain at 9 V. The scale bar is 2 mm (Reproduced with permission from Ref. [140]; Copyright (2022), The Authors, under exclusive license to Springer Nature Ltd.). (f) 3D Simulation of aggregated morphology for SY combined with PU-PCL. Large-area stretchable electrodes and PLED arrays (Reproduced with permission from Ref. [141]; Copyright (2025), Wiley-VCH GmbH). (g) Atomic force microscopy topography images of AgNW before and after welding using MXene solution, carrier mobility of electrodes. Photographs of the biaxially stretched and twisted ExciPh films. Energy-level alignment of the fully stretchable OLEDs (Reproduced with permission from Ref. [142]; Copyright (2026), The Authors, under exclusive license to Springer Nature Ltd.).

release cycles under 40% strain. This strategy demonstrated excellent universality in both polymer small-molecule and all-small-molecule systems, offering a new pathway toward stretchable OPVs with both high efficiency and robust mechanical stability.

For stretchable electrodes, Lee *et al.*[136] developed an InMiG electrode with a metal interlayer via physical vapor deposition (PVD) for use in ISOPVs. Using Cu as an interlayer material achieved the lowest sheet resistance of 0.55 $\Omega \cdot sq^{-1}$ and exceptional stretchability, with a 1.9-fold increase in resistance under 100% strain. The incorporation of InCuG electrodes into ISOPVs significantly improved charge transport and extraction, which was attributed to the dense and uniform formation of liquid metal (Fig. 7b). The well-adhered InCuG electrode also effectively dissipated stress in ISOPVs, alleviating crack initiation and propagation in the underlying layers and consequently enhancing their resilience to tensile strains. The InCuG-based ISOPVs demonstrated high performance (PCE=14.60% and FF=0.75) and excellent mechanical robustness ($PCE_{70\%}$ strain=63%).

Research has often focused on enhancing the intrinsic stretchability of individual layers such as substrates, active layers, and electrodes. However, synergistic optimization of multiple components is critical.[137] Lee *et al.*[138] proposed a double-locked substrate/transparent electrode platform for stretchable optoelectronics. The physical adsorption of PEDOT:PSS onto the stretchable TPU substrate was first induced, followed by chemical cross-linking *via* doping with (3-glycidyloxypropyl)trimethoxysilane. This dual-locking mechanism significantly enhanced the interfacial adhesion (Fig. 7c). As a result, the intrinsically stretchable organic photovoltaic based on the PM6:Y6-BO:N2200 bulk heterojunction system

exhibited no cracking under 40% strain and retained 79.7% of its initial power conversion efficiency (10.2%).

Chen *et al*.[54] systematically optimized both materials and device architectures using a multi-strategy approach to achieve high-performance ISOPVs. First, the stretchability of the active layer was enhanced by incorporating the styrene-ethylene-propylene-styrene (SEPS) elastomer. A SEPS content below 10 wt% had a negligible impact on the crystalline behavior of the active layer and overall device performance. Second, the stretchability and conductivity of the opaque electrode were improved by using a conductive polymer/metal composite strategy (M-PH1000@Ag). The M-PH1000 matrix provided stretchability and formed a continuous conductive network, whereas the deposited Ag layer enhanced the electrical conductivity and improved the light-harvesting efficiency, collectively boosting the device performance. Third, the optical and electrical properties of the AgNWs-based transparent electrode were improved *via* solvent vapor annealing (SVA), a process that precisely modulates the surface tension of the substrate and dispersant. The resulting ISOPVs achieved an initial PCE of 16.23% and retained over 80% of this efficiency after 200 stretching cycles at a 10% strain.

Despite pioneering progress, the efficiency of current ISOPVs still lags significantly behind their rigid and flexible counterparts. Achieving a combination of high PCE and robust mechanical stability remains an unresolved challenge, necessitating continued research in this field.

3.4 Organic Light-emitting Diodes

Since the development of polymer-based light-emitting diodes (PLEDs) in the 1990s, light-emitting polymers have been widely adopted in display devices owing to their convenient solution processability and favorable mechanical properties, making them promising candidates for realizing stretchable electronics.

In recent years, significant research has been focused on the molecular design of intrinsically stretchable electroluminescent polymers. In 2022, Lai *et al*.[143] synthesized a triblock copolymer, SBSPy-16, *via* the anionic polymerization of pyrene, styrene, and butadiene. The self-constrained, balanced rigid/flexible chain dynamics significantly reduced the modulus of the elastomer and substantially suppressed aggregation-induced quenching. The SBSPy-16 thin film achieved a maximum strain of 806% and high photoluminescence quantum yield (PLQY) of 53%. Xie *et al*.[144] incorporated flexible segments (oxyalkyl chains) into a fluorene-based polymer backbone, realizing flexible functionalization of a blue-light-emitting molecule with excellent performance and aging resistance. Huang *et al*.[145] introduced phenyl ester-based plasticizers into the side chains of deep-blue-emitting conjugated polymers (PF-MC4, PF-MC6, and PF-MC8). The rigid and polar phenyl ester core not only suppressed interchain interactions to facilitate polymer chain sliding and alignment but also maintained relatively dense interchain packing. The freestanding PF-MC8 film exhibited excellent intrinsic stretchability (fracture strain of 25%) along with highly efficient and stable deep-blue emission (PLQY>50%). An asymmetric substitution strategy, which disrupts the regularity and ordered crystallization ability of conjugated polymer chains, has also been reported for the fabrication of intrinsically stretchable, deep-blue-emitting, fully π-conjugated polymers (FπCPs).[146] Furthermore, stretchable active layers for ISOLEDs can be alternatively achieved by blending with plasticizing molecules[139,147,148] or soft elastic insulators.[149]

Although the performance of stretchable light-emitting polymers has been significantly improved, intrinsically stretchable OLEDs have rarely been demonstrated. In 2021, Kim and Park[139] reported an intrinsically stretchable organic light-emitting diode by blending the poly(phenylene vinylene) (PPV) derivative "Super Yellow" (SY) with a nonionic surfactant (Triton X-100) featuring a large hydrophobic head and a hydrophilic tail (Fig. 7d). This approach enhanced stretchability and induced a nanofibril-like morphology. The addition of Triton X-100 triggered a conformational transition of the polymer from a coiled to linear form, increasing the COS from 40% (0 wt%) to 110% (67 wt%) without significantly compromising its electrical properties. A Triton X-100 content of 33 wt% was identified as the optimal composition, achieving a balanced trade-off between mechanical stretchability and electrical performance. The device reached a maximum luminance of 2500 cd·m^{-2} at 11 V and maintained its electroluminescence performance under strains of up to 80%. However, the operational stability of this ISOLED is limited, and the high operating voltage leads to elevated device temperatures. The formation of nanoscale protrusions on the anode surface likely caused current concentration during operation, resulting in severe degradation of the organic layers.

Bao *et al*.[140] reported a strategy for constructing high-brightness stretchable OLEDs using an emitting layer with a nanoconfined polymer architecture. The SY nanofibers were uniformly distributed within the PU matrix (Fig. 7e). Facilitated by polar interactions, this configuration prevented phase separation and delayed crack formation, while simultaneously enhancing both stretchability and charge transport. By integrating this stretchable emitting layer with transparent, stretchable, and highly conductive polymer electrodes, along with appropriate interfacial modifications to both the anode and cathode, they realized a fully stretchable all-polymer light-emitting diode (APLED). The resulting device achieved a notable brightness of approximately 7450 cd·m^{-2}, withstood up to 100% strain, and exhibited an overall modulus of approximately 1 MPa.

Our group[150] developed a self-assembled 3D interpenetrating nanonetwork as the emitting layer for intrinsically stretchable PLEDs (ISPLEDs), based on a blend strategy employing high-molecular-weight styrylene-ethynylene (L-SY-PPV) and polyacrylonitrile (PAN). A stretchable electron-injection layer was fabricated using a hybrid material comprising polyethylenimine ethoxylated (PEIE), 1,10-phenanthroline monohydrate (pBphen), and Triton X-100 (TR) to form a Zn-PEIE-pBphen-TR complex. This composite layer exhibited enhanced electron injection and transport capabilities. The resulting ISPLEDs exhibited a high current efficiency of 8.13 cd·A^{-1} and retained 54% of its maximum luminescence when stretched to 30% strain. Recently, our group[141] proposed a novel and universal strategy for developing high-performance ISPLEDs by incorporating a microcrystalline elastomer (PU-PCL) into light-emitting polymer matrices (including SY, MDMO-PPV, PFOPV, and PFB) to construct submicron optical self-gain structures. This approach enabled the formation of

submicron optical self-gain structures in light-emitting polymers, and the confined polymers formed a nanofiber morphology through spatial nanoconfinement effects, which improved polymer crystallinity, facilitated carrier transport, and enhanced light outcoupling efficiency through increased reflection and scattering (Fig. 7f). Leveraging these synergistic advantages, the ISPLEDs achieved a current efficiency (CE) of 13.70 cd·A^{-1}, an EQE of 4.70%, a low turn-on voltage of 3.70 V, a maximum luminance of 32013 cd·m^{-2} at 9 V and demonstrated stable operation under 50% strain. Furthermore, a 12 × 12 array of ISPLEDs was successfully fabricated *via* electrohydrodynamic (EHD) printing, demonstrating excellent optoelectronic stability under both tensile and bending strains.

The maximum theoretical quantum yield for fluorescence emission relying on singlet excitons is limited to 25%, as constrained by the spin statistics. Stretchable thermally activated delayed fluorescence (TADF) polymers offer a promising pathway for achieving ideal electroluminescence and mechanical properties. Wang *et al*.[151] proposed a molecular design strategy for stretchable TADF polymers by embedding flexible alkyl chains between the TADF units in the polymer backbone. The resulting polymer PDKCD exhibited substantial stretchability, well above 100% strain, maintaining an EQE as high as about 10%, which is twice the theoretical limit (5%) of fluorescent polymers. The fully stretchable TADF-OLEDs exhibited a high EQE of 3.3%, current efficiency of 10.2 cd·A^{-1}, low turn-on voltage of 4.75 V and skin-like stretchability of 60%.

Tensile strain can weaken spin-orbit coupling (SOC) in TADF systems, thereby suppressing reverse intersystem crossing (RISC) and reducing triplet harvesting efficiency. In contrast, phosphorescent materials, owing to their strong SOC, exhibit a stable triplet-harvesting capability in stretchable OLEDs. Lee, Gogotsi and co-workers[142] developed an intrinsically stretchable exciplex-assisted phosphorescent layer (ExciPh). The ExciPh layer consists of the phosphorescent dopant bis(2-phenylpyridine)(acetylacetonate) iridium(III) (Ir(ppy)$_2$-acac), an exciplex co-host system of tris(4-carbazoyl-9-ylphenyl)amine (TCTA) and 2,2′,2″-(1,3,5-benzinetriyl)-tris(1-phenyl-1-*H*-benzimidazole) (TPBi), and a stretchable PU elastomer matrix. It demonstrated stretchability exceeding 200% and an EQE of 21.7%. Furthermore, they developed MXene-contact stretchable electrodes (MCSEs) with tunable work functions (3.79–5.71 eV) and two-dimensional electrical contacts. The MCSEs consisted of a 2D MXene interlayer deposited on top of AgNW-based stretchable electrodes, diluted MXene was used as a conductive binder to connect ("weld") AgNW/AgNW and AgNW/MXene interfaces, which greatly reduced contact resistance and enhanced charge-carrier mobility from 1.4 cm^2·V^{-1}·s^{-1} to 85.9 cm^2·V^{-1}·s^{-1}. When paired with a stretchable gradient hole-injection layer (SGraHIL), the charge injection efficiency was further enhanced (Fig. 7g). The resulting ISOLEDs, built on these components, exhibited a low turn-on voltage of <5.0 V, peak luminance of 4840 cd·m^{-2}, and record EQE of 17.0%. The devices exhibited minimal luminance loss (10.6%) under 60% strain and retained over 83% of their initial efficiency after 100 stretch-release cycles at 20% strain. This study significantly narrows the efficiency gap between rigid and intrinsically stretchable OLEDs, providing a promising pathway toward high-performance stretchable optoelectronics.

Table 1 summarizes the key performance parameters of representative ISOLEDs reported in recent years, covering aspects such as emissive layer materials, device structures, maximum tensile strain, luminance, and efficiency to facilitate an intuitive comparison for readers.

3.5 Organic Luminescent Electrochemical Cells

As one of the simplest electroluminescent devices, an OLEC is composed of a light-emitting layer containing both ionic and electronic conductors sandwiched between two electrodes, a structure that supports charge injection, transport, and emissive recombination.[153] The working mechanism of OLEC is described as follows: When a voltage is applied to an OLEC, ions in the emission layer are redistributed to form an electrical double layer at the anode and cathode interfaces to allow easy hole and electron injection, respectively, leading to electrochemical doping to form a light-emitting PIN junction.

In 2011, Pei *et al*.[38] reported the first all-organic light-emitting device, OLEC, a luminescent polymer layer consisting of a blue emissive polyfluorene copolymer (PF-B), an ionic conductor (poly(ethylene oxide) dimethacrylate ether (PEO-DMA)), and a salt (lithium trifluoromethane sulfonate (LiTf)) laminated between two single-walled carbon nanotube (SWNT)-polymer electrodes. The device could withstand deformations of up to 45% linear strain without compromising the electroluminescence characteristics. However, the limited stretchability and conductivity of the electrodes, low electroluminescent performance, and complicated processing methods constitute significant obstacles to the fabrication of stretchable displays based on these light-emitting device architectures. In 2013, they reported an elastic polymer light-emitting electrochemical cell (EPLEC).[152] The composite electrode was based on a thin silver nanowire network inlaid on the surface layer of a rubbery poly(urethane acrylate) (PUA) matrix, endowing it with high visual transparency, good surface electrical conductivity, high stretchability, and high surface smoothness. The electroluminescent polymer layer consisted of a blend of yellow light-emitting polymer (Super Yellow), ethoxylated trimethylolpropane triacrylate (ETPTA), polyethylene oxide (PEO), and LiTf. The device exhibited a maximum luminance of 2200 cd·m^{-2} and an efficiency of 5.7 cd·A^{-1}. It could withstand a maximum linear strain of up to 120% and maintain a reasonably stable current efficiency and luminance over 1000 stretch-release cycles at 30% strain. This paved the way for fully stretchable active-matrix displays capable of high-resolution information display.

4 INTEGRATED APPLICATION OF DEVICES

4.1 Human-machine Interaction/Intelligent Interfaces

4.1.1 Stretchable optoelectronic displays and information feedback

Active-matrix platforms are widely adopted for pixel multiplexing in light-emitting display devices owing to their distinctive features: minimal interpixel crosstalk, high pixel density, and a reduced number of interconnects. To achieve fully stretchable skin-like displays, two key components are required: an array of intrinsically stretchable light-emitting devices, and an intrinsically stretchable active backplane driven by thin-film transistors

https://doi.org/10.1007/s10118-026-3652-3

Table 1 The key performance parameters of representative ISOLEDs reported in recent years.

Year	Stretchable EML	Device structure	L_{max} (cd·m^{-2})	CE (cd·A^{-1})	EQE (%)	V_{on} (V)	Mechanical properties	Maximum stretchability (%)	Ref.
2013	Super Yellow/ ETPTA/ PEO/LiTf	TCPU/ AgNWs-PUA/ PEDOT:PSS/ EML/ AgNWs-PUA TCPU	2200 (@21 V)	5.7 (max)	4.0	6.8	1000 Stretching-releasing cycles (30% strain)	120	[152]
2021	SuperYellow: Triton X	AgNWs- JIOS Aerogel-PDMS/ Triton X- PEDOT:PSS (Al4083)/EML/ ZnO- d-PEIE/ AgNWs-ETL	2500 (@11 V)	1.6	–	8.3	200 Stretching-releasing cycles (0%–40% strain)	80	[139]
2022	SuperYellow: PU	PEDOT:PSS-PR/ PEDOT: PSS-Triton X/ TFB-PU EML/ PFN-Br-PEIE/ PEDOT:PSS-PR	7450 (@15 V)	5.3±0.3	–	5	85% Of its original brightness value after stretching for 100 cycles to 40% strain	100	[140]
2022	L-SY-PPV: PAN	Serpentine Au/Au interlayer /PEDOT:PSS-TX/EML /PMMA/Zn-PEIE-pBphen-TR/Ag interlayer/AgNWs/PDMS	3780 (@6.5 V)	2.35	2.64	6.5	50 Stretching–releasing cycles (0%–15% strain) V_{on}=7.3 V, L_{max}=1740 cd·m^{-2}; etched up to 30% while retaining 54% of initial luminescence	30	[150]
2022	SBSPy-16	PEDOT: PSS(PH 1000)/PEDOT:PSS(Al 4083)/EML/TPBi/LiF/Al	3274 (28.5 V)	5.32	2.08	9.3	With 50% strain, the initial luminance and current efficiency of the stretchable OLED decreased to 73% and 70% of its initial values	54	[143]
2023	PDKCD	AgNWs/ PEDOT: PSS-PFI/EML/ PFN-Br-PEIE/ AgNWs	About 5000	–	3.3	4.75	60% Of its initial luminance value under 60% strain	60	[151]
2025	SY: PU-PCL	Semi-reflective anode/ (PEDOT:PSS/TX-100)/EML/PEIE-PFNBr/Total reflection cathode	32013 (@9 V)	13.70	4.70	3.70	Stable device operation under 50% strain, maintained normal operation after 100 cycles (0%–20% cyclic strain)	100	[141]
2026	Ir(ppy)2acac:TCTA:TPBi:PU	A-MCSE/SGraHIL/ EML/C-MCSE	4840	47.9	17	< 5	10.6% Decrease in luminance and a 22.0% drop in EQE at 60% strain, more than 83% of its initial efficiency after 100 cycles (0%–20% cyclic strain)	60	[142]

(TFTs). Stretchable interconnects, capable of vertically linking individual light-emitting pixels with their switching transistors while maintaining the overall stretchability of the monolithic device, are essential for enhancing spatial resolution and contrast.

The development of active-matrix platforms requires high-performance stretchable transistor arrays capable of delivering the current density necessary to drive stretchable OLECs. In 2020, Bao *et al*.[154] developed a stretchable, chemically orthogonal, and photo-patternable perfluorinated elastomer as a gate dielectric layer for transistors. This material allowed for direct, large-area, uniform solution processing of the semiconductor layer on top. The introduction of a crosslinker containing flexible polydimethylsiloxane enhances the stretchability of the semiconducting polymer and achieves better interfacial bonding with the dielectric layer. The fabricated 5 × 5 active-matrix transistor array exhibited an average saturation mobility of (0.56±0.17) cm^2·V^{-1}·s^{-1}, which could be stretched up to 100% and cycled 1000 times with less than one order of magnitude reduction in both mobility and on-current. For stretchable OLECs, PUA-AgNWs and PEDOT:PSS were used as the electrode and hole injection layers, respectively. The light-emitting layer comprised the luminescent polymer SY, the ionic conductive polymer PEO, ethoxylated trimethylolpropane triacrylate (ETT-15), and LiTf. The device was able to withstand a tensile strain of 30%. Finally, an active-matrix OLEC (AMOLEC) array was completed by vertically stacking the fully stretchable active backplane with the OLEC array. The TFTs provide an average drain current of (0.16±0.04) mA. The AMOLEC array possessed mechanical softness (about 50 MPa) and could be flexibly bent, twisted, and stretched without compromising the device performance. Negligible delamination of the multilayer structure was observed, even after 20 cycles at 30% strain. However, challenges remain in on-skin integration, including the array's relatively low pixel density and high operating voltage.

Benefiting from the integration of material innovation, manufacturing process design, device engineering, and circuit design, in 2024, they fabricated a high-performance stretchable transistor array using high-purity semiconducting

carbon nanotubes (S-CNTs) as the channel material, a high-*k* elastic nitrile-butadiene rubber (NBR) dielectric layer, low-contact-resistance metallic CNT/palladium (M-CNT/Pd) source-drain electrodes with interface modification, a smooth PEDOT:PSS gate electrode, and highly conductive stretchable EGaIn interconnects.[155] The array achieved an exceptional transistor density of up to 10^5 transistors/cm^2, a mobility exceeding 20 cm^2·V^{-1}·s^{-1} under 100% strain, and a drive current of approximately 2.0 μA·μm^{-1} at a low operating voltage of 5 V. Leveraging the high device density, fast operating speed, and high driving current of the stretchable transistor array, a high-resolution braille sensing array was constructed, which conformally adhered to a human finger (Fig. 8a). When the loading pressure on the tactile sensor reached approximately 20 kPa, the on-state current (I_{on}) of the access transistor in the corresponding pixel increased from <1 nA to >1 μA (Fig. 8a). The large current response and small pixel size (200 μm) enabled the precise mapping of tiny objects and allowed for the recognition of shapes (including triangles, circles, and rectangles), orientations, locations, and sizes (down to <1 mm). A record-high sensing density of 2500 units per cm^2 was achieved, surpassing the mechanical receptor density of the human fingertip by more than ten times. This enabled Braille recognition at a resolution finer than that of human perception, and the sensing array could read an entire word within an area of just 8 mm^2 (Fig. 8b). Furthermore, an LED display driven by this transistor array successfully displayed different numbers, letters, and symbols, with a refresh rate above 60 Hz (Fig. 8c). Both the transistor current and LED brightness remained stable even under significant deformation. This study provides a key building block for the diversification of practical on-skin applications.

Recently, Son *et al.*[156] proposed a reconfigurable and scalable (RS) assembly method to construct a user-interactive system that integrates self-healing, stretchable transistor arrays, tactile sensors, and light-emitting cells. A self-healing polymer (SHP) based on dynamic hydrogen bonds, specifically a poly(dimethylsiloxane) derivative, served as a universal matrix. Semiconducting nanocomposites and electrodes with self-healing capability and stretchability were prepared by blending SHP with a semiconducting polymer (DPP-DTT) and conductive CNTs, respectively. All functional layers (dielectric, semiconductor, and electrode) were integrated through self-assembly and transfer-printing processes, resulting in an intrinsically stretchable and self-healing thin-film transistor (SS-TFT). Based on this, the authors constructed a 5 × 5 active-matrix transistor array (AM-SS-TFT) and fabricated a wearable user-interactive system integrating a 5 × 5 SS-CNT array, AM-

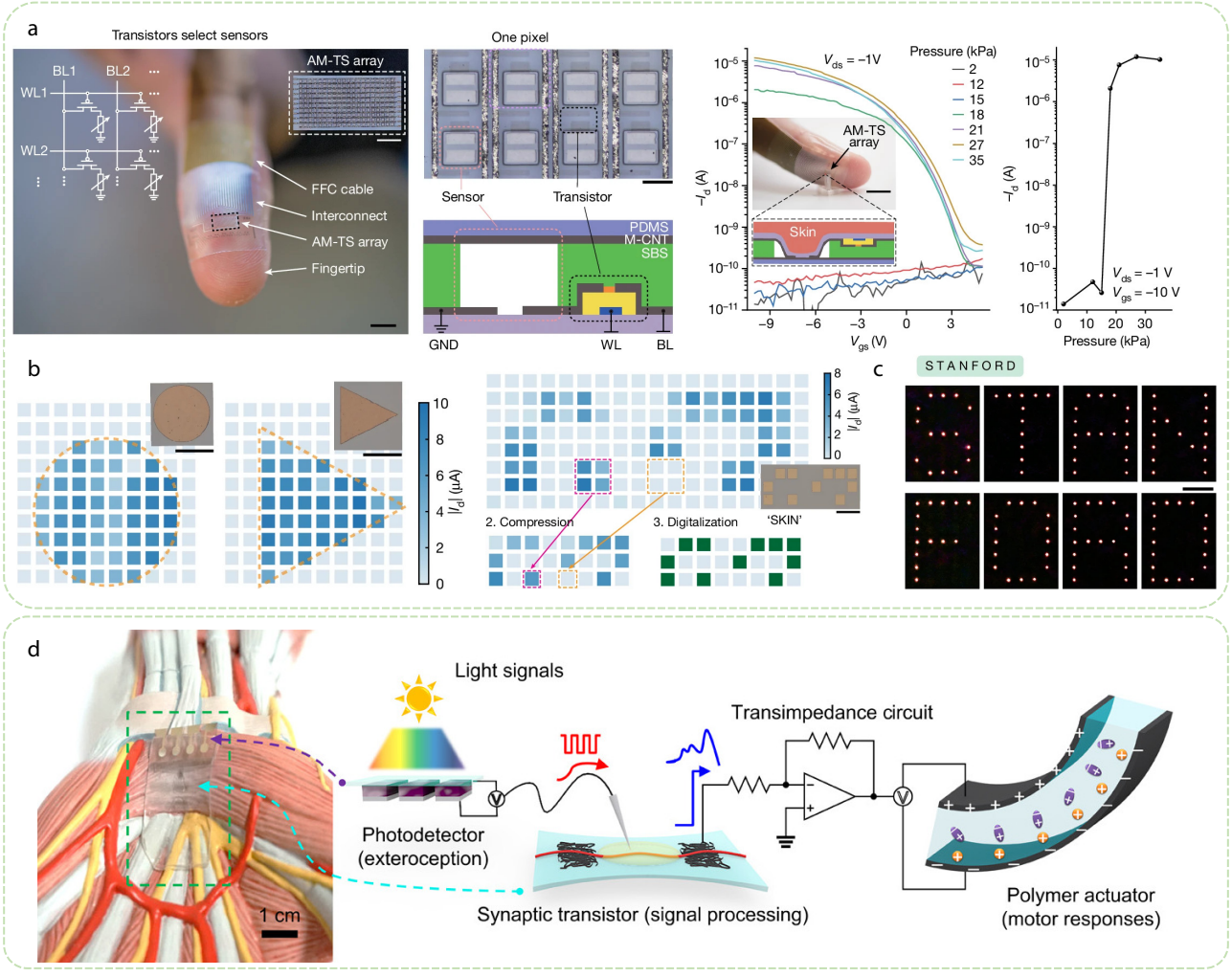

https://doi.org/10.1007/s10118-026-3652-3

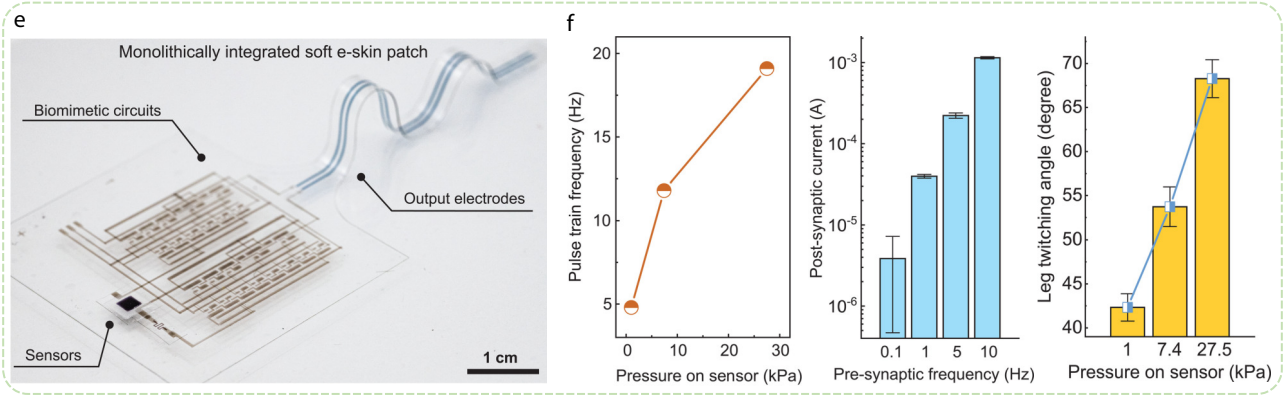

Fig. 8 (a) Schematic, photo and microscope image of an active-matrix sensor array (AM-TS). Transfer curves of a single pixel and extracted drain current, under different pressure. (b) On-state current distribution of AM-TS when pressing on different shapes. (c) Photos of LED displays with different letters (Reproduced with permission from Ref. [155]; Copyright (2024), The Authors, under exclusive license to Springer Nature Ltd.). (d) Organic optoelectronic synapse and neuromuscular electronic system (Reproduced with permission from Ref. [157]; Copyright (2024), The Authors, under exclusive license to Springer Nature Ltd.). (e) Photo showing the components of a monolithically integrated, soft e-skin patch; (f) Pulse-train output frequencies under different pressure levels applied on a pressure sensor, and correlation between leg twitching angle and applied pressure (Reproduced with permission from Ref. [158]; Copyright (2023), The American Association for the Advancement of Science).

SS-TFT array, and self-healable LEC (SS-LEC) array. Tactile sensing was successfully performed by detecting the change in the resistance of each row and column in the SS-CNT array. The top and bottom CNT interconnects were electrically isolated using passive capacitive architecture. The tactile sensor signals recorded by the SS-CNT array upon pressure application were directly transmitted to the AM-SS-TFT module *via* a PXI switch module (Pickering) and source measurement unit. These modules sequentially activated individual transistors at the points where deformation occurred in the SS-CNT array, thereby controlling the SS-LEC units. This setup achieved real-time, spatially correlated closed-loop interaction from "tactile input" to "optical feedback."

4.1.2 Neuromorphic electronic skin

Stretchable organic optoelectronic devices have achieved breakthroughs in realizing fundamental neuromorphic functions, including synaptic plasticity, and the construction of integrated neuromorphic electronic skin systems capable of adaptive perception, information preprocessing, and learning has become a major focus of research. Current explorations in this field advance primarily along two critical dimensions. The first involves emulating the adaptive and protective mechanisms inherent to biological sensory systems, such as visual adaptation, nociceptive sensitization, and memory formation. The second focuses on constructing low-power pattern recognition and decision-making systems based on local sensing-processing units.[159] These developments are opening new avenues for next-generation autonomous soft robotics and immersive human-machine interaction.

Lee *et al.*[157] developed a stretchable organic nanowire synaptic transistor (s-ONWST) that demonstrated stable *I-V* characteristics and a range of representative postsynaptic behaviors. These include excitatory postsynaptic current (EPSC), PPF, spike voltage-dependent plasticity (SVDP), spike number-dependent plasticity (SNDP), spike frequency-dependent plasticity (SFDP), and high-pass filtering at both 0% and 100% strains. Furthermore, they reported the first neuromorphic organic optoelectronic sensorimotor synapse based on s-ONWST, which successfully mimicked biological synapses within the sensorimotor nervous system. Specifically, this system utilizes the output voltage of a photodetector to convert light signals into presynaptic spikes, thereby triggering postsynaptic potentiation in an artificial synapse. This synaptic response subsequently drives an artificial muscle actuator, producing a motor response analogous to the tension response of a biological muscle during contraction (Fig. 8d). s-ONWST could also react to patterned visible light representing the International Morse code, where each letter of the English alphabet induced a distinct EPSC amplitude response. Remarkably, the device showed no significant change in these responses, even under 100% tensile strain, highlighting its potential for light-fidelity optical wireless communication in human-machine interfaces.

Yu *et al.*[160] reported a fully rubber-based stretchable synaptic transistor and neurologically integrated devices. The synaptic transistor exhibits functions analogous to those of biological synapses, including EPSC, PPF, short-term memory (STM), long-term memory (LTM), and filtering characteristics. These properties remained stable even after mechanical stretching to 50%. Based on an array of pressure-sensitive rubber mechanoreceptors and fully rubbery synaptic transistors, they developed neurologically integrated tactile sensory skin. Mechanoreceptors respond to physical contact by generating presynaptic pulses, which excite synaptic transistors to produce postsynaptic potentials. The mapping of these postsynaptic potentials from the arrayed sensory pixels was achieved even when the skin was stretched. Building on this, they created a soft adaptive neurologically integrated robot by covering a soft pneumatic robot with a functional elastic skin that incorporated triboelectric nanogenerators (TENGs) and synaptic transistors. This system achieves a closed-loop "sense-process-actuate" cycle. It was capable of sensing physical taps and adaptively driving locomotion in a programmed manner through signals encoded by synaptic memory.

Bao *et al.*[158] developed an organic transistor featuring a trilayer, high-*k* elastomeric dielectric. The device demonstrat-

ed low-voltage operation (3 V), high performance, low subthreshold swing (about 85 mV per decade) comparable to that of poly-Si transistors, and stretchability up to 100% strain. These transistors are further integrated to form low-voltage functional circuits. The system incorporates sensors to collect external stimuli, ring oscillators (ROs) to modulate the sensor signals, and edge detectors (EDs) to generate action potential-like pulse-train signals. This integration resulted in a monolithic electronic skin (e-skin) patch that emulated the natural mechanoreceptor and thermoreceptor functions (Fig. 8e). By encoding different stimuli into pulse trains within distinct frequency bands, the system achieved multimodal perception. A fully stretchable all-solid-state synaptic transistor array was fabricated to complete the sensorimotor loop. Digital inputs mimicking somatic sensory cortex signals have been successfully used to elicit responses in the motor cortex of live rats. Specifically, the captured signals were amplified and processed to serve as the gate input for the synaptic transistors, causing the amplitude of the postsynaptic currents to scale proportionally to the applied pressure. The synaptic channel was interfaced with the sciatic nerve via a low-impedance PEDOT:PSS electrode, leading to the contraction of the biceps femoris muscle. Analogous to natural sensory feedback, in which stronger stimuli trigger more intense reactions, this bidirectional e-skin system also elicited stronger leg twitching in response to increased pressure (Fig. 8f). This study demonstrated the potential feasibility of such artificial e-skin systems for neuroprosthetic applications.

Cao *et al*.[161] developed a broad-spectrum responsive stretchable organic optoelectronic synaptic transistor (s-OOST) based on an intrinsically stretchable, high-mobility, narrow-bandgap, and high-relaxation-time organic semiconductor PTDPPSe-6Si. This device achieves brain-inspired memory/computation, and retina-inspired visual perception/adaptation. The s-OOST exhibits a high transconductance (86 mS) at a low operating voltage (−1 V), withstands multidirectional strains of up to 50%, and retains full neuromorphic characteristics including PPF, short-term/long-term plasticity, and "learning-forgetting-relearning" behavior. By leveraging its ultra-broad spectral response from UV to NIR light (365-1050 nm), a single-pixel NIR imaging system was successfully constructed, achieving high-contrast imaging of an "SU" pattern. Owing to the significant variation in relaxation time with the wavelength of incident light, the s-OOST demonstrated human-retina-like functionalities such as photoplasticity, color recognition, and visual self-adaptation. This capability further enhanced the security of "encryption" and "decryption" in optical communication, paving the way for constructing artificial systems integrating dual modes of neuromorphic computing and visual perception.

4.2 Wearable Health Monitoring

Traditional rigid wearable devices face inherent limitations in terms of long-term comfort and signal fidelity. Particularly during motion, the relative displacement between the device and skin can generate significant motion artifacts, compromising the accuracy of the monitoring data. In contrast, intrinsically flexible/stretchable organic optoelectronic devices can conformally adhere to the human body like a "second skin." Their mechanical compliance and/or stretchability help minimize the pressure and discomfort arising from their conformability and softness, thereby providing a promising platform for continuous, precise, and unobtrusive health monitoring.

Someya *et al*.[162]demonstrated an ultraflexible photonic skin based on highly efficient three-color PLEDs and OPDs. By integrating green and red PLEDs as light sources and an OPD as the detector, they developed an ultraflexible reflective pulse oximeter that can be directly laminated onto a finger. This device measured the pulse waveform and blood oxygen saturation in real time and noninvasively by detecting the differential absorption of light at different wavelengths by blood, demonstrating its potential for physiological monitoring under dynamic wearable conditions. Kim *et al*.[163] developed a standalone health-monitoring patch by integrating a stretchable OLED array and PPG sensor on an all-elastomer substrate, enabling real-time heart rate monitoring and display. The skin-attachable PPG sensor, which consisted of two red OLEDs and one OPD, exhibited a high signal-to-noise ratio of >21 dB. Owing to its conformal contact with the wrist, mechanical stability, and high detectivity, the heart rate measurement demonstrated greater robustness during wrist movement (repetitive flexion and extension) than a silicon-based PPG sensor. The incorporation of micro-cracked gold interconnects and stress relief layers effectively distributed the external stress, allowing the integrated device to operate stably under up to 30% strain. The patch layout was optimized based on the skin strain distribution and, combined with a customized processing module and flexible battery, formed a complete standalone monitoring system.

As wearable electronics evolve from data acquisition to long-term continuous health management, self-sustaining power capabilities have emerged as a pivotal requirement for practical system deployment. The integration of intrinsically flexible/stretchable organic optoelectronic devices with energy-harvesting units presents a viable route toward building genuinely autonomous wearable systems. Someya *et al*.[164] fabricated highly efficient OPVs with a one-dimensional dual-grating structure on a 1-μm-thick flexible substrate *via* a DVD-R template and room-temperature molding process. This design effectively enhanced light trapping and scattering, raising the power conversion efficiency to 10.49% and achieving a high power-per-weight ratio of 11.46 $W \cdot g^{-1}$, while demonstrating excellent stability under mechanical compression and varying illumination angles. The OPVs were integrated with organic electrochemical transistors (OECTs) on an ultrathin 1-μm parylene substrate to form a monolithic "sensing-powering" system. The OECTs exhibited a transconductance as high as 0.8 mS and a response speed faster than 1 kHz. This integrated system was successfully applied to monitor electrocardiographic (ECG) signals on the surface of a live rat heart, achieving a maximum signal-to-noise ratio of 40.02 dB for cardiac signal detection.

Furthermore, they[165] adopted an inverted device architecture and used lithium-salt-doped polyethylenimine ethoxylate (PEIE:Liq) as the electron transport layer, successfully fabricating an air-stable ultraflexible PLED with an operational lifetime of 11.3 h in an unencapsulated state. By integrating this air-stable PLED with an OPV and an OPD, they developed an ultraflexible self-powered organic optical system, complet-

https://doi.org/10.1007/s10118-026-3652-3

ing a closed-loop of signal "emission-powering-detection" for photoplethysmography (PPG) monitoring. The ultraflexible OPV module harvested energy from the ambient light to directly drive the PLED, which emitted yellow-green light with a peak wavelength of 590 nm. This wavelength has suitable penetration characteristics for human tissue. The OPD is responsible for precisely detecting reflected light signals. The system successfully demonstrated fully self-powered, battery-free PPG monitoring on the human skin, recording a real-time pulse rate of 77 beats per minute. This work represents the first realization of self-powered biosensing based on all-organic, ultraflexible optoelectronic device integration, paving the way for the development of comfortable, long-lasting, wearable health-monitoring electronic skin.

5 SUMMARY AND OUTLOOK

In recent years, the field of intrinsically stretchable organic optoelectronic devices has advanced from proof-of-concept demonstrations to the integration of functional systems. Focusing on this theme, this review systematically summarizes representative progress in fundamental material design, key device architecture, and frontier integrated applications. Overall, molecular engineering and composite strategies have yielded intrinsically stretchable organic/polymer semiconductors with fracture strains exceeding 100%, moduli as low as the MPa range, and high electrical performance. Through multiscale structural design and interface engineering, devices capable of stable operation under 50%–100% tensile strain and thousands of deformation cycles have been realized. Furthermore, by combining such devices with other electronic components, preliminary prototype systems have been built for optical human-machine interfaces, visual neuromorphic computing, and health monitoring, highlighting promising prospects for wearable and implantable optoelectronics.[5]

Despite remarkable progress, many studies remain at an early stage, and system-level integration applications for complex functions remain limited. Most current intrinsically stretchable materials inevitably sacrifice charge-carrier mobility, luminescence efficiency, or photoconversion efficiency in exchange for their high ductility and low modulus. In particular, the development of n-type semiconductors has lagged significantly behind that of p-type materials,[103] mainly because of (1) the high sensitivity of electrons as charge carriers to trap states such as water and oxygen in air, resulting in poor environmental stability and (2) the rigid planar structures of many high-performance n-type molecular semiconductors, which hinder the realization of high stretchability without compromising the continuity of charge transport pathways. Future molecular designs should go beyond simple rigid-flexible block concepts and explore more sophisticated molecular conformations that can maintain effective orbital overlap under dynamic deformation, thereby enabling the development of air-stable, mechanically stretchable, high-performance n-type and p-type materials. For wearable and implantable applications, the devices must operate under low-voltage conditions. The development of gate dielectrics that combine high-*k*, low leakage current, and stretchability is expected to significantly lower the operating voltage and energy consumption.[30] At the molecular level, introducing highly polar, low-hysteresis functional groups into the polymer backbone or designing block copolymers with intrinsic microphase-separated structures enables nanoscale control over the polarization and mechanical properties. For composite strategies, a thorough investigation into the surface chemical modification of high-*k* nanofillers and their spatial distribution within the elastic matrix is essential to prevent aggregation-induced electric field concentration and increased leakage current.

Microcracks and interfacial fatigue induced by repeated stretching can lead to performance degradation of high-performance devices under large strains and prolonged cycling. Synchrotron-based X-ray scattering and imaging tools, such as *in situ* grazing-incidence wide-angle X-ray scattering (GIWAXS),[166] grazing-incidence small-angle X-ray scattering (GISAXS),[167] and wide-angle X-ray scattering (WAXS),[168] have provided new insights into the dynamic evolution of molecular packing, phase separation, and microcrack formation during mechanical deformation. For instance, Ye *et al*.[166] recently developed an in situ stretching GIWAXS method capable of simultaneously probing the microstructural evolution both parallel and perpendicular to the strain direction. This approach revealed that a styrene-isoprene-styrene (SIS) elastomer can induce strain-enhanced π-π stacking coherence in PM6:PY-IT all-polymer blend films, demonstrating how synchrotron-based *in situ* characterization can uncover non-intuitive design rules and guide the rational selection of elastomeric additives. Future work should integrate multiscale simulations with *in situ* characterization to elucidate the microstructural evolution and failure mechanisms of intrinsically stretchable devices under stress. Such an integrated approach will enable the co-optimization of materials and devices from the molecular and morphological levels to the device architecture, ultimately leading to robust integrated systems.

Most organic and hybrid materials used in intrinsically stretchable devices are highly sensitive to environmental moisture and oxygen. For wearable or implantable applications, ensuring biocompatibility requires resistance to bodily fluid erosion. Elastomer-based organic encapsulation materials exhibit excellent intrinsic stretchability, biocompatibility, and ease of processing, allowing them to integrate seamlessly and synergistically deform with flexible substrates and devices. However, their relatively high water vapor and oxygen transmission rates (WVTR/OTR) often fail to satisfy the stringent encapsulation requirements of optoelectronic devices. In contrast, inorganic materials with their dense atomic packing structure serve as ideal gas barrier layers, offering extremely low WVTR/OTR. However, their inherent brittleness is incompatible with the mechanical requirements of stretchable devices. To address this trade-off, Deng *et al*.[169] innovatively introduced liquid metal EGaIn and glass microbead spacers between the PDMS encapsulation layers, creating an adaptively deformable sealing layer. This approach offers a promising route for fabricating soft, stretchable devices capable of long-term, stable operation. Bao *et al*.[170] developed a method to directly tether a nanostructured fluorinated molecular protective layer onto stretchable semiconductor films, achieving moisture barrier performance comparable to

https://doi.org/10.1007/s10118-026-3652-3

that of certain inorganic materials. Moving forward, an important research direction is to combine stretchable seal design with functional layer engineering to ensure both outstanding barrier properties and strong adhesion while maintaining compatibility with the overall mechanical and optical performance of the system.

Equally critical is the development of deformable and stretchable energy devices to realize self-powered systems. Stretchable batteries capable of maintaining stable performance under repeated mechanical deformation are fundamental for driving wearable and implantable optoelectronics without compromising motion comfort. However, significant challenges remain, including low energy density, difficulties in encapsulation, and insufficient system level integration.[171] Harvesting energy efficiently from the environment is another key pathway toward self-powered systems. In addition to solar cells, thermoelectric conversion, which directly converts temperature gradients into voltage, offers sustainable energy-harvesting technology. Lei *et al.*[172] reported the first n-type thermoelectric elastomer, achieving simultaneous optimization of the mechanical and thermoelectric performance through a synergistic strategy combining uniform bulk nanophase separation, thermally activated crosslinking, and targeted doping. Both in-plane and out-of-plane elastic thermoelectric generators based on this elastomer maintained a stable voltage output under dynamic bending and stretching cycles and conformally adhered to human skin, providing a critical material foundation for constructing fully self-powered, skin-adaptable wearable optoelectronic systems, and are promising candidates for low-grade heat harvesting.

The ability of electronic devices to self-heal, allowing them to autonomously recover their structure and function after damage, similar to that of biological skin, has emerged as an important goal in material and device design. Although self-healing materials based on dynamic chemical bonds have shown initial progress, most cannot fully restore their intricate internal charge-transport networks, such as π–π stacking in semiconductors or percolation pathways in conductors, after mechanical repair. The resulting defects act as charge traps or scattering centers, leading to significant performance loss. Furthermore, many current healing strategies depend on external stimuli, such as heat, light, or solvents,[80,173] which are often impractical in real-world settings. Future research should look beyond simple mechanical recovery to achieve molecular-level healing. This requires that dynamic bonds not only reconnect broken interfaces but also guide functional molecules to reassemble into ordered structures, ultimately enabling truly self-healing electronic systems.

Currently, many high-performance devices with small-area samples and low pixel density remain at the laboratory scale. Developing scalable manufacturing techniques compatible with stretchable materials, improving patterning precision and yield,[174] and achieving million-pixel intrinsically stretchable optoelectronic arrays are crucial steps toward practical products. Most current wearable/implantable electronics are still in the proof-of-concept stage,[175] and future research should increasingly focus on constructing closed-loop intelligent systems capable of "sensing-processing-feedback." This requires not only the co-design and integration of hardware with flexible sensors, wireless communication, and power management modules but also the incorporation of algorithms leveraging machine learning and neuromorphic computing. By fully exploiting the inherent synaptic-like properties and structural plasticity of the devices, their applications in smart wearables, brain-computer interfaces, and soft robotics can be significantly advanced.

In summary, with the continuous refinement of design principles for intrinsically stretchable semiconductors and conductors, the maturation of high-barrier flexible encapsulation and large-area fabrication technologies, and the deepening convergence of materials science, mechanics, electronics, and biomedicine, stretchable organic optoelectronic devices are poised to transition from laboratory to real-world scenarios. This promises to provide a novel technological platform for advancing human-machine interaction, personalized healthcare, and intelligent perception.

BIOGRAPHY

Yun-Long Guo received his Ph.D. degree in Physical Chemistry from the Institute of Chemistry, Chinese Academy of Sciences (ICCAS), in 2010. He is currently a professor at ICCAS. His research interests include intrinsically flexible organic-inorganic hybrid perovskite electronics and functional organic field-effect transistors.

Conflict of Interests

The authors declare no interest conflict.

ACKNOWLEDGMENTS

This work was financially supported by the National Natural Science Foundation of China (Nos. 22525506, U22A6002, and T2441002), Strategic Priority Research Program of CAS (No. XDB0520101), CAS Project for Young Scientists in Basic Research (No. YSBR-053), and Beijing Natural Science Foundation (No. Z250016).

REFERENCES

1 Kim, D. C.; Choi, M. K.; Kim, D.-H.; Yang, J. Rise of intrinsically stretchable electroluminescent materials: toward free-form displays. *npj Flex. Electron.* **2025**, *9*, 50.
2 Takei, K.; Gao, W.; Wang, C.; Javey, A. Physical and chemical sensing with electronic skin. *Proc. IEEE* **2019**, *107*, 2155–2167.
3 Qian, Y.; Zhang, X.; Xie, L.; Qi, D.; Chandran, B. K.; Chen, X.; Huang, W. Stretchable Organic Semiconductor Devices. *Adv. Mater.* **2016**, *28*, 9243–9265.
4 Zheng, Y.; Zhang, S.; Tok, J. B. H.; Bao, Z. Molecular design of stretchable polymer semiconductors: current progress and future directions. *J. Am. Chem. Soc.* **2022**, *144*, 4699–4715.
5 Li, C.; Bian, Y.; Zhao, Z.; Liu, Y.; Guo, Y. Advances in biointegrated wearable and implantable optoelectronic devices for cardiac healthcare. *Cyborg Bionic Syst.* **2024**, *5*, 0172.
6 Lee, H.; Jiang, Z.; Yokota, T.; Fukuda, K.; Park, S.; Someya, T. Stretchable organic optoelectronic devices: design of materials, structures, and applications. *Mater. Sci. Eng.: R: Rep.* **2021**, *146*, 100631.

Graphical Abstract

Stretchable Organic Photoelectric Conversion Systems: From Molecular Design to Device Applications

Yue-Yue Zhang, Yi-Li Wang, Yun-Qi Liu, and Yun-Long Guo

Institute of Chemistry Chinese Academy of Sciences; University of Chinese Academy of Sciences

This review summarizes molecular/structural design strategies for intrinsically stretchable organic optoelectronics and discusses their integration and potential in human-machine interfaces, neuromorphic electronics, and wearable health monitoring.

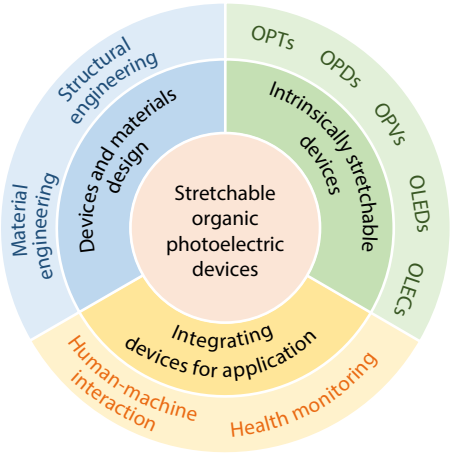

Chinese J. Polym. Sci., 2026 *https://doi.org/10.1007/s10118-026-3652-3*

7 Xue, X.; Li, C.; Shangguan, Z.; Gao, C.; Chenchai, K.; Liao, J.; Zhang, X.; Zhang, G.; Zhang, D. Intrinsically stretchable and healable polymer semiconductors. *Adv. Sci.* **2024**, *11*, 2305800.
8 Ko, H. C.; Stoykovich, M. P.; Song, J.; Malyarchuk, V.; Choi, W. M.; Yu, C.-J.; Geddes Iii, J. B.; Xiao, J.; Wang, S.; Huang, Y.; Rogers, J. A. A hemispherical electronic eye camera based on compressible silicon optoelectronics. *Nature* **2008**, *454*, 748–753.
9 Lipomi, D. J.; Tee, B. C. K.; Vosgueritchian, M.; Bao, Z. Stretchable organic solar cells. *Adv. Mater.* **2011**, *23*, 1771–1775.
10 Ashizawa, M.; Zheng, Y.; Tran, H.; Bao, Z. Intrinsically stretchable conjugated polymer semiconductors in field effect transistors. *Prog. Polym. Sci.* **2020**, *100*, 101181.
11 Mun, J.; Ochiai, Y.; Wang, W.; Zheng, Y.; Zheng, Y.-Q.; Wu, H.-C.; Matsuhisa, N.; Higashihara, T.; Tok, J. B. H.; Yun, Y.; Bao, Z. A design strategy for high mobility stretchable polymer semiconductors. *Nat. Commun.* **2021**, *12*, 3572.
12 Wang, B.; Bao, S.; Vinnikova, S.; Ghanta, P.; Wang, S. Buckling analysis in stretchable electronics. *npj Flex. Electron.* **2017**, *1*, 5.
13 White, M. S.; Kaltenbrunner, M.; Głowacki, E. D.; Gutnichenko, K.; Kettlgruber, G.; Graz, I.; Aazou, S.; Ulbricht, C.; Egbe, D. A. M.; Miron, M. C.; Major, Z.; Scharber, M. C.; Sekitani, T.; Someya, T.; Bauer, S.; Sariciftci, N. S. Ultrathin, highly flexible and stretchable PLEDs. *Nat. Photonics* **2013**, *7*, 811–816.
14 Lee, I.; Park, C.; Kim, T. S.; Kang, M.; Oh, H.; Jang, J.; Park, J.; Yuk, J. M.; Lee, H.; Park, C. B.; Choi, S. Y.; Kang, K.; Lee, W.; Bae, B. S. Water-stable and photo-patternable siloxane-encapsulated upconversion nanoparticles toward flexible near-infrared phototransistors. *Adv. Opt. Mater.* **2023**, *11*, 2202469.
15 Kaltenbrunner, M.; White, M. S.; Głowacki, E. D.; Sekitani, T.; Someya, T.; Sariciftci, N. S.; Bauer, S. Ultrathin and lightweight organic solar cells with high flexibility. *Nat. Commun.* **2012**, *3*, 770.
16 Chortos, A.; Liu, J.; Bao, Z. Pursuing prosthetic electronic skin. *Nat. Mater.* **2016**, *15*, 937–950.
17 Yin, D.; Feng, J.; Ma, R.; Liu, Y. F.; Zhang, Y. L.; Zhang, X. L.; Bi, Y. G.; Chen, Q. D.; Sun, H. B. Efficient and mechanically robust stretchable organic light-emitting devices by a laser-programmable buckling process. *Nat. Commun.* **2016**, *7*, 11573.
18 Yin, D.; Jiang, N. R.; Liu, Y. F.; Zhang, X. L.; Li, A. W.; Feng, J.; Sun, H. B. Mechanically robust stretchable organic optoelectronic devices built using a simple and universal stencil-pattern transferring technology. *Light Sci. Appl.* **2018**, *7*, 35.
19 Lim, Y.; Yoon, J.; Yun, J.; Kim, D.; Hong, S. Y.; Lee, S. J.; Zi, G.; Ha, J. S. Biaxially stretchable, integrated array of high performance microsupercapacitors. *ACS Nano* **2014**, *8*, 11639–11650.
20 Kim, T.; Lee, H.; Jo, W.; Kim, T. S.; Yoo, S. Realizing stretchable OLEDs: a hybrid platform based on rigid island arrays on a stress-relieving bilayer structure. *Adv. Mater. Technol.* **2020**, *5*, 2000494.
21 Sekitani, T.; Noguchi, Y.; Hata, K.; Fukushima, T.; Aida, T.; Someya, T. A rubberlike stretchable active matrix using elastic conductors. *Science* **2008**, *321*, 1468–1472.
22 Dai, Y.; Hu, H.; Wang, M.; Xu, J.; Wang, S. Stretchable transistors and functional circuits for human-integrated electronics. *Nat. Electron.* **2021**, *4*, 17–29.
23 Lim, M. S.; Nam, M.; Choi, S.; Jeon, Y.; Son, Y. H.; Lee, S. M.; Choi, K. C. Two-dimensionally stretchable organic light-emitting diode with elastic pillar arrays for stress relief. *Nano Lett.* **2020**, *20*, 1526–1535.
24 Seiberlich, M.; Rainer, C.; Skarjan, L.; Ruiz-Preciado, L. A.; Perevedentsev, A.; Xia, K.; Krebsbach, P.; Schlisske, S.; Lemmer, U.; Hernandez-Sosa, G. Streamlined inkjet-printing of stretchable organic photodetectors. *Adv. Mater. Technol.* **2025**, *10*, 2401413.
25 Drack, M.; Graz, I.; Sekitani, T.; Someya, T.; Kaltenbrunner, M.; Bauer, S. An imperceptible plastic electronic wrap. *Adv. Mater.* **2015**, *27*, 34–40.
26 Cai, M.; Nie, S.; Du, Y.; Wang, C.; Song, J. Soft elastomers with programmable stiffness as strain-isolating substrates for

stretchable electronics. *ACS Appl. Mater. Interfaces* **2019**, *11*, 14340−14346.
27 Wang, W.; Wang, S.; Rastak, R.; Ochiai, Y.; Niu, S.; Jiang, Y.; Arunachala, P. K.; Zheng, Y.; Xu, J.; Matsuhisa, N.; Yan, X.; Kwon, S.-K.; Miyakawa, M.; Zhang, Z.; Ning, R.; Foudeh, A. M.; Yun, Y.; Linder, C.; Tok, J. B. H.; Bao, Z. Strain-insensitive intrinsically stretchable transistors and circuits. *Nat. Electron.* **2021**, *4*, 143−150.
28 Trung, T. Q.; Lee, N. E. Recent progress on stretchable electronic devices with intrinsically stretchable components. *Adv. Mater.* **2017**, *29*, 1603167.
29 Sun, J.; Tang, Q.; Liu, Y. Research progress in skin-like ultraflexible organic field-effect transistors. *Sci. Sin. Chim.* **2022**, *52*, 1925−1947.
30 Liu, K.; Wang, C.; Liu, B.; Bian, Y.; Kuang, J.; Hou, Y.; Pan, Z.; Liu, G.; Huang, X.; Zhu, Z.; Qin, M.; Zhao, Z.; Jiang, C.; Liu, Y.; Guo, Y. Low-voltage intrinsically stretchable organic transistor amplifiers for ultrasensitive electrophysiological signal detection. *Adv. Mater.* **2023**, *35*, 2207006.
31 Kim, S.; Kim, T.; Kim, D.; Ju, B. K. Layer-by-layer assembled nanocomposite multilayer gas barrier film manufactured with stretchable substrate. *Appl. Sci.* **2021**, *11*, 5794.
32 Kim, C. Y.; Ku, M. J.; Qazi, R.; Nam, H. J.; Park, J. W.; Nam, K. S.; Oh, S.; Kang, I.; Jang, J. H.; Kim, W. Y.; Kim, J. H.; Jeong, J.-W. Soft subdermal implant capable of wireless battery charging and programmable controls for applications in optogenetics. *Nat. Commun.* **2021**, *12*, 535.
33 Liang, J.; Li, L.; Chen, D.; Hajagos, T.; Ren, Z.; Chou, S. Y.; Hu, W.; Pei, Q. Intrinsically stretchable and transparent thin-film transistors based on printable silver nanowires, carbon nanotubes and an elastomeric dielectric. *Nat. Commun.* **2015**, *6*, 7647.
34 Liang, J.; Tong, K.; Pei, Q. A water-based silver-nanowire screen-print ink for the fabrication of stretchable conductors and wearable thin-film transistors. *Adv. Mater.* **2016**, *28*, 5986−5996.
35 Wang, C.; Bian, Y.; Liu, K.; Qin, M.; Zhang, F.; Zhu, M.; Shi, W.; Shao, M.; Shang, S.; Hong, J.; Zhu, Z.; Zhao, Z.; Liu, Y.; Guo, Y. Strain-insensitive viscoelastic perovskite film for intrinsically stretchable neuromorphic vision-adaptive transistors. *Nat. Commun.* **2024**, *15*, 3123.
36 Kang, J.; Son, D.; Wang, G.-J. N.; Liu, Y.; Lopez, J.; Kim, Y.; Oh, J. Y.; Katsumata, T.; Mun, J.; Lee, Y.; Jin, L.; Tok, J. B. H.; Bao, Z. Tough and water-insensitive self-healing elastomer for robust electronic skin. *Adv. Mater.* **2018**, *30*, 1706846.
37 Vo, N. T. P.; Nam, T. U.; Jeong, M. W.; Kim, J. S.; Jung, K. H.; Lee, Y.; Ma, G.; Gu, X.; Tok, J. B. H.; Lee, T. I.; Bao, Z.; Oh, J. Y. Autonomous self-healing supramolecular polymer transistors for skin electronics. *Nat. Commun.* **2024**, *15*, 3433.
38 Yu, Z.; Niu, X.; Liu, Z.; Pei, Q. Intrinsically stretchable polymer light-emitting devices using carbon nanotube-polymer composite electrodes. *Adv. Mater.* **2011**, *23*, 3989−3994.
39 Yuan, S.; Wang, G.; Fan, Z.; Wang, Y.; Zhang, J.; Yu, G.; Chai, Z.; Zhao, D.; Lu, X. Stretchable serpentine electrodes with high fidelity fabricated using orientation-controlled surface energy-directed assembly. *Adv. Funct. Mater.* **2025**, *35*, 2423987.
40 Yang, S.; Cao, Y. J.; Han, K.; Guo, J. T.; Zheng, P. L.; Wang, L. Y.; Cheng, T.; Zhang, Y. Z.; Lai, W. Y. Stretchable transparent electrodes based on metal grid hybrids for skin-like multimodal sensing and flexible touch panel. *Nano Energy* **2025**, *139*, 110942.
41 Park, Y.; Fuentes-Hernandez, C.; Kim, K.; Chou, W. F.; Larrain, F. A.; Graham, S.; Pierron, O. N.; Kippelen, B. Skin-like low-noise elastomeric organic photodiodes. *Sci. Adv.* **2021**, *7*, eabj6565.
42 Guo, C. F.; Sun, T.; Liu, Q.; Suo, Z.; Ren, Z. Highly stretchable and transparent nanomesh electrodes made by grain boundary lithography. *Nat. Commun.* **2014**, *5*, 3121.
43 Liu, J.; Xiao, L.; Rao, Z.; Dong, B.; Yin, Z.; Huang, Y. High-performance, micrometer thick/conformal, transparent metal-network electrodes for flexible and curved electronic devices. *Adv. Mater. Technol.* **2018**, *3*, 1800155.
44 Wu, F.; Liu, Y.; Zhang, J.; Duan, S.; Ji, D.; Yang, H. Recent advances in high-mobility and high-stretchability organic field-effect transistors: from materials, devices to applications. *Small Methods* **2021**, *5*, 2100676.
45 Kim, Y.; Zhu, J.; Yeom, B.; Di Prima, M.; Su, X.; Kim, J. G.; Yoo, S. J.; Uher, C.; Kotov, N. A. Stretchable nanoparticle conductors with self-organized conductive pathways. *Nature* **2013**, *500*, 59−63.
46 Yao, S.; Zhu, Y. Nanomaterial-enabled stretchable conductors: strategies, materials and devices. *Adv. Mater.* **2015**, *27*, 1480−1511.
47 Sun, Y.; Chang, M.; Meng, L.; Wan, X.; Gao, H.; Zhang, Y.; Zhao, K.; Sun, Z.; Li, C.; Liu, S.; Wang, H.; Liang, J.; Chen, Y. Flexible organic photovoltaics based on water-processed silver nanowire electrodes. *Nat. Electron.* **2019**, *2*, 513−520.
48 Akter, T.; Kim, W. S. Reversibly stretchable transparent conductive coatings of spray-deposited silver nanowires. *ACS Appl. Mater. Interfaces* **2012**, *4*, 1855−1859.
49 Zhao, J.; Bu, T.; Zhang, X.; Pang, Y.; Li, W.; Zhang, Z.; Liu, G.; Wang, Z. L.; Zhang, C. Intrinsically stretchable organic-tribotronic-transistor for tactile sensing. *Research* **2020,** *2020*.
50 Lin, Y.; Fang, T.; Bai, C.; Sun, Y.; Yang, C.; Hu, G.; Guo, H.; Qiu, W.; Huang, W.; Wang, L.; Tao, Z.; Lu, Y. Q.; Kong, D. Ultrastretchable electrically self-healing conductors based on silver nanowire/liquid metal microcapsule nanocomposites. *Nano Lett.* **2023**, *23*, 11174−11183.
51 Azani, M. R.; Hassanpour, A.; Torres, T. Benefits, problems, and solutions of silver nanowire transparent conductive electrodes in indium tin oxide (ITO)-free flexible solar cells. *Adv. Energy Mater.* **2020**, *10*, 2002536.
52 Sim, H.; Bok, S.; Kim, B.; Kim, M.; Lim, G. H.; Cho, S. M.; Lim, B. Organic-stabilizer-free polyol synthesis of silver nanowires for electrode applications. *Angew. Chem. Int. Ed.* **2016**, *55*, 11814−11818.
53 Huang, J.; Lu, Z.; He, J.; Hu, H.; Liang, Q.; Liu, K.; Ren, Z.; Zhang, Y.; Yu, H.; Zheng, Z.; Li, G. Intrinsically stretchable, semi-transparent organic photovoltaics with high efficiency and mechanical robustness via a full-solution process. *Energy Environ. Sci.* **2023**, *16*, 1251−1263.
54 Zheng, X.; Wu, X.; Wu, Q.; Han, Y.; Ding, G.; Wang, Y.; Kong, Y.; Chen, T.; Wang, M.; Zhang, Y.; Xue, J.; Fu, W.; Luo, Q.; Ma, C.; Ma, W.; Zuo, L.; Shi, M.; Chen, H. Thorough optimization for intrinsically stretchable organic photovoltaics. *Adv. Mater.* **2024**, *36*, 2307280.
55 Zhang, H.; Shao, Y.; Xia, R.; Chen, G.; Xiang, X.; Yu, Y. Stretchable electrodes with interfacial percolation network. *Adv. Mater.* **2024**, *36*, 2401550.
56 Han, D.; Zhou, K.; Li, X.; Lv, P.; Wu, J.; Ke, H.; Zhao, W.; Ye, L. Intrinsically stretchable organic solar cells and sensors enabled by extensible composite electrodes. *Adv. Funct. Mater.* **2024**, *34*, 2407392.
57 Zhou, H.; Han, S. J.; Harit, A. K.; Kim, D. H.; Kim, D. Y.; Choi, Y. S.; Kwon, H.; Kim, K. N.; Go, G. T.; Yun, H. J.; Hong, B. H.; Suh, M. C.; Ryu, S. Y.; Woo, H. Y.; Lee, T. W. Graphene-based intrinsically stretchable 2D-contact electrodes for highly efficient organic light-emitting diodes. *Adv. Mater.* **2022**, *34*, 2203040.
58 Liu, N.; Chortos, A.; Lei, T.; Jin, L.; Kim, T. R.; Bae, W.-G.; Zhu, C.; Wang, S.; Pfattner, R.; Chen, X.; Sinclair, R.; Bao, Z. Ultratransparent and stretchable graphene electrodes. *Sci. Adv.* **2017**, *3*, e1700159.
59 Park, J. S.; Kim, G. U.; Lee, S.; Lee, J. W.; Li, S.; Lee, J. Y.; Kim, B. J.

Material design and device fabrication strategies for stretchable organic solar cells. *Adv. Mater.* **2022**, *34*, 2201623.
60 Wang, Y.; Zhu, C.; Pfattner, R.; Yan, H.; Jin, L.; Chen, S.; Molina-Lopez, F.; Lissel, F.; Liu, J.; Rabiah, N. I.; Chen, Z.; Chung, J. W.; Linder, C.; Toney, M. F.; Murmann, B.; Bao, Z. A highly stretchable, transparent, and conductive polymer. *Sci. Adv.* **2017**, *3*, e1602076.
61 Wang, J.; Ochiai, Y.; Wu, N.; Adachi, K.; Inoue, D.; Hashizume, D.; Kong, D.; Matsuhisa, N.; Yokota, T.; Wu, Q.; Ma, W.; Sun, L.; Xiong, S.; Du, B.; Wang, W.; Shih, C.-J.; Tajima, K.; Aida, T.; Fukuda, K.; Someya, T. Intrinsically stretchable organic photovoltaics by redistributing strain to PEDOT:PSS with enhanced stretchability and interfacial adhesion. *Nat. Commun.* **2024**, *15*, 4902.
62 Jiang, Y.; Zhang, Z.; Wang, Y. X.; Li, D.; Coen, C. T.; Hwaun, E.; Chen, G.; Wu, H. C.; Zhong, D.; Niu, S.; Wang, W.; Saberi, A.; Lai, J. C.; Wu, Y.; Wang, Y.; Trotsyuk, A. A.; Loh, K. Y.; Shih, C. C.; Xu, W.; Liang, K.; Zhang, K.; Bai, Y.; Gurusankar, G.; Hu, W.; Jia, W.; Cheng, Z.; Dauskardt, R. H.; Gurtner, G. C.; Tok, J. B. H.; Deisseroth, K.; Soltesz, I.; Bao, Z. Topological supramolecular network enabled high-conductivity, stretchable organic bioelectronics. *Science* **2022**, *375*, 1411–1417.
63 Bai, Y.; Li, W.; Tie, Y.; Kou, Y.; Wang, Y.-X.; Hu, W. A stretchable polymer conductor through the mutual plasticization effect. *Adv. Mater.* **2023**, *35*, 2303245.
64 Yao, Y.; Dong, H.; Hu, W. Charge transport in organic and polymeric semiconductors for flexible and stretchable devices. *Adv. Mater.* **2016**, *28*, 4513–4523.
65 Guo, S.; Tong, Y.; Tang, Q. Recent progress in intrinsically stretchable polymer semiconductors for stretchable electronics. *Macromol. Chem. Phys. n/a*, e00336.
66 Wei, X.; Wen, W.; Shi, W.; Liu, Y.; Sun, J.; Dai, X.; Guo, Y.; Liu, Y. Intrinsically stretchable light-emitting polymer semiconductors with high charge mobility through micro-crystalline aggregation-limited morphology. *Adv. Funct. Mater.* **2024**, *34*, 2310558.
67 Zhao, Y.; Zhao, X.; Zang, Y.; Di, C.-a.; Diao, Y.; Mei, J. Conjugation-break spacers in semiconducting polymers: impact on polymer processability and charge transport properties. *Macromolecules* **2015**, *48*, 2048–2053.
68 Zhao, X.; Zhao, Y.; Ge, Q.; Butrouna, K.; Diao, Y.; Graham, K. R.; Mei, J. Complementary semiconducting polymer blends: the influence of conjugation-break spacer length in matrix polymers. *Macromolecules* **2016**, *49*, 2601–2608.
69 Mun, J.; Wang, G. J. N.; Oh, J. Y.; Katsumata, T.; Lee, F. L.; Kang, J.; Wu, H. C.; Lissel, F.; Rondeau-Gagné, S.; Tok, J. B. H.; Bao, Z. Effect of nonconjugated spacers on mechanical properties of semiconducting polymers for stretchable transistors. *Adv. Funct. Mater.* **2018**, *28*, 1804222.
70 Galuska, L. A.; McNutt, W. W.; Qian, Z.; Zhang, S.; Weller, D. W.; Dhakal, S.; King, E. R.; Morgan, S. E.; Azoulay, J. D.; Mei, J.; Gu, X. Impact of backbone rigidity on the thermomechanical properties of semiconducting polymers with conjugation break spacers. *Macromolecules* **2020**, *53*, 6032–6042.
71 Lin, Y. C.; Matsuda, M.; Chen, C. K.; Yang, W. C.; Chueh, C. C.; Higashihara, T.; Chen, W. C. Investigation of the mobility–stretchability properties of naphthalenediimide-based conjugated random terpolymers with a functionalized conjugation break spacer. *Macromolecules* **2021**, *54*, 7388–7399.
72 Lin, Y. C.; Matsuda, M.; Sato, K. I.; Chen, C. K.; Yang, W. C.; Chueh, C. C.; Higashihara, T.; Chen, W. C. Intrinsically stretchable naphthalenediimide–bithiophene conjugated statistical terpolymers using branched conjugation break spacers for field–effect transistors. *Polym. Chem.* **2021**, *12*, 6167–6178.
73 Matsuda, M.; Lin, C. Y.; Enomoto, K.; Lin, Y. C.; Chen, W. C.; Higashihara, T. Impact of the heteroatoms on mobility–stretchability properties of n-type semiconducting polymers with conjugation break spacers. *Macromolecules* **2023**, *56*, 2348–2361.
74 Zhang, S.; Ocheje, M. U.; Huang, L.; Galuska, L.; Cao, Z.; Luo, S.; Cheng, Y.-H.; Ehlenberg, D.; Goodman, R. B.; Zhou, D.; Liu, Y.; Chiu, Y. C.; Azoulay, J. D.; Rondeau-Gagné, S.; Gu, X. The critical role of electron-donating thiophene groups on the mechanical and thermal properties of donor–acceptor semiconducting polymers. *Adv. Electron. Mater.* **2019**, *5*, 1800899.
75 Lu, C.; Lee, W. Y.; Gu, X.; Xu, J.; Chou, H. H.; Yan, H.; Chiu, Y. C.; He, M.; Matthews, J. R.; Niu, W.; Tok, J. B. H.; Toney, M. F.; Chen, W. C.; Bao, Z. Effects of molecular structure and packing order on the stretchability of semicrystalline conjugated poly(tetrathienoacene-diketopyrrolopyrrole) polymers. *Adv. Electron. Mater.* **2017**, *3*, 1600311.
76 Zheng, Y.; Wang, G. J. N.; Kang, J.; Nikolka, M.; Wu, H. C.; Tran, H.; Zhang, S.; Yan, H.; Chen, H.; Yuen, P. Y.; Mun, J.; Dauskardt, R. H.; McCulloch, I.; Tok, J. B. H.; Gu, X.; Bao, Z. An intrinsically stretchable high-performance polymer semiconductor with low crystallinity. *Adv. Funct. Mater.* **2019**, *29*, 1905340.
77 Liu, D.; Mun, J.; Chen, G.; Schuster, N. J.; Wang, W.; Zheng, Y.; Nikzad, S.; Lai, J.-C.; Wu, Y.; Zhong, D.; Lin, Y.; Lei, Y.; Chen, Y.; Gam, S.; Chung, J. W.; Yun, Y.; Tok, J. B. H.; Bao, Z. A design strategy for intrinsically stretchable high-performance polymer semiconductors: incorporating conjugated rigid fused-rings with bulky side groups. *J. Am. Chem. Soc.* **2021**, *143*, 11679–11689.
78 Yue, H.; Wang, Y.; Luo, S.; Guo, J.; Jin, J.; Li, G.; Meng, Z.; Zhang, L.; Zhou, D.; Zhen, Y.; Hu, W. *In situ* continuous hydrogen-bonded engineering for intrinsically stretchable and healable high-mobility polymer semiconductors. *Sci. Adv*. **2024,** *10*, eadq0171.
79 Wu, H. C.; Lissel, F.; Wang, G. J. N.; Koshy, D. M.; Nikzad, S.; Yan, H.; Xu, J.; Luo, S.; Matsuhisa, N.; Cheng, Y.; Wang, F.; Ji, B.; Li, D.; Chen, W. C.; Xue, G.; Bao, Z. Metal–ligand based mechanophores enhance both mechanical robustness and electronic performance of polymer semiconductors. *Adv. Funct. Mater.* **2021**, *31*, 2009201.
80 Oh, J. Y.; Rondeau-Gagné, S.; Chiu, Y.-C.; Chortos, A.; Lissel, F.; Wang, G.-J. N.; Schroeder, B. C.; Kurosawa, T.; Lopez, J.; Katsumata, T.; Xu, J.; Zhu, C.; Gu, X.; Bae, W. G.; Kim, Y.; Jin, L.; Chung, J. W.; Tok, J. B. H.; Bao, Z. Intrinsically stretchable and healable semiconducting polymer for organic transistors. *Nature* **2016**, *539*, 411–415.
81 Zheng, Y.; Ashizawa, M.; Zhang, S.; Kang, J.; Nikzad, S.; Yu, Z.; Ochiai, Y.; Wu, H.-C.; Tran, H.; Mun, J.; Zheng, Y. Q.; Tok, J. B. H.; Gu, X.; Bao, Z. Tuning the mechanical properties of a polymer semiconductor by modulating hydrogen bonding interactions. *Chem. Mater.* **2020**, *32*, 5700–5714.
82 Yu, X.; Chen, L.; Li, C.; Gao, C.; Xue, X.; Zhang, X.; Zhang, G.; Zhang, D. Intrinsically stretchable polymer semiconductors with good ductility and high charge mobility through reducing the central symmetry of the conjugated backbone units. *Adv. Mater.* **2023**, *35*, 2209896.
83 Zhu, M.; Li, Y.; Wang, C.; Shao, Z.; Shi, W.; Chen, J.; Yang, Z.; Bian, Y.; Qin, M.; Zhu, Z.; Zhao, Z.; Wang, H.; Guo, Y.; Liu, Y. Atom-knotting enables high-performance intrinsically stretchable polymer semiconductors. *Chem. Mater.* **2024**, *36*, 8274–8285.
84 Zhu, M.; Shao, Z.; Li, Y.; Xiong, Z.; Yang, Z.; Chen, J.; Shi, W.; Wang, C.; Bian, Y.; Zhao, Z.; Guo, Y.; Liu, Y. Molecular-scale geometric design: zigzag-structured intrinsically stretchable polymer semiconductors. *J. Am. Chem. Soc.* **2024**, *146*, 27429–27442.
85 Savagatrup, S.; Makaram, A. S.; Burke, D. J.; Lipomi, D. J.

Mechanical properties of conjugated polymers and polymer-fullerene composites as a function of molecular structure. *Adv. Funct. Mater.* **2014**, *24*, 1169–1181.
86 Zhang, S.; Alesadi, A.; Mason, G. T.; Chen, K. L.; Freychet, G.; Galuska, L.; Cheng, Y. H.; St. Onge, P. B. J.; Ocheje, M. U.; Ma, G.; Qian, Z.; Dhakal, S.; Ahmad, Z.; Wang, C.; Chiu, Y.-C.; Rondeau-Gagné, S.; Xia, W.; Gu, X. Molecular origin of strain-induced chain alignment in PDPP-based semiconducting polymeric thin films. *Adv. Funct. Mater.* **2021**, *31*, 2100161.
87 Wu, H. C.; Hung, C. C.; Hong, C. W.; Sun, H. S.; Wang, J. T.; Yamashita, G.; Higashihara, T.; Chen, W. C. Isoindigo-based semiconducting polymers using carbosilane side chains for high performance stretchable field-effect transistors. *Macromolecules* **2016**, *49*, 8540–8548.
88 Chiang, Y. C.; Wu, H. C.; Wen, H. F.; Hung, C. C.; Hong, C. W.; Kuo, C. C.; Higashihara, T.; Chen, W. C. Tailoring carbosilane side chains toward intrinsically stretchable semiconducting polymers. *Macromolecules* **2019**, *52*, 4396–4404.
89 Dai, Y.; Dai, S.; Li, N.; Li, Y.; Moser, M.; Strzalka, J.; Prominski, A.; Liu, Y.; Zhang, Q.; Li, S.; Hu, H.; Liu, W.; Chatterji, S.; Cheng, P.; Tian, B.; McCulloch, I.; Xu, J.; Wang, S. Stretchable redox-active semiconducting polymers for high-performance organic electrochemical transistors. *Adv. Mater.* **2022**, *34*, 2201178.
90 Sun, Y.; Luo, J.; Cai, S.; Deng, C.; Peng, Q.; Shi, Y.; Li, H.; Chen, J.; Ding, J. Side-chain engineering enabled stretchable indacenodithiophene-based polymers for high-performance organic electrochemical transistors. *Chin. J. Chem.* **2025**, *43*, 3065–3074.
91 Wen, H. F.; Wu, H. C.; Aimi, J.; Hung, C. C.; Chiang, Y. C.; Kuo, C. C.; Chen, W. C. Soft poly(butyl acrylate) side chains toward intrinsically stretchable polymeric semiconductors for field-effect transistor applications. *Macromolecules* **2017**, *50*, 4982–4992.
92 Yao, J.; Yu, C.; Liu, Z.; Luo, H.; Yang, Y.; Zhang, G.; Zhang, D. Significant improvement of semiconducting performance of the diketopyrrolopyrrole–quaterthiophene conjugated polymer through side-chain engineering *via* hydrogen-bonding. *J. Am. Chem. Soc.* **2016**, *138*, 173–185.
93 Galuska, L. A.; Ocheje, M. U.; Chase, Z. A.; Rondeau-Gagné, S.; Gu, X. Elucidating the role of hydrogen bonds for improved mechanical properties in a high-performance semiconducting polymer. *Chem. Mater.* **2022**, *34*, 2259–2267.
94 Ocheje, M. U.; Selivanova, M.; Zhang, S.; Van Nguyen, T. H.; Charron, B. P.; Chuang, C. H.; Cheng, Y. H.; Billet, B.; Noori, S.; Chiu, Y. C.; Gu, X.; Rondeau-Gagné, S. Influence of amide-containing side chains on the mechanical properties of diketopyrrolopyrrole-based polymers. *Polym. Chem.* **2018**, *9*, 5531–5542.
95 Lin, Y. C.; Chen, C. K.; Chiang, Y. C.; Hung, C. C.; Fu, M. C.; Inagaki, S.; Chueh, C. C.; Higashihara, T.; Chen, W. C. Study on intrinsic stretchability of diketopyrrolopyrrole-based π-conjugated copolymers with poly(acryl amide) side chains for organic field-effect transistors. *ACS Appl. Mater. Interfaces* **2020**, *12*, 33014–33027.
96 Gasperini, A.; Wang, G. J. N.; Molina-Lopez, F.; Wu, H.-C.; Lopez, J.; Xu, J.; Luo, S.; Zhou, D.; Xue, G.; Tok, J. B. H.; Bao, Z. Characterization of hydrogen bonding formation and breaking in semiconducting polymers under mechanical strain. *Macromolecules* **2019**, *52*, 2476–2486.
97 Ocheje, M. U.; Charron, B. P.; Cheng, Y. H.; Chuang, C. H.; Soldera, A.; Chiu, Y. C.; Rondeau-Gagné, S. Amide-containing alkyl chains in conjugated polymers: effect on self-assembly and electronic properties. *Macromolecules* **2018**, *51*, 1336–1344.
98 Lee, M. Y.; Dharmapurikar, S.; Lee, S. J.; Cho, Y.; Yang, C.; Oh, J. H. Regular H-bonding-containing polymers with stretchability up to 100% external strain for self-healable plastic transistors. *Chem. Mater.* **2020**, *32*, 1914–1924.
99 Wang, G. J. N.; Shaw, L.; Xu, J.; Kurosawa, T.; Schroeder, B. C.; Oh, J. Y.; Benight, S. J.; Bao, Z. Inducing elasticity through oligo-siloxane crosslinks for intrinsically stretchable semiconducting polymers. *Adv. Funct. Mater.* **2016**, *26*, 7254–7262.
100 Liu, D.; Lei, Y.; Ji, X.; Wu, Y.; Lin, Y.; Wang, Y.; Zhang, S.; Zheng, Y.; Chen, Y.; Lai, J. C.; Zhong, D.; Cheng, H. W.; Chiong, J. A.; Gu, X.; Gam, S.; Yun, Y.; Tok, J. B. H.; Bao, Z. Tuning the mechanical and electric properties of conjugated polymer semiconductors: side-chain design based on asymmetric benzodithiophene building blocks. *Adv. Funct. Mater.* **2022**, *32*, 2203527.
101 Huang, Y. W.; Lin, Y. C.; Yen, H. C.; Chen, C. K.; Lee, W. Y.; Chen, W. C.; Chueh, C. C. High mobility preservation of near amorphous conjugated polymers in the stretched states enabled by biaxially-extended conjugated side-chain design. *Chem. Mater.* **2020**, *32*, 7370–7382.
102 Ding, Y.; Yuan, Y.; Wu, N.; Wang, X.; Zhang, G.; Qiu, L. Intrinsically stretchable n-type polymer semiconductors through side chain engineering. *Macromolecules* **2021**, *54*, 8849–8859.
103 Sun, H.; Guo, X.; Facchetti, A. High-performance n-type polymer semiconductors: applications, recent development, and challenges. *Chem* **2020**, *6*, 1310–1326.
104 Sekitani, T.; Nakajima, H.; Maeda, H.; Fukushima, T.; Aida, T.; Hata, K.; Someya, T. Stretchable active-matrix organic light-emitting diode display using printable elastic conductors. *Nat. Mater.* **2009**, *8*, 494–499.
105 Yan, C.; Wang, J.; Wang, X.; Kang, W.; Cui, M.; Foo, C. Y.; Lee, P. S. An intrinsically stretchable nanowire photodetector with a fully embedded structure. *Adv. Mater.* **2014**, *26*, 943–950.
106 Shin, M.; Oh, J. Y.; Byun, K.-E.; Lee, Y. J.; Kim, B.; Baik, H.-K.; Park, J.-J.; Jeong, U. Polythiophene nanofibril bundles surface-embedded in elastomer: a route to a highly stretchable active channel layer. *Adv. Mater.* **2015**, *27*, 1255–1261.
107 Xu, J.; Wang, S.; Wang, G.-J. N.; Zhu, C.; Luo, S.; Jin, L.; Gu, X.; Chen, S.; Feig, V. R.; To, J. W. F.; Rondeau-Gagné, S.; Park, J.; Schroeder, B. C.; Lu, C.; Oh, J. Y.; Wang, Y.; Kim, Y. H.; Yan, H.; Sinclair, R.; Zhou, D.; Xue, G.; Murmann, B.; Linder, C.; Cai, W.; Tok, J. B. H.; Chung, J. W.; Bao, Z. Highly stretchable polymer semiconductor films through the nanoconfinement effect. *Science* **2017**, *355*, 59–64.
108 Xu, J.; Wu, H.-C.; Zhu, C.; Ehrlich, A.; Shaw, L.; Nikolka, M.; Wang, S.; Molina-Lopez, F.; Gu, X.; Luo, S.; Zhou, D.; Kim, Y.-H.; Wang, G.-J. N.; Gu, K.; Feig, V. R.; Chen, S.; Kim, Y.; Katsumata, T.; Zheng, Y.-Q.; Yan, H.; Chung, J. W.; Lopez, J.; Murmann, B.; Bao, Z. Multi-scale ordering in highly stretchable polymer semiconducting films. *Nat. Mater.* **2019**, *18*, 594–601.
109 Peña-Alcántara, A.; Nikzad, S.; Michalek, L.; Prine, N.; Wang, Y.; Gong, H.; Ponte, E.; Schneider, S.; Wu, Y.; Root, S. E.; He, M.; Tok, J. B. H.; Gu, X.; Bao, Z. Effect of molecular weight on the morphology of a polymer semiconductor–thermoplastic elastomer blend. *Adv. Electron. Mater.* **2023**, *9*, 2201055.
110 Zheng, Y.; Yu, Z.; Zhang, S.; Kong, X.; Michaels, W.; Wang, W.; Chen, G.; Liu, D.; Lai, J. C.; Prine, N.; Zhang, W.; Nikzad, S.; Cooper, C. B.; Zhong, D.; Mun, J.; Zhang, Z.; Kang, J.; Tok, J. B. H.; McCulloch, I.; Qin, J.; Gu, X.; Bao, Z. A molecular design approach towards elastic and multifunctional polymer electronics. *Nat. Commun.* **2021**, *12*, 5701.
111 Weng, Y. C.; Kang, C. C.; Chang, T. W.; Tsai, Y. T.; Khan, S.; Hung, T. M.; Shih, C. C. Design principles for enhancing both carrier mobility and stretchability in polymer semiconductors *via* Lewis acid doping. *Adv. Mater.* **2025**, *37*, 2411572.
112 Mun, J.; Kang, J.; Zheng, Y.; Luo, S.; Wu, H. C.; Matsuhisa, N.; Xu, J.; Wang, G.-J. N.; Yun, Y.; Xue, G.; Tok, J. B. H.; Bao, Z. Conjugated carbon cyclic nanorings as additives for intrinsically stretchable

semiconducting polymers. *Adv. Mater.* **2019**, *31*, 1903912.
113 Mun, J.; Kang, J.; Zheng, Y.; Luo, S.; Wu, Y.; Gong, H.; Lai, J. C.; Wu, H. C.; Xue, G.; Tok, J. B.-H.; Bao, Z. F4-TCNQ as an additive to impart stretchable semiconductors with high mobility and stability. *Adv. Electron. Mater.* **2020**, *6*, 2000251.
114 Xu, J.; Wu, H. C.; Mun, J.; Ning, R.; Wang, W.; Wang, G.-J. N.; Nikzad, S.; Yan, H.; Gu, X.; Luo, S.; Zhou, D.; Tok, J. B. H.; Bao, Z. Tuning conjugated polymer chain packing for stretchable semiconductors. *Adv. Mater.* **2022**, *34*, 2104747.
115 Kang, H.; Lee, Y.; Lee, G. H.; Chung, J. W.; Kwon, Y.-N.; Kim, J.-Y.; Kuzumoto, Y.; Gam, S.; Kang, S. G.; Jung, J. Y.; Choi, A.; Yun, Y. Strain-tolerant, high-detectivity, and intrinsically stretchable all-polymer photodiodes. *Adv. Funct. Mater.* **2023**, *33*, 2212219.
116 Qin, M.; Bian, Y.; Wang, C.; Sun, J.; Shi, W.; Liu, K.; Zheng, Y.; Zhang, F.; Liu, G.; Shao, M.; Wen, W.; Zhu, Z.; Zhu, M.; Zhao, Z.; Wang, H.; Liu, Y.; Yuan, G.; Guo, Y. Intrinsically stretchable organic photodiodes for faint near-infrared light detection and extendable cryptographic imaging. *Adv. Funct. Mater.* **2024**, *34*, 2403770.
117 Mao, P.; Li, H.; Shan, X.; Davis, M.; Tang, T.; Zhang, Y.; Tong, X.; Xin, Y.; Cheng, J.; Li, L.; Yu, Z. Stretchable photodiodes with polymer-engineered semiconductor nanowires for wearable photoplethysmography. *ACS Appl. Mater. Interfaces* **2023**, *15*, 33797−33808.
118 Kang, C. C.; Hung, T. M.; Lu, S. T.; Lu, T. C.; Shih, C. C. Dipole-tailored isomeric linker enables decoupling of aggregation and crystallinity in conjugated polymers for stretchable transistors and photodiodes. *J. Am. Chem. Soc.* **2025**, *147*, 29282−29291.
119 Liu, K.; Bian, Y.; Kuang, J.; Huang, X.; Li, Y.; Shi, W.; Zhu, Z.; Liu, G.; Qin, M.; Zhao, Z.; Li, X.; Guo, Y.; Liu, Y. Ultrahigh-performance optoelectronic skin based on intrinsically stretchable perovskite-polymer heterojunction transistors. *Adv. Mater.* **2022**, *34*, 2107304.
120 Song, J.-K.; Kim, J.; Yoon, J.; Koo, J. H.; Jung, H.; Kang, K.; Sunwoo, S. H.; Yoo, S.; Chang, H.; Jo, J.; Baek, W.; Lee, S.; Lee, M.; Kim, H. J.; Shin, M.; Yoo, Y. J.; Song, Y. M.; Hyeon, T.; Kim, D. H.; Son, D. Stretchable colour-sensitive quantum dot nanocomposites for shape-tunable multiplexed phototransistor arrays. *Nat. Nanotechnol.* **2022**, *17*, 849−856.
121 Nam, T. U.; Jeong, J. H.; Vo, N. T. P.; Jeong, M. W.; Ma, J. H.; Park, M. H.; Park, J.; Kang, S. J.; Oh, J. Y. Intrinsically stretchable phototransistors with polymer-QD-polymer multi-layered hybrid films for visible-NIR perspective electronic skin sensors. *Chem. Eng. J.* **2024**, *492*, 152143.
122 Bian, Y.; Liu, K.; Ran, Y.; Li, Y.; Gao, Y.; Zhao, Z.; Shao, M.; Liu, Y.; Kuang, J.; Zhu, Z.; Qin, M.; Pan, Z.; Zhu, M.; Wang, C.; Chen, H.; Li, J.; Li, X.; Liu, Y.; Guo, Y. Spatially nanoconfined N-type polymer semiconductors for stretchable ultrasensitive X-ray detection. *Nat. Commun.* **2022**, *13*, 7163.
123 Bian, Y.; Zhu, M.; Wang, C.; Liu, K.; Shi, W.; Zhu, Z.; Qin, M.; Zhang, F.; Zhao, Z.; Wang, H.; Liu, Y.; Guo, Y. A detachable interface for stable low-voltage stretchable transistor arrays and high-resolution X-ray imaging. *Nat. Commun.* **2024**, *15*, 2624.
124 Pei, L.; Han, D.; Wang, Y.; Gao, M.; Wu, J.; Sun, C.; Yu, M.; Wang, Y. X.; Ke, H.; Li, X.; Ye, L. Advancing intrinsically stretchable organic photovoltaics with a nearly amorphous polymer semiconductor. *Adv. Funct. Mater.* **2025**, *35*, 2425892.
125 Lee, J. W.; Seo, S.; Lee, S. W.; Kim, G. U.; Han, S.; Phan, T. N. L.; Lee, S.; Li, S.; Kim, T. S.; Lee, J. Y.; Kim, B. J. Intrinsically stretchable, highly efficient organic solar cells enabled by polymer donors featuring hydrogen-bonding spacers. *Adv. Mater.* **2022**, *34*, 2207544.
126 Luo, X.; Liu, X.; Lin, Y.; Li, M.; Yang, Z.; Xiong, Z.; Wang, Y.; Peng, F.; Zhong, W.; Li, N.; Ying, L. Modular design of polymer donors regulates solution aggregation and stretchability of organic solar cells. *Angew. Chem. Int. Ed.* **2025**, *64*, e202514985.
127 Zhang, D.; Wang, Z.; Liu, J.; He, J.; Zhou, R.; Wang, Z.; Li, R.; Yang, L.; Gao, X.; Liu, Z.; Shao, M. "Twisted" terpolymer donor enabling high-performance intrinsically stretchable organic solar cells. *Angew. Chem. Int. Ed*. **2025,** *64*, e202509160.
128 Wang, Z.; Zhang, D.; Yang, L.; Allam, O.; Gao, Y.; Su, Y.; Xu, M.; Mo, S.; Wu, Q.; Wang, Z.; Liu, J.; He, J.; Li, R.; Jia, X.; Li, Z.; Yang, L.; Weber, M. D.; Yu, Y.; Zhang, X.; Marks, T. J.; Stingelin, N.; Kacher, J.; Jang, S. S.; Facchetti, A.; Shao, M. Mechanically robust and stretchable organic solar cells plasticized by small-molecule acceptors. *Science* **2025**, *387*, 381−387.
129 Lee, J. W.; Sun, C.; Lee, S. W.; Kim, G. U.; Li, S.; Wang, C.; Kim, T. S.; Kim, Y. H.; Kim, B. J. Sequentially regular polymer acceptors featuring flexible spacers for high-performance and mechanically robust all-polymer solar cells. *Energy Environ. Sci.* **2022**, *15*, 4672−4685.
130 Ding, Y.; Xiong, S.; Memon, W. A.; Zhang, D.; Wang, Z.; Li, M.; Deng, Z.; Li, H.; Shao, M.; He, F. High-performance intrinsically-stretchable organic solar cells enabled by electron acceptors with flexible linkers. *Angew. Chem. Int. Ed.* **2025**, *64*, e202421430.
131 Hu, H.; Ye, L.; Ghasemi, M.; Balar, N.; Rech, J. J.; Stuard, S. J.; You, W.; O'Connor, B. T.; Ade, H. Highly efficient, stable, and ductile ternary nonfullerene organic solar cells from a two-donor polymer blend. *Adv. Mater.* **2019**, *31*, 1808279.
132 Lee, J.-W.; Kim, G.-U.; Kim, D. J.; Jeon, Y.; Li, S.; Kim, T.-S.; Lee, J. Y.; Kim, B. J. Intrinsically-stretchable, efficient organic solar cells achieved by high-molecular-weight, electro-active polymer acceptor additives. *Adv. Energy Mater.* **2022**, *12*, 2200887.
133 Peng, Z.; Xian, K.; Cui, Y.; Qi, Q.; Liu, J.; Xu, Y.; Chai, Y.; Yang, C.; Hou, J.; Geng, Y.; Ye, L. Thermoplastic elastomer tunes phase structure and promotes stretchability of high-efficiency organic solar cells. *Adv. Mater.* **2021**, *33*, 2106732.
134 Sun, M.; Wang, C.; Xiao, M.; Sun, F.; Wang, H.; Xu, Y.; Fu, Z.; Zhang, W.; Xia, X.; Yin, H.; Zhang, M.; Ye, L.; Du, X.; Hao, X. T. Control of effective elastomer density enables mechanically robust and high-efficiency intrinsically stretchable organic solar cells. *Adv. Mater*. **2025,** *n/a*, e14031.
135 Li, S.; Wang, Y.; Sun, C.; Feng, J.; Zuo, J.; Sun, B.; Han, D.; Gao, M.; Li, X.; Xiao, B.; Zhao, W.; Kuvondikov, V.; Nematov, S.; Jia, T.; Zhang, G.; Ye, L. A general elastomeric agent to addressing embrittlement in high-efficiency organic solar cells. *Adv. Mater.* **2026**, *38*, e16229.
136 Lee, S.; Oh, S.; Han, S.; Lee, D.; Lee, J.; Kim, Y.; Jeong, H.-Y.; Lee, J. W.; Lee, M. H.; Ying, W. B.; Jeong, S.; Lee, S.; Kim, J.; Kim, Y. H.; Kim, B. J.; Jeon, E. C.; Kim, T. S.; Cho, S.; Lee, J. Y. Advancing high-efficiency, stretchable organic solar cells: novel liquid metal electrode architecture. *Energy Environ. Sci.* **2024**, *17*, 8915−8925.
137 Qin, J.; Lan, L.; Chen, S.; Huang, F.; Shi, H.; Chen, W.; Xia, H.; Sun, K.; Yang, C. Recent progress in flexible and stretchable organic solar cells. *Adv. Funct. Mater.* **2020**, *30*, 2002529.
138 Lee, S.; Jeon, Y.; Lee, S. Y.; Ma, B. S.; Song, M.; Jeong, D.; Jo, J.; Kim, G. U.; Lee, J.; Kim, T. S.; Kim, B. J.; Lee, J. Y. Intrinsically stretchable organic solar cells without cracks under 40% strain. *Adv. Energy Mater.* **2023**, *13*, 2300533.
139 Kim, J.-H.; Park, J.-W. Intrinsically stretchable organic light-emitting diodes. *Sci. Adv.* **2021**, *7*, eabd9715.
140 Zhang, Z.; Wang, W.; Jiang, Y.; Wang, Y.-X.; Wu, Y.; Lai, J. C.; Niu, S.; Xu, C.; Shih, C. C.; Wang, C.; Yan, H.; Galuska, L.; Prine, N.; Wu, H. C.; Zhong, D.; Chen, G.; Matsuhisa, N.; Zheng, Y.; Yu, Z.; Wang, Y.; Dauskardt, R.; Gu, X.; Tok, J. B. H.; Bao, Z. High-brightness all-polymer stretchable LED with charge-trapping dilution. *Nature* **2022**, *603*, 624−630.
141 Shi, W.; Hua, C.; Cao, Y.; Liu, W.; Liu, Y.; Sun, J.; Guo, A.; Qin, M.; Wang, C.; Bian, Y.; Wen, W.; Liu, Y.; Wang, F.; Ma, C.; Wang, J.; Liu,

K.; Hua, J.; Li, J.; Zhao, Z.; Guo, Y.; Liu, Y. Submicron structure confined polymers for high-performance intrinsically stretchable light-emitting diodes. *Adv. Mater.* **2025,** *n/a*, e19650.

142 Zhou, H.; Kim, H.-W.; Han, S. J.; Zhang, D.; Jeong, W. J.; Yu, H.; Tsuchiya, Y.; Hu, B.; Huh, J.; Zhang, T.; Cho, S.; Kim, J. S.; Kim, D.-H.; Yun, H. J.; Park, J.; Jang, K. Y.; Yoon, E.; Harit, A. K.; Sung, M. J.; Ahn, Y.; Chen, H.; Zeng, Q.; Park, C. Y.; Kim, K. N.; Ayuningtias, L.; Yang, H.; Kim, J. C.; Kim, Y.-H.; Woo, H. Y.; Adachi, C.; Gogotsi, Y.; Lee, T. W. Exciplex-enabled high-efficiency, fully stretchable OLEDs. *Nature* **2026**, *649*, 604–611.

143 Li, X. C.; Yao, L.; Song, W.; Liu, F.; Wang, Q.; Chen, J.; Xue, Q.; Lai, W. Y. Intrinsically stretchable electroluminescent elastomers with self-confinement effect for highly efficient non-blended stretchable OLEDs. *Angew. Chem. Int. Ed.* **2023**, *62*, e202213749.

144 Li, H.; Yu, M.; Gu, J.; Bao, Q.; Wang, Y.; Li, Y.; Ma, Y.; Bai, L.; Zhuo, Z.; Zhang, Y.; Zhang, J.; Wang, Y.; Luo, M.; Liu, Y.; Li, C.; Lin, J.; Zhang, X.; Feng, Q.; Xie, L. Intrinsically flexible and aging resistant fluorene-based rod-coil copolymer for bendable deep-blue PLEDs. *Adv. Funct. Mater.* **2023**, *33*, 2303947.

145 Zhuo, Z.; Ni, M.; An, X.; Bai, L.; Liang, X.; Yang, J.; Zheng, Y.; Liu, B.; Sun, N.; Sun, L.; Wei, C.; Yu, N.; Chen, W.; Li, M.; Xu, M.; Lin, J.; Huang, W. Intrinsically stretchable and efficient fully π-conjugated polymer via internal plasticization for flexible deep-blue polymer light-emitting diodes with CIEy = 0.08. *Adv. Mater.* **2023**, *35*, 2303923.

146 Ni, M.; Zhuo, Z.; Liu, B.; Han, X.; Yang, J.; Sun, L.; Yang, Y.; Cai, J.; An, X.; Bai, L.; Xu, M.; Lin, J.; Feng, Q.; Xie, G.; Wu, Y.; Huang, W. Intrinsically stretchable fully π-conjugated polymers with inter-aggregate capillary interaction for deep-blue flexible inkjet-printed light-emitting diodes. *Nat. Commun.* **2025**, *16*, 330.

147 Zhuo, Z.; Ni, M.; Yu, N.; Zheng, Y.; Lin, Y.; Yang, J.; Sun, L.; Wang, L.; Bai, L.; Chen, W.; Xu, M.; Huo, F.; Lin, J.; Feng, Q.; Huang, W. Intrinsically stretchable fully π-conjugated polymer film *via* fluid conjugated molecular external-plasticizing for flexible light-emitting diodes. *Nat. Commun.* **2024**, *15*, 7990.

148 Ma, J.; Xu, M.; Zhuo, Z.; Wang, K.; Li, Q.; Li, H.; Feng, Q.; Chen, W.; Yu, N.; Li, M.; Xie, L.; Lin, J. Plasticizer design principle of "like dissolves like": semiconductor fluid plasticized stretchable fully π-conjugated polymers films for uniform large-area and flexible deep-blue polymer light-emitting diodes. *Adv. Mater.* **2024**, *36*, 2411449.

149 Jeong, M. W.; Ma, J. H.; Shin, J. S.; Kim, J. S.; Ma, G.; Nam, T. U.; Gu, X.; Kang, S. J.; Oh, J. Y. Intrinsically stretchable three primary light-emitting films enabled by elastomer blend for polymer light-emitting diodes. *Sci. Adv.* **2023**, *9*, eadh1504.

150 Liu, Y.; Zhu, M.; Sun, J.; Shi, W.; Zhao, Z.; Wei, X.; Huang, X.; Guo, Y.; Liu, Y. A Self-assembled 3D penetrating nanonetwork for high-performance intrinsically stretchable polymer light-emitting diodes. *Adv. Mater.* **2022**, *34*, 2201844.

151 Liu, W.; Zhang, C.; Alessandri, R.; Diroll, B. T.; Li, Y.; Liang, H.; Fan, X.; Wang, K.; Cho, H.; Liu, Y.; Dai, Y.; Su, Q.; Li, N.; Li, S.; Wai, S.; Li, Q.; Shao, S.; Wang, L.; Xu, J.; Zhang, X.; Talapin, D. V.; de Pablo, J. J.; Wang, S. High-efficiency stretchable light-emitting polymers from thermally activated delayed fluorescence. *Nat. Mater.* **2023**, *22*, 737–745.

152 Liang, J.; Li, L.; Niu, X.; Yu, Z.; Pei, Q. Elastomeric polymer light-emitting devices and displays. *Nat. Photon.* **2013**, *7*, 817–824.

153 Filiatrault, H. L.; Porteous, G. C.; Carmichael, R. S.; Davidson, G. J. E.; Carmichael, T. B. Stretchable light-emitting electrochemical cells using an elastomeric emissive material. *Adv. Mater.* **2012**, *24*, 2673–2678.

154 Liu, J.; Wang, J.; Zhang, Z.; Molina-Lopez, F.; Wang, G. J. N.; Schroeder, B. C.; Yan, X.; Zeng, Y.; Zhao, O.; Tran, H.; Lei, T.; Lu, Y.; Wang, Y.-X.; Tok, J. B. H.; Dauskardt, R.; Chung, J. W.; Yun, Y.; Bao, Z. Fully stretchable active-matrix organic light-emitting electrochemical cell array. *Nat. Commun.* **2020**, *11*, 3362.

155 Zhong, D.; Wu, C.; Jiang, Y.; Yuan, Y.; Kim, M. G.; Nishio, Y.; Shih, C. C.; Wang, W.; Lai, J. C.; Ji, X.; Gao, T. Z.; Wang, Y.-X.; Xu, C.; Zheng, Y.; Yu, Z.; Gong, H.; Matsuhisa, N.; Zhao, C.; Lei, Y.; Liu, D.; Zhang, S.; Ochiai, Y.; Liu, S.; Wei, S.; Tok, J. B. H.; Bao, Z. High-speed and large-scale intrinsically stretchable integrated circuits. *Nature* **2024**, *627*, 313–320.

156 Jang, J.; Choo, H.; Lee, S.; Song, J.; Park, K.; Yoon, J.; Seong, D.; An, S.; Jung, H.; Ju, J.; Kang, J.; Kang, J.; Kim, I. S.; Shin, M.; Park, J. H.; Son, D. Reconfigurable assembly of self-healing stretchable transistors and circuits for integrated systems. *Nat. Electron.* **2025**, *8*, 474–484.

157 Lee, Y.; Oh, J. Y.; Xu, W.; Kim, O.; Kim, T. R.; Kang, J.; Kim, Y.; Son, D.; Tok, J. B. H.; Park, M. J.; Bao, Z.; Lee, T. W. Stretchable organic optoelectronic sensorimotor synapse. *Sci. Adv.* **2018**, *4*, eaat7387.

158 Wang, W.; Jiang, Y.; Zhong, D.; Zhang, Z.; Choudhury, S.; Lai, J. C.; Gong, H.; Niu, S.; Yan, X.; Zheng, Y.; Shih, C. C.; Ning, R.; Lin, Q.; Li, D.; Kim, Y. H.; Kim, J.; Wang, Y. X.; Zhao, C.; Xu, C.; Ji, X.; Nishio, Y.; Lyu, H.; Tok, J. B. H.; Bao, Z. Neuromorphic sensorimotor loop embodied by monolithically integrated, low-voltage, soft e-skin. *Science* **2023**, *380*, 735–742.

159 Bian, Y.; Liu, Y.; Guo, Y. Intrinsically stretchable organic optoelectronic devices and arrays: progress and perspective. *Sci. Bull.* **2023**, *68*, 975–980.

160 Shim, H.; Sim, K.; Ershad, F.; Yang, P.; Thukral, A.; Rao, Z.; Kim, H. J.; Liu, Y.; Wang, X.; Gu, G.; Gao, L.; Wang, X.; Chai, Y.; Yu, C. Stretchable elastic synaptic transistors for neurologically integrated soft engineering systems. *Sci. Adv.* **2019**, *5*, eaax4961.

161 Lan, L.; Huang, B.; Li, Y.; Wang, C.; Pan, J.; Huang, J.; Chen, B.; zhou, Q.; Qiu, L.; Ding, Y.; Wan, Q.; Ji, Z.; Li, Y.; Peng, J.; Cao, Y. Stretchable optoelectronic synapses with ultraviolet to near-infrared perception for retina-inspired computing and vision-adaptive sensing. *npj Flex. Electron.* **2025**, *9*, 16.

162 Yokota, T.; Zalar, P.; Kaltenbrunner, M.; Jinno, H.; Matsuhisa, N.; Kitanosako, H.; Tachibana, Y.; Yukita, W.; Koizumi, M.; Someya, T. Ultraflexible organic photonic skin. *Sci. Adv.* **2016**, *2*, e1501856.

163 Lee, Y.; Chung, J. W.; Lee, G. H.; Kang, H.; Kim, J. Y.; Bae, C.; Yoo, H.; Jeong, S.; Cho, H.; Kang, S. G.; Jung, J. Y.; Lee, D. W.; Gam, S.; Hahm, S. G.; Kuzumoto, Y.; Kim, S. J.; Bao, Z.; Hong, Y.; Yun, Y.; Kim, S. Standalone real-time health monitoring patch based on a stretchable organic optoelectronic system. *Sci. Adv.* **2021**, *7*, eabg9180.

164 Park, S.; Heo, S. W.; Lee, W.; Inoue, D.; Jiang, Z.; Yu, K.; Jinno, H.; Hashizume, D.; Sekino, M.; Yokota, T.; Fukuda, K.; Tajima, K.; Someya, T. Self-powered ultra-flexible electronics *via* nano-grating-patterned organic photovoltaics. *Nature* **2018**, *561*, 516–521.

165 Jinno, H.; Yokota, T.; Koizumi, M.; Yukita, W.; Saito, M.; Osaka, I.; Fukuda, K.; Someya, T. Self-powered ultraflexible photonic skin for continuous bio-signal detection *via* air-operation-stable polymer light-emitting diodes. *Nat. Commun.* **2021**, *12*, 2234.

166 Sun, C.; Li, S.; Feng, J.; Zhao, W.; Chen, Y.; Gao, M.; Kuvondikov, V.; Nematov, S.; Ye, L. Elasticization enables strain-tolerant microstructure and enhanced performance in stretchable polymer solar cells. *Adv. Mater. n/a*, e20990.

167 Peng, Z.; Xian, K.; Liu, J.; Zhang, Y.; Sun, X.; Zhao, W.; Deng, Y.; Li, X.; Yang, C.; Bian, F.; Geng, Y.; Ye, L. Unraveling the stretch-induced microstructural evolution and morphology–stretchability relationships of high-performance ternary organic photovoltaic blends. *Adv. Mater.* **2023**, *35*, 2207884.

168 Peng, Z.; Li, S.; Zhou, K.; Zhang, Y.; Li, M.; Li, X.; Yang, C.; Bian, F.; Geng, Y.; Ye, L. Unveiling the strain-induced microstructural

evolution and morphology-stretchability correlations of intrinsically stretchable organic photovoltaic films. *Adv. Energy Mater.* **2024**, *14*, 2304286.
169 Shen, Q.; Jiang, M.; Wang, R.; Song, K.; Vong, M. H.; Jung, W.; Krisnadi, F.; Kan, R.; Zheng, F.; Fu, B.; Tao, P.; Song, C.; Weng, G.; Peng, B.; Wang, J.; Shang, W.; Dickey, M. D.; Deng, T. Liquid metal-based soft, hermetic, and wireless-communicable seals for stretchable systems. *Science* **2023**, *379*, 488–493.
170 Zheng, Y.; Michalek, L.; Liu, Q.; Wu, Y.; Kim, H.; Sayavong, P.; Yu, W.; Zhong, D.; Zhao, C.; Yu, Z.; Chiong, J. A.; Gong, H.; Ji, X.; Liu, D.; Zhang, S.; Prine, N.; Zhang, Z.; Wang, W.; Tok, J. B. H.; Gu, X.; Cui, Y.; Kang, J.; Bao, Z. Environmentally stable and stretchable polymer electronics enabled by surface-tethered nano-structured molecular-level protection. *Nat. Nanotechnol.* **2023**, *18*, 1175–1184.
171 Mackanic, D. G.; Kao, M.; Bao, Z. Enabling deformable and stretchable batteries. *Adv. Energy Mater.* **2020**, *10*, 2001424.
172 Liu, K.; Wang, J.; Pan, X.; Tian, S.-Y.; Liu, Y.; Zhang, Z.; Di, Y.; Chen, J.; Wu, C.; Deng, X. Y.; Wang, D.; Li, P.; Pan, C. K.; Qi, F.; Liu, J.; Hua, J.; Pei, J.; Di, C. A.; Guo, Y.; Liu, Y.; Lei, T. n-Type thermoelectric elastomers. *Nature* **2025**, *644*, 920–926.
173 Bauer, S.; Kaltenbrunner, M. Semiconductors that stretch and heal. *Nature* **2016**, *539*, 365–367.
174 Wang, C.; Liu, Y.; Guo, Y. Research progress of intrinsically flexible/stretchable organic photoelectric materials and devices. *Sci. Sin. Chim.* **2025**, *55*, 1444–1470.
175 Gao, W. C.; Qiao, J.; Hu, J.; Guan, Y. S.; Li, Q. Recent advances in intrinsically stretchable electronic materials and devices. *Responsive Mater.* **2024**, *2*, e20230022.

https://doi.org/10.1007/s10118-026-3652-3